Pharmacokinetic properties of D-peptides designed for treatment of Alzheimer's disease

Inaugural-Dissertation

zur Erlangung des Doktorgrades
der Mathematisch-Naturwissenschaftlichen Fakultät
der Heinrich-Heine-Universität Düsseldorf

vorgelegt von

Leonie Leithold geb. Hofmann
aus Aachen

Düsseldorf, Juni 2015

Aus dem Institut für Physikalische Biologie

der Heinrich-Heine-Universität Düsseldorf

Gedruckt mit der Genehmigung der
Mathematisch-Naturwissenschaftlichen Fakultät der
Heinrich-Heine-Universität Düsseldorf

Referent: Prof. Dr. Dieter Willbold

Korreferent: Prof. Dr. med. Karl-Josef Langen

Tag der mündlichen Prüfung: 07.07.2015

I Eidesstattliche Erklärung

Hiermit erkläre ich an Eides statt, dass ich die vorliegende Dissertation selbständig verfasst und keine anderen als die von mir angegebenen Quellen und Hilfsmittel verwendet und Zitate kenntlich gemacht habe.

Ferner erkläre ich, dass ich in keinem anderen Dissertationsverfahren mit oder ohne Erfolg versucht habe, diese Dissertation einzureichen

Der Mensch wird alt wie eine Kuh und lernt doch immer noch dazu.

II Acknowledgement

I would like to express my gratitude to Prof Dr Dieter Willbold for the possibility to work at his institute and complete this interesting project around Alzheimer's disease, development of therapeutics and preclinical studies.

Additionally, I want to thank Prof Dr Karl-Josef Langen for being my second examiner and for allowing me to perform the largest part of my experiments in his lab.

Special thanks go to Dr Antje Willuweit for her excellent supervision and guidance.

Furthermore, I would like to thank all the members of the ICS-6 and INM-4 for professional and personal support. Special thanks go to Dr Dagmar Jürgens and Dr Janine Kutzsche for always lending an open ear and having good suggestions.

I would also like to thank my office colleagues Tina and Antonia for their suggestions, chats and help concerning all sorts of things. I also thank Nan Jiang, Julia Post, Jennifer Cohnen, Elias Bissong, Elena Schartmann, Nicole Niemietz, Tamar Ziehm and Daniela Schumacher for helping me in all sorts of ways with my experiments. Further thanks go to Kateryna Kravchenko, Claudia Börger, Carina Stegmayr, Christina Dammers, Sarah Schemmert, Franziska Weirich, Katrin Röllen, Michael Schöneck, Prof Dr Aileen Funke, Dr Kerstin Reiß, Dr Stephan Weber and Dr Alexandra Boeske.

I also would like to thank the always helpful people from the animal facility: Nikola Kornadt-Beck, Larissa Damm, Tanja Juraschek and Michaela Bohlen.

Thanks also go to my friends who supported me, but probably more importantly, distracted me in hard times and motivated me to keep going.

Finally, I specially want to thank Maxi and my mother for their support and motivation. Without you, this would not have been possible.

III Table of contents

IV List of publications

Year	Publication
2015	N Jiang, **LHE Leithold**, J Post, T Ziehm, J Mauler, L Gremer, M Cremer, E Schartmann, NJ Shah, J Kutzsche, KJ Langen, J Breitkreutz, D Willbold, A Willuweit (2015). Preclinical pharmacokinetic studies of the tritium labelled D-enantiomeric peptide D3 developed for the treatment of Alzheimer´s disease. *PloS One, 10(6), DOI 10.1371/journal.pone.0128553*
	LHE Leithold, N Jiang, J Post, T Ziehm, J Kutzsche, NJ Shah, J Breitkreutz, KJ Langen, A Willuweit, D Willbold (2015). Pharmacokinetic properties of a novel D-peptide developed to be therapeutically active against toxic beta-amyloid oligomers. *Pharmaceutical Research, DOI 10.1007/s11095-015-1791-2*
	LHE Leithold, N Jiang, J Post, N Niemietz, E Schartmann, T Ziehm, J Kutzsche, NJ Shah, J Breitkreutz, KJ Langen, A Willuweit, D Willbold. Pharmacokinetic properties of tandem D-peptides. *European Journal of Pharmaceutical Sciences (submitted)*

Year	Conference abstracts
2015	**LHE Leithold**, N Jiang, J Post, J Kutzsche, D Jürgens, KJ Langen, A Willuweit, D Willbold (2015). D-peptides developed to be therapeutically active against beta-amyloid oligomers show promising pharmacokinetic properties. *AD/PD 2015 - The 12th international conference on Alzheimer's & Parkinson's diseases*
	N Jiang, **L Leithold**, J Kutzsche, D Jürgens, KJ Langen, A Willuweit, D Willbold (2015). Preclinical pharmacokinetic studies of tritium labelled D-enantiomeric peptide D3 for the treatment of Alzheimer's disease. *AD/PD 2015 - The 12th international conference on Alzheimer's & Parkinson's diseases*
	LHE Leithold, N Jiang, J Post, T Ziehm, J Kutzsche, KJ Langen, A Willuweit, D Willbold (2015). Pharmacokinetic properties of RD2, a D-peptide as potential candidate for the treatment of Alzheimer's disease. *Düsseldorf-Jülich Symposium on Neurodegenerative Diseases (Düsseldorf, Germany)*
2014	**L Hofmann**, N Jiang, J Kutzsche, J Mauler, D Jürgens, KJ Langen, A Willuweit, D Willbold (2014). Pharmacokinetic properties of D-peptides developed to be therapeutically active against beta-amyloid oligomers. *NeuroVisionen 10*
	N Jiang, **L Hofmann**, J Mauler, L Gremer, D Jürgens, J Kutzsche, KJ Langen, A Willuweit, D Willbold (2014). Preclinical pharmacokinetic studies of tritium labelled D-Enantiomeric Peptide D3 in mouse models. *NeuroVisionen 10*

V List of figures

VI Abbreviations

Abbreviation	Meaning
%ID	Relative injected dose
AD	Alzheimer's disease
ADL	Activity of daily living
ADME	Absorption, distribution, metabolism, excretion
AGP	α_1-acid glycoprotein
APP	Amyloid precursor protein
AUC	area under the concentration-time curve
Aβ	β-amyloid
C_{max}	Peak concentration
Cl	Clearance
CSF	Cerebrospinal fluid
F	Bioavailability
HSA	Human serum albumin
i.p.	Intraperitoneal
i.v.	Intravenous
inf	Infinity
λ_z	Terminal eliminiation rate constant
MCI	Mild cognitive impairment
NMDA	*N*-methyl-D-aspartate
p.o.	Oral
PET	Positron emission tomography
PS1	Presenilin 1
PS2	Presenilin 2
s.c.	Subcutaneous
$t_{1/2}$	Terminal half-life
t_{max}	Timepoint of maximal concentration
V_d	Distribution volume

VII Deutsche Zusammenfassung

Die Alzheimer‘sche Demenz ist die häufigste Form von Demenz in Senioren und es wird erwartet, dass Patientenzahlen durch die demografische Alterung der Gesellschaft zunehmen werden. Dies führt zu einer zunehmenden Belastung für Patienten, Pflegende und das öffentliche Gesundheitssystem. Die Alzheimer’sche Demenz ist eine fortschreitende neurodegenerative Erkrankung mit weitgehenden Symptomen wie unter anderem Gedächtnisstörungen und Veränderungen der Persönlichkeit. Die Hauptkennzeichen der Pathologie umfassen Aggregation und Ablagerung der Proteine Amyloid β (Aβ) und Tau. Bis zum heutigen Tage führen Behandlungsmethoden für die Alzheimer’sche Demenz lediglich zu symptomatischer Verbesserung, die zugrundeliegenden Pathologien werden jedoch nicht aufgehalten. Bei dem Versuch eine ursächliche Behandlung zu finden werden verschiedene Ansätze untersucht. Ein Beispiel für eine vielversprechende Kategorie sind Peptide. Allerdings werden Peptide häufig proteolytisch degradiert und anschließend schnell vom Körper ausgeschieden. Um dem entgegenzuwirken können die Peptide in ihrer D-enantiomeren Form verwendet werden. Dieser Ansatz wurde bei dem Peptid D3 verwendet, welches sich bereits in transgenen Mäusen als therapeutisch effektiv zeigte und dort die Kognition verbesserte und sowohl Aβ Ablagerungen als auch Neuroinflammation verminderte.

In der vorliegenden Arbeit wurden die proteolytische Stabilität und pharmakokinetischen Eigenschaften des Tritium-markierten D-Peptids D3 in Mäusen untersucht. Des Weiteren wurde das D3-Derivat RD2 untersucht, welches aus denselben Aminosäuren besteht, lediglich die Sequenz wurde nach rationalen Gesichtspunkten neu geordnet. Zusätzlich wurden die Tandempeptide D3D3 und RD2D3 analysiert und die pharmakokinetischen Eigenschaften aller vier Peptide verglichen, sowie verschiedene verwendete Administrationsrouten. Schließlich wurde *in vitro* die Bindung der Peptide an das humane Serumalbumin und das saure α_1-Glykoprotein untersucht, um den Anteil freien Peptids in Plasma abzuschätzen.

Die Ergebnisse zeigen, dass alle vier D-Peptide für mindestens einen Tag im Plasma stabil vorliegen. Im Vergleich zu den einfachen Peptiden zeigen die Tandempeptide unvorteilhafte pharmakokinetische Eigenschaften. Hier ist von Interesse, dass RD2D3 etwas positivere Werte aufweist als D3D3. Insgesamt zeigt RD2 die vorteilhaftesten Eigenschaften, wie etwa die längste Halbwertszeit mit etwa 60 Stunden. Alle Peptide erreichen zudem das Gehirn, wo sie ihre therapeutische Wirkung entfalten sollen. Die Tandempeptide zeigen eine starke Bindung an Plasmaproteine, im Gegensatz zu D3 und RD2, von denen 8 bzw. 11,5 % frei im Plasma vorliegen. Nach oraler Gabe zeigen sowohl D3 als auch RD2 sehr vorteilhafte pharmakokinetische Eigenschaften, ebenso wie RD2 nach subkutaner Administration. Zusammengefasst kann man sagen, dass D3 und RD2 vielversprechende pharmakokinetische Eigenschaften zeigen, die sie für weitere therapeutische Untersuchungen ausweisen. Von besonderem Interesse für präklinische Studien ist RD2, was eine höhere Spezifität zu Aβ Oligomeren aufweist.

VIII Abstract

Alzheimer's disease (AD) is the most common form of dementia in the elderly, and with demographic ageing the prevalence of AD will increase and become a burden on patients, caregivers and the public health systems. AD is a progressive neurodegenerative disorder and its symptoms are broad and include memory deficits as well as personality changes. The major hallmark of AD pathology is aggregation and deposition of the proteins β-amyloid (Aβ) and tau. To date, treatment of AD provides symptomatic relief, but the underlying pathologies are not ameliorated. Different approaches are exploited in the effort to uncover the cause of AD and find a curative treatment. One approach considers peptides as drug category. However, peptides often undergo protease degradation and are rapidly cleared from the organism. To counteract this, peptides consisting of D-enantiomeric amino acids can be employed. One promising D-peptide is D3, which was shown to be effective in mice where treatment lead to improved cognition as well as reduced plaque load and neuroinflammation.

In the present work we analysed proteolytic stability and pharmacokinetic properties of ^{3}H-labelled D3 in mice. Additionally, we investigated the D3 derivative RD2 which contains the same amino acids, but with a reordered sequence. Furthermore, we analysed the tandem peptides D3D3 and RD2D3 and compared pharmacokinetic properties of these peptides as well as different routes of administration. Finally, *in vitro* binding to α_1-acid glycoprotein and human serum albumin is assessed in order to estimate the fraction of the peptide remaining unbound in plasma.

Results show, that all four D-peptides remain stable in plasma for at least one day, while the control L-peptide is quickly degraded. Interestingly, the tandem peptides do not fare well in the comparison of the pharmacokinetic properties with the single peptides. They show a relatively short plasma half-life of maximally only few hours and high rates of clearance. It is noteworthy, that RD2D3 exhibits more favourable properties than D3D3. This seems to originate from the sequence of RD2, which shows the longest half-life of about 60 hours compared to about 40 hours for D3, as well as the lowest clearance. All peptides are found to enter the brain where they are thought to exhibit their therapeutic function. Plasma protein binding is high for the tandem peptides and RD2 shows the lowest binding with an estimated 11.5 % remaining unbound in plasma. Furthermore, both D3 and RD2 show promising pharmacokinetic parameters after oral administration and RD2 shows excellent results upon subcutaneous administration.

In summary, both D3 and RD2 show promising pharmacokinetic parameters qualifying them for further therapeutic research. Considering the higher Aβ oligomer specificity of RD2 together with its slightly more favourable parameters, the focus regarding preclinical studies should be on RD2.

1 Introduction

1.1 Alzheimer's disease

Alzheimer's disease (AD) is the most common type of dementia as well as the most prevalent age-related neurodegenerative disorder. In 2001 dementia had a prevalence of over 5.4 % for people aged 60 years or older living in Western Europe (Ferri *et al.* 2005). Currently, over 35 million people worldwide are suffering from dementia and in the future this number is expected to increase largely, with estimations ranging up to 115 million people by 2050 (figure 1; Alzheimer's Disease International 2013b). AD currently affects about 25 million people, but to date no curative treatment exists (Alzheimer's Disease International 2014).

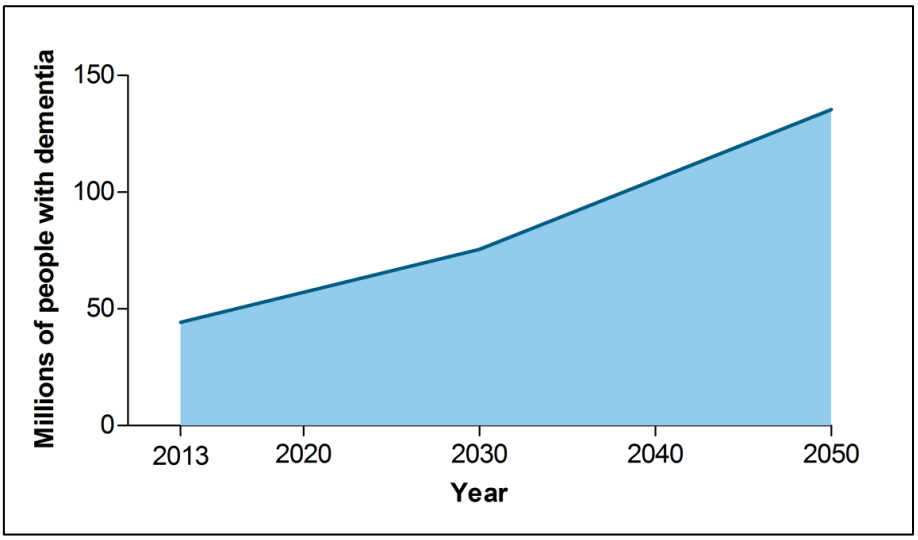

Figure 1: Estimated number of people with dementia worldwide from 2013 to 2050. Numbers according to Alzheimer's disease International (2013a).

AD is marked by a progressing inexorable course of disease. It is frequently grouped in different stages. At a preclinical stage changes already occur in the brain, but have little impact on a patient's life. Patients then experience mild cognitive impairment (MCI) before the disease advances into dementia. Alzheimer's patients initially experience deficits to memorise new information and while growing older cognition declines further, accompanied by attention and problem-solving difficulties. Other symptoms become apparent at later stages: language dysfunction, visuospatial difficulties, loss of insight and personality changes (Holtzman *et al.* 2011; Thies *et al.* 2013). With progressing AD, patients experience more and more difficulties performing the basic activities of daily living (ADLs) such as dressing, eating and personal hygiene. Patients therefore need social care, resulting in an increasing global economic impact of AD (Alzheimer's Disease International 2010).

The biggest risk factor for AD is age. Hereditary factors also play a role in increasing the chance of developing AD, including having a family history of AD as well as the presence of selected genes (Reitz & Mayeux 2014). One example of a gene enhancing the risk of developing AD is the presence of one or two apolipoprotein E ε4 alleles (Corder *et al.* 1993). Other factors that influence disease progression include cardiovascular health, head trauma and education levels (reviewed in Alzheimer's Association 2011; and Holtzman *et al.* 2011). The risk of developing dementia is influenced by early-life IQ, hypertension, diabetes, physical fitness and education (Deary *et al.* 2009).

AD can also occur due to genetic reasons. A number of genetic variants were found in families with a history of early onset AD (< 60 years) and are inherited in a Mendelian pattern, mostly autosomal dominant (Bertram *et al.* 2010; Reitz & Mayeux 2014). These so-called "familial" AD patients account for only < 1 % of AD cases with the majority of AD cases being due to sporadic AD (Thies *et al.* 2013). Amongst others, mutations causing familial AD were found in three genes that are involved in amyloid precursor protein (APP) cleavage and Aβ formation: the gene for APP itself as well as the genes for presenilin 1 and 2 (PS1 and PS2) (Bird 2008). To date, over 200 mutations have been identified in those three genes leading to early onset AD, many are point mutations but also deletions are found to cause familial forms of AD (Bertram *et al.* 2010). Usually, familial AD patients experience an early onset of the disease with symptoms occurring at middle age (Thies *et al.* 2013). An example for these mutations, is the so called Swedish mutation, a double point mutation of APP, which leads to an increase of Aβ production by enhancing β-secretase processing of APP (Citron *et al.* 1992; Mullan *et al.* 1992).

1.1.1 Pathology

To date, the underlying cause of AD remains to be unravelled; however, protein deposits are thought to contribute to neuronal and synaptic loss. The most prominent pathology in brains of AD patients are aggregation pathologies such as amyloid plaques consisting of β-amyloid (Aβ) peptides that accumulate extracellularly and intraneuronal neurofibrillary tangles formed of tau protein with altered phosphorylation (figure 2) (Blennow *et al.* 2006).

These protein deposits are thought to contribute to neuronal and synaptic loss by hampering the physiological functioning of the neurons (Ballard *et al.* 2011). Furthermore, loss of cholinergic function in the central nervous system has been shown to contribute to the cognitive decline and glutamatergic overstimulation of the postsynaptic *N*-methyl-D-aspartate (NMDA) receptors is thought to lead to neuronal damage, indicating more facets to the development of AD (Blennow *et al.* 2006).

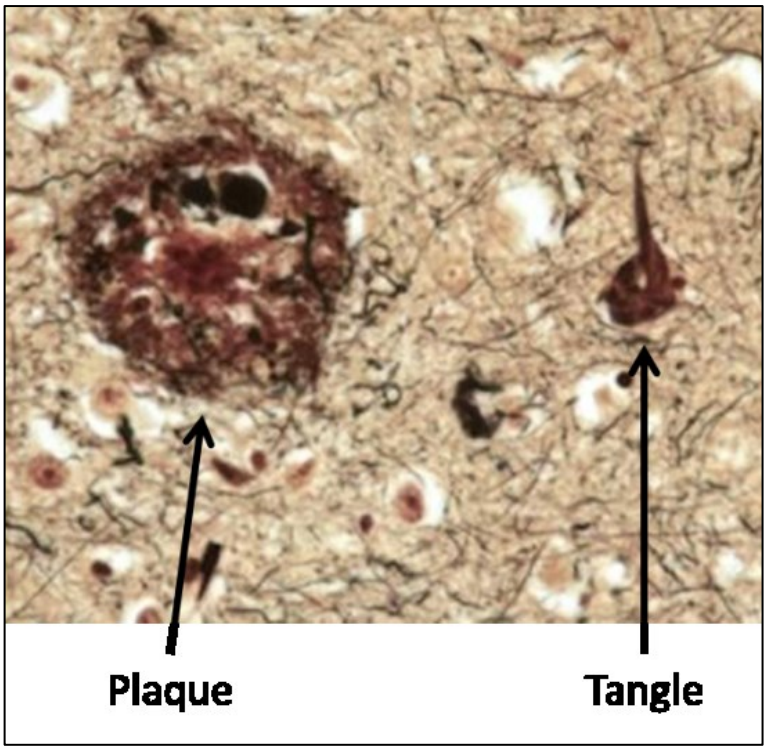

Figure 2: Silver staining showing both plaque and tangle. Both pathologies are found in Alzheimer's disease (adapted from Serrano-Pozo *et al.* 2011)

1.1.1.1 Amyloid β

The Aβ peptide is the main component of the plaques that are a hallmark of AD pathology and mostly comprised of Aβ fibrils (Hutton & Hardy 1997). There are different subtypes of plaques, ranging from plaques with a dense central core (figure 2) formed of aggregated Aβ which are associated with neuron loss in their surroundings, to more diffuse plaques consisting of amorphous Aβ aggregates (Hutton & Hardy 1997).

Under physiological conditions, APP is mainly cleaved by the α-secretase (see figure 3). The α-secretase cleavage site is positioned inside the Aβ region, therefore leading to formation of non-amyloidogenic fragments (Esch *et al.* 1990). In AD, proteolytic cleavage of APP by β- and γ-secretase complexes (figure 3) leads to production of a series of Aβ fragments (Kummer & Heneka 2014). The γ-secretase has multiple possible cleavage positions in APP (red arrows) resulting in Aβ fragments differing in length (Benilova *et al.* 2012), the main forms are $A\beta_{1-40}$ and $A\beta_{1-42}$ with their length denoted in subscript.

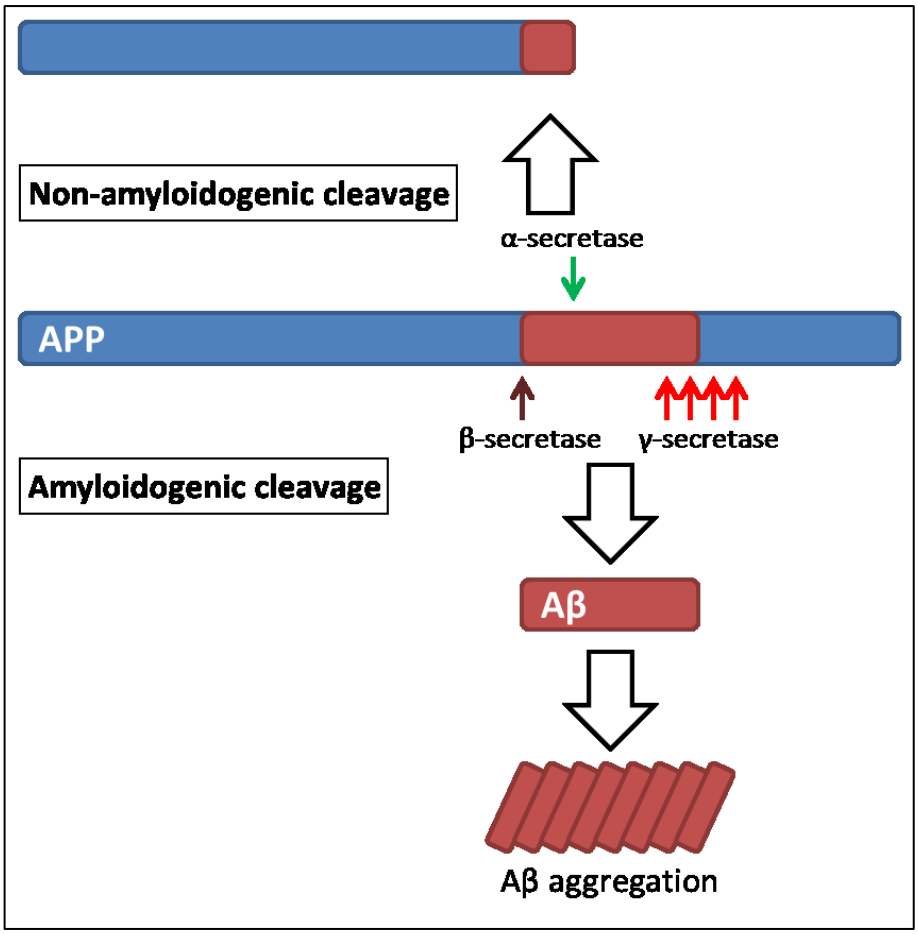

Figure 3: Processing of APP and formation of Aβ. Non-amyloidogenic cleavage of APP (top) is performed by the α-secretase (green arrow). Abnormal cleavage (bottom) by the β- and γ-secretase (dark red and red arrows) leads to formation of Aβ and aggregation (after Benilova *et al.* 2012).

One long-standing hypothesis trying to explain the development of AD is the amyloid cascade hypothesis, which indicates a major role for Aβ in the pathogenesis of AD (figure 4). It states that the imbalance between production and clearance of Aβ in the brain is the main event ultimately leading to neuronal degeneration (Selkoe 1991; Hardy & Higgins 1992; Soto 1999; Pimplikar 2009). The importance of Aβ in the development of AD is supported by the mutations found in familial AD. Mutations were found in the pathway leading to Aβ formation, in the APP gene as well as in the genes encoding PS1 and PS2 which are part of the γ-secretase complex and therefore enzymes necessary for Aβ generation (Citron *et al.* 1992; de Silva & Patel 1997). Furthermore, people with Down's syndrome, who possess an additional APP gene, are reported to develop Aβ plaques at an early age (Wilcock & Griffin 2013).

Which form of Aβ is the toxic one leading to AD pathogenesis is controversially discussed in the literature (Walsh & Selkoe 2007; Liu *et al.* 2012). Nowadays, soluble Aβ oligomers are viewed as the toxic amyloid species ultimately leading to AD (Ferreira *et al.* 2007; Decker *et al.* 2010; DaRocha-Souto *et al.* 2011; Benilova *et al.* 2012).

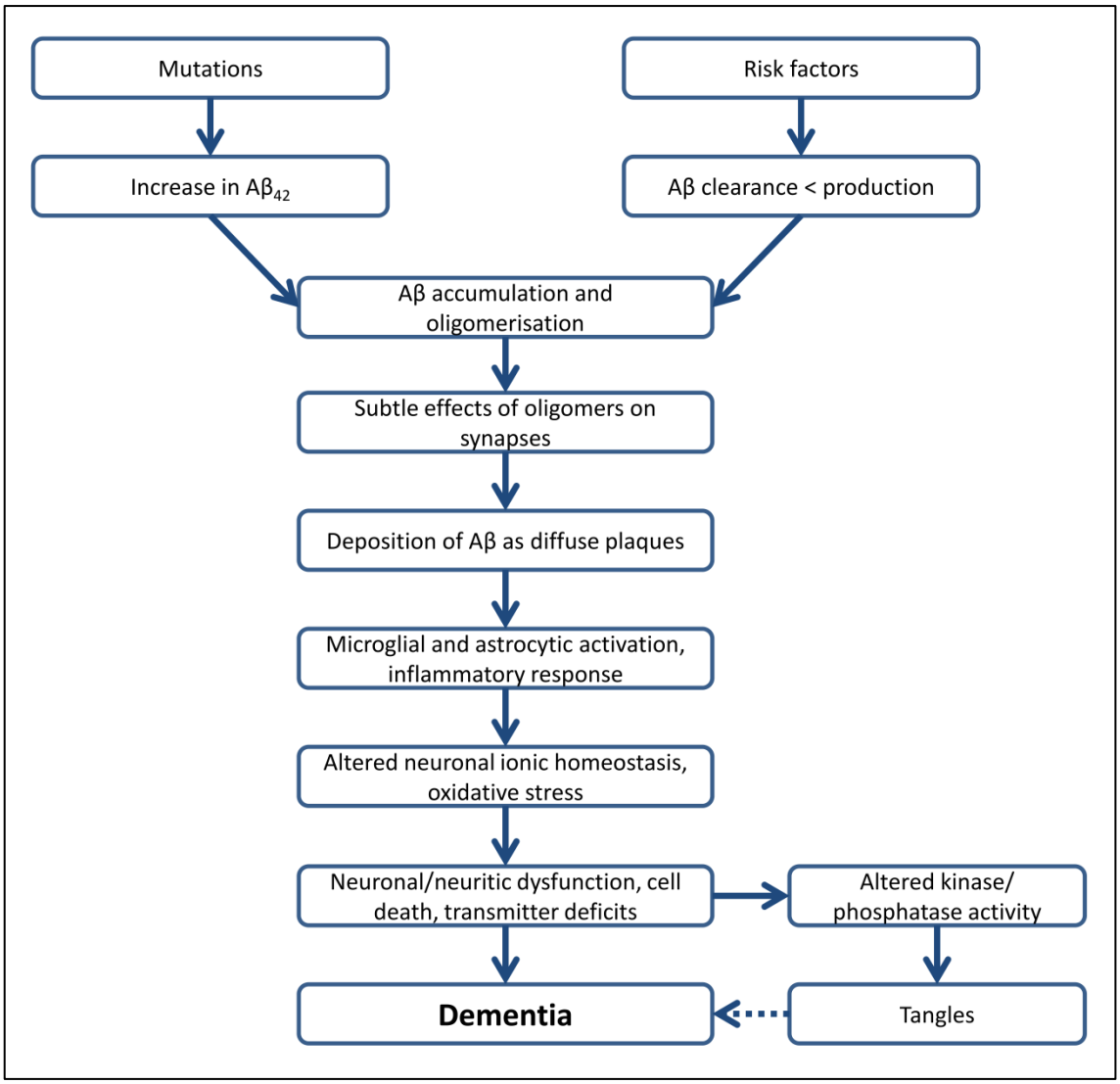

Figure 4: Amyloid cascade hypothesis. This hypothesis claims that the imbalance between Aβ production and clearance ultimately leads to dementia. Tau pathology is considered a contributing downstream event (figure after: Hardy & Selkoe 2002; Blennow *et al.* 2006).

1.1.1.2 Tau

Intraneuronal neurofibrillary tangles are made up of the microtubule-associated protein tau in a hyper-phosphorylated state. The abnormal disengagement of tau from microtubules leads to an increase in the cytosolic tau concentration. This is thought to be the primary process leading to the formation of the tangles due to an increased misfolding likelihood of the unbound protein (reviewed in Ballatore *et al.* 2007). Causes for the abnormal disengagement of tau from the microtubules include an imbalance of tau kinases and phosphatases, genetic mutations and covalent tau modifications (Ballatore *et al.* 2007). It was found that a mutation in tau alone is able to cause frontotemporal dementia (Hutton *et al.* 1998). Pathological functions of hyperphosphorylated tau and the tangles could result in neurodegeneration as well as loss of normal function of tau (Ballatore *et al.* 2007). Especially the latter is thought to be an important factor in development of neurodegeneration (Roy *et al.* 2005; Trojanowski *et al.* 2005).

1.1.1.3 Neuroinflammation

Increasing evidence is found that there are common links between the two pathological hallmarks, such as the development of neuroinflammation which is considered a third hallmark of AD by some researchers (reviewed in McNaull *et al.* 2010). Oxidative stress is thought to be one of the earliest events in AD pathogenesis, potentially caused by reduced cerebral blood flow (Zhu *et al.* 2007; Chang *et al.* 2011). Oxidative stress can lead to activation of inflammatory cells such as microglia (Rojo *et al.* 2008). Microglia are commonly found surrounding Aβ plaques, they also show increased chemotaxis towards them (Rogers & Lue 2001; Tuppo & Arias 2005). Furthermore, increased numbers of reactive astrocytes are found in the brains of AD patients as well as surrounding Aβ plaques (Pike *et al.* 1995; McNaull *et al.* 2010). However, the connection between neuroinflammation and AD remains unclear. It is not yet known whether neuroinflammation contributes to development of the disease, it may also be caused by it (Tuppo & Arias 2005).

1.1.2 Diagnosis of AD

Diagnosis of AD remains difficult. AD is most commonly diagnosed by physicians based on medical and familiar history, input from close family members, physical and neurological examinations as well as cognitive tests (Blennow *et al.* 2006). However, it is still difficult to distinguish AD from other dementias.

Biomarker tests may help diagnosing AD at early, preclinical stages and thereby give the ability to start treatment before clinical symptoms manifest. To date, a number of biomarker tests have been developed, however, their efficacy depends on the stage of the disease and type of dementia (reviewed in Bloudek *et al.* 2011). Biomarkers can most conveniently be assessed in plasma or the cerebrospinal fluid (CSF); especially total tau, phosphorylated tau and $A\beta_{1\text{-}42}$ are under investigation as promising biomarkers (Blennow *et al.* 2010). Furthermore, imaging methods such as magnetic resonance imaging (detecting medial temporal lobe atrophy) or positron emission tomography (PET) using tracers against Aβ, tau or glucose metabolism can be used for diagnosis of AD (Blennow *et al.* 2006; Ikonomovic *et al.* 2008; Zhang *et al.* 2012b).

In recent years the United States' National Institute on Aging together with the Alzheimer's Association developed new criteria and guidelines for the diagnosis of AD as well as for the evaluation of the occurring pathology (McKhann *et al.* 2011; Hyman *et al.* 2012). They included biomarker diagnostics (analysis of CSF and PET) and assessment of neuronal injury as well as preclinical stages of AD to allow for better diagnostic differentiation between the different stages of AD and to distinguish them from other neurodegenerative diseases (McKhann *et al.* 2011; Hyman *et al.* 2012).

1.1.3 Treatment of AD

Despite intensive research, causal treatment to AD remains to be developed. The available medications slow down progression of the symptoms but do not stop the underlying neurodegeneration (Alzheimer's Association 2011). Especially the individual differences in response to the available drugs pose a major problem in clinical trials as well as in clinical praxis, leading to therapeutic failure or adverse drug reactions (Meyer 2000).

To date, available treatment focusses on the imbalance of the neurotransmitters acetylcholine and glutamate. However, improvement remains symptomatic and does not include neuroprotection (Massoud & Léger 2011). The cholinergic hypothesis states that loss of cholinergic function in the cortex is associated with behavioural changes present in AD (Terry & Buccafusco 2003). Three acetylcholinesterase inhibitors donepezil, galantamine and rivastigmine are currently used for treatment of mild to moderate AD and meta-analyses show improvements in cognitive function, ADLs and general behaviour, though the effects remain relatively small (Lanctot *et al.* 2003; Birks 2006). However, they also found that all three acetylcholinesterase inhibitors evoke adverse drug reactions such as nausea, vomiting, diarrhoea and anorexia (Lanctot *et al.* 2003; Massoud & Léger 2011). Memantine is a NMDA receptor antagonist and is licensed as treatment for moderate to severe AD (Noetzli & Eap 2013). It is a relatively new drug and shows small but significant benefits for cognition, ADLs, global functioning and neuropsychiatric symptoms and mostly only mild side effects (van Marum 2009).

Many strategies for the development of AD therapeutics address Aβ, thereby trying to reduce its production, inhibit aggregation or enhance its clearance (Soto 1999; Hardy & Selkoe 2002). The main focus so far has been on modulation of secretases as well as on immunotherapy and inhibition of Aβ fibril formation (Blennow *et al.* 2006). Furthermore, anti-inflammatory agents, cholesterol-lowering drugs and antioxidants are suggested to have positive effects (Blennow *et al.* 2006).

Many studies on potential therapeutics considered peptides, e.g. designed to prevent β-sheet conformation (Soto 1999; Sun *et al.* 2012). However, many peptides showed severe disadvantages since they can be immunogenic, instable due to degradation by proteases and often show rapid clearance, low oral bioavailability and short *in vivo* half-lives (Pauletti *et al.* 1997; Sato *et al.* 2006).

1.2 D-enantiomeric peptides

D-peptides are peptides which are entirely composed of D-enantiomeric amino acid residues. For *in vivo* administration, e.g. as medication, their use can be advantageous to that of L-peptides. D-peptides are more protease resistant than L-peptides, due to the stereoisomeric selectivity of most proteolytic enzymes (Soto *et al.* 1996; van Regenmortel & Muller 1998). As a result, system elimination is slower and they remain stable in the body for longer periods of time than L-peptides, thereby providing more time to be therapeutically active *in vivo* (Dintzis *et al.* 1993; Sela & Zisman 1997). This was for instance shown for D-enantiomeric peptides in rat plasma (Poduslo *et al.* 1999) and CSF of Rhesus monkeys (Findeis *et al.* 1999). In addition it has been shown that they are not immunogenic or at least significantly less than L-peptides (Dintzis *et al.* 1993).

D-amino acid containing peptides are an increasingly emerging therapeutic approach for AD therapy (Kumar & Sim 2014). It has been previously shown that short synthetic peptides containing D-amino acids are able to reduce fibril formation and toxicity *in vitro* (Soto *et al.* 1996; Blanchard *et al.* 1997; Tjernberg *et al.* 1997; Chalifour *et al.* 2003). Some also have shown promising results *in vivo* by reducing amyloid deposits and improving cognition in transgenic AD mice. Examples are the peptides NH_2-D-Trp-Aib-OH (Frydman-Marom *et al.* 2009), D-4F (Handattu *et al.* 2009) and D3, which is discussed in detail in the next paragraph.

1.2.1 D-peptide D3

To identify Aβ binding D-peptides, mirror image phage display was performed using a large phage library and selecting for binding to $A\beta_{1-42}$ under conditions where monomers were expected to be the dominating species (Schumacher *et al.* 1996; Wiesehan & Willbold 2003). D3 consists of 12 D-amino acid residues (rprtrlhthrnr) and was first described in 2008 (van Groen *et al.* 2008). It was investigated in several *in vitro* and *in vivo* assays showing the results described below.

Van Groen *et al.* (2008) showed *in vitro* that D3 is able to decrease the formation of Thioflavin T positive aggregates, to prevent Aβ aggregation and to disassemble Aβ aggregates. Further *in vitro* investigations showed that D3 is able to reverse Aβ cytotoxicity, to completely rescue cell viability and was found to be non-toxic to cells in concentrations of up to 200 µM. Consequently, D3 was assessed *in vivo* in transgenic AD mice after 30 days of hippocampal infusion. They found that D3 had reduced the Aβ load as well as the inflammation occurring near plaques (van Groen *et al.* 2008).

Furthermore, it was shown by administration of fluorescently labelled D3 to brains of transgenic AD mice that D3 evokes no inflammatory response, can be taken up into neurons and pericytes and preferably binds to $A\beta_{1-42}$ (van Groen *et al.* 2009). The latter was confirmed by a study by Bartnik *et al.* (2010) who additionally showed that D3 has a clear preference for binding to $A\beta_{1-42}$ oligomers compared to fibrils and monomers.

Further *in vivo* studies were carried out, administering D3 orally in the drinking water or via brain infusion to transgenic AD mice for 8 weeks. They showed that learning in cognitive paradigms such as the Morris water maze was improved (Funke *et al.* 2010). Furthermore, consistent experiments indicated that D3 reduces Aβ load and plaque-associated inflammation in the transgenic mice (Funke *et al.* 2010; van Groen *et al.* 2012; van Groen *et al.* 2013). Additionally, direct infusion of lower doses of D3 into the stomach of transgenic mice showed the same results, proving the efficacy of D3 even at lower doses (Funke *et al.* 2010). However, in contrast to prior studies, no improvement of cognition relative to the control mice was visible after 4 weeks of treatment via hippocampal infusion (van Groen *et al.* 2012). Only slight improvements were detectable after 8 weeks of hippocampal infusion to aged transgenic mice (van Groen *et al.* 2013), with both studies using partially or completely fluorescently labelled D3.

To investigate the mechanism of D3 action, further *in vitro* assays were performed and showed that D3 induces the formation of large amorphous Aβ particles that do not contain oligomers or regular fibrils (Funke *et al.* 2010). Furthermore, it was shown that D3 inhibits fibrillogenesis of Aβ in seeding experiments (Funke *et al.* 2010), and cell culture experiments also indicated that D3 is able to cross the blood-brain barrier by transcytosis (Liu *et al.* 2010). D3 was shown to be able to form interactions with negatively charged groups of Aβ that reduce solubility and advance Aβ aggregation (Funke *et al.* 2010). This was confirmed by Olubiyi and Strodel (2012) who also showed that the five positively charged arginine residues of D3 are the main interaction partners and that binding induces large conformational changes in Aβ. Thereby β-sheet units were reduced which might explain the observed inhibition of fibrillisation. Later, it was shown that also the non-arginine residues contribute to the strong binding of D3 to Aβ (Olubiyi *et al.* 2014).

1.2.2 Derivatives of D3

RD2 is a derivative of D3 containing the same 12 D-amino acid residues, but with a rationally designed sequence where all arginine residues were placed together at the C-terminus (ptlhthnrrrrr). Both D3 and RD2 therefore are positively charged and have a low molecular weight of 1.6 kDa. It was demonstrated previously that RD2 exhibits strong binding to Aβ, similar to that observed with D3 but with higher affinity to Aβ oligomers, and RD2 was shown to inhibit amyloid fibril formation in an *in vitro* assay (Olubiyi *et al.* 2014).

Consequently, tandem peptides of D3 and RD2 were created in order to gain higher affinities to Aβ. This is based on the expectation that multivalent D-peptides target their multivalent target molecules, here the Aβ oligomer, with increased efficiency. D3D3 is the head-to-tail tandem version of D3 and RD2D3 is a head-to-tail heteropeptide that combines RD2 and D3. Both peptides therefore consist of 24 D-amino acid residues and have a higher molecular weight of approximately 3.2 kDa.

1.3 Pharmacokinetics

Pharmacology investigates drugs and their effects *in vivo*. It is divided in pharmacokinetics and pharmacodynamics (Brenner & Stevens 2010). Pharmacokinetic studies examine mathematically the time-dependent fate of a drug administered into a living organism. In contrast, pharmacodynamic studies examine the drug's impact on the organism it is applied to.

The drug's concentration over time, and therefore its pharmacokinetic properties, depends on different factors and processes (figure 5). The first step is the drug's absorption, followed by distribution, metabolism and excretion, which is generally abbreviated by ADME. These steps depend on different factors such as the administered dose, the administration route and the drug's formulation as well as the organism's constitution and indication of the drug (Caldwell *et al.* 1995).

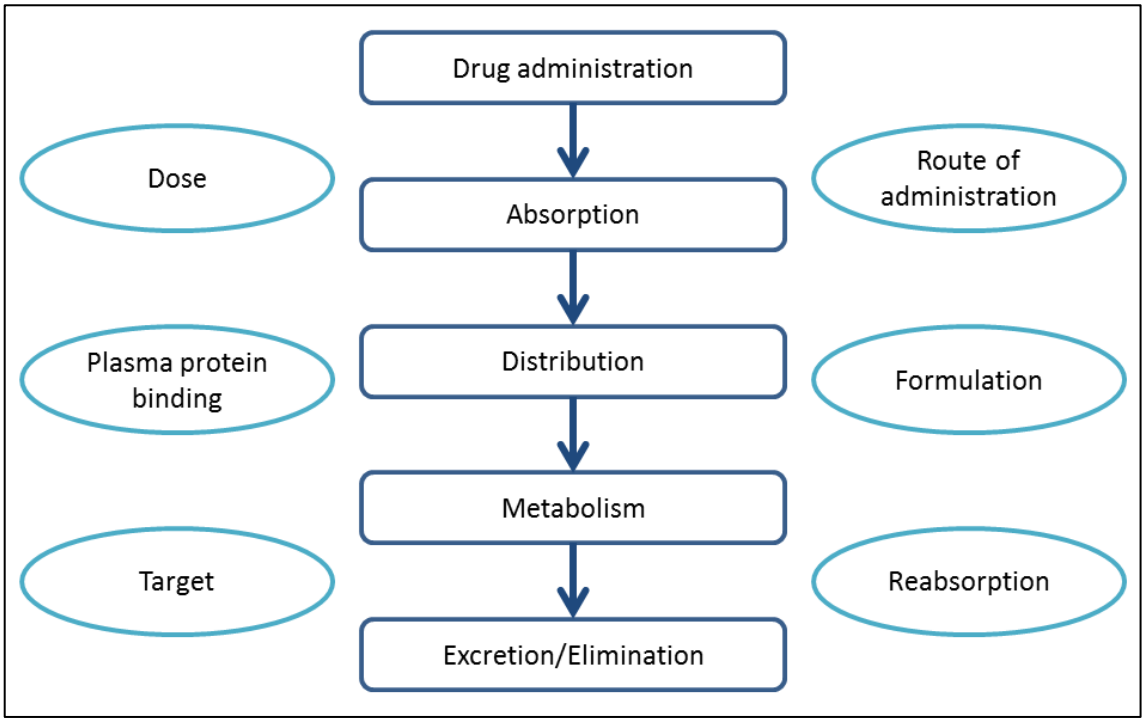

Figure 5: Schematic representation showing processes of pharmacokinetics and influencing factors. After drug administration, it is absorbed into the circulation and distributed through the organism. Thereby, drugs can be affected by metabolism before they are excreted from the organism. Many factors influence this process, some of which are shown in the ellipses.

For ethical reasons, extensive pharmacokinetic studies are carried out either *in vitro* or in laboratory animals before a drug is first administered to humans (Leucuta & Vlase 2006). Therefore, knowledge of the pharmacokinetic ADME profile of a drug candidate is essential to predict its efficacy *in vivo*. However, it is important to understand that pharmacokinetic and safety assessment of drugs in animals and extrapolation to humans remain critical steps since adverse reactions can be species specific. The individual response to a drug depends on the target mechanism, the sensitivity to the compound, the metabolism and the distribution of the compound all of which can

differ between species as well as from person to person (Caldwell *et al.* 1995; Noetzli & Eap 2013).

In pharmacology, stereoisomerism is an important factor since receptor and enzyme affinities can be specific to the enantiomers. It is long known that this can result in pharmacodynamic and pharmacokinetic differences between two enantiomers (Williams 1990; Wang *et al.* 2005). Furthermore, stereoselectivity also results in metabolism differences (Campo *et al.* 2009; Niwa *et al.* 2011).

1.3.1 Routes of administration

There are different routes to administer a drug to living organisms. Enteral administration routes include oral and rectal administration which lead to the drug being absorbed from the gastrointestinal tract (Brenner & Stevens 2010). For oral administration (*per os*, p.o.), which is the most common route of administration, the drug is swallowed and absorbed from the stomach and small intestines. Therefore, this route is convenient, relatively safe and economical. However, absorption can vary widely, drugs can be inactivated by gastric acid and first-pass metabolism (see 1.3.4) can occur, additionally, depending on the patient's condition, this route may not be applicable (Brenner & Stevens 2010; Feucht & Patel 2011).

Upon parenteral administration routes, the drug does not pass the gastrointestinal tract but is immediately systemically bioavailable or able to reach the target. Intravenous (i.v.) administration gives the greatest control over the dose reaching the circulation due to the avoidance of absorption processes. This is often used for compounds with short half-lives and if careful titration of the dose is needed. However, it is potentially the most dangerous route of administration, as for instance the fast administration can lead to toxicity (Brenner & Stevens 2010). Intramuscular and subcutaneous (s.c.) administration of drugs can be used for drug solutions and suspensions, yet they can cause pain or skin irritation and cannot be used for large volumes (Brenner & Stevens 2010). Suspensions are often used because they result in slower absorption and therefore prolong a drug's duration of action (Brenner & Stevens 2010). In small animals intraperitoneal (i.p.) administration is frequently used, in human patients it is less often performed but is used for certain indications such as chemotherapy or other indications where the target is within the peritoneum or close by (Chaudhary *et al.* 2010).

1.3.2 Absorption

Absorption refers to the way a drug enters the blood circulation or possibly directly its target from the site of administration. This is important especially for orally delivered drugs as the gastrointestinal tract is the most important site of absorption (Caldwell *et al.* 1995). Further sites of absorption are the peritoneum, the skin and the respiratory tract.

Absorption requires a drug to cross one or more layers of cell membranes. This can take place either by passive or facilitated diffusion or by active transport (Brenner & Stevens 2010). The rate limiting determinants are concentration gradients, the lipid/water partition coefficient of the drug and the presence of active carrier molecules. Furthermore, active transport across cell membranes tends to show stereoselectivity (Caldwell *et al.* 1995).

1.3.3 Distribution

A drug is mainly distributed via the blood circulation, thereby reaching organs and tissues. The distribution of a drug through the body is dependent on hemodynamics, passive diffusion across lipid membranes, presence of active transport molecules and binding of proteins in plasma and tissue (Caldwell *et al.* 1995). Highly perfused organs such as the heart, liver, kidney and brain are reached swiftly, enabling a fast onset of drug action (Brenner & Stevens 2010). Plasma proteins (detailed in 1.3.7) play an important role in binding of drugs and preventing them from reaching their target or delivering them to their respective target organ (Bohnert & Gan 2013).

Furthermore, knowledge of possible accumulation sites is important in many ways. Accumulation of a drug can provide a reservoir to prolong the presence of the drug in the organism. If drugs accumulate, they usually do so in certain tissues and are slowly released as plasma concentrations decrease (Caldwell *et al.* 1995). In this case, termination of drug action depends on metabolism and excretion of the drug and can lead to (potentially adverse) side effects (Caldwell *et al.* 1995).

1.3.4 Metabolism

Many drugs are metabolised and thereby transformed into one or more different metabolites. This can leave activity unaffected, but can also render a potent agent ineffective or lead to adverse effects caused by the metabolites (Leucuta & Vlase 2006). Furthermore, some drugs are applied as inactive agent and are then activated by metabolic reactions (Brenner & Stevens 2010). Metabolism can be affected by many factors, either physiological, endogenous (e.g. age, sex and genetic polymorphisms) or exogenous (e.g. nutrition, daytime) (Caldwell *et al.* 1995).

Metabolism can be caused enzymatically or by spontaneous chemical transformation (Caldwell *et al.* 1995). Enzymatic metabolism for example takes place in liver and kidney. Potential metabolic pathways include demethylation, conjugation, dealkylation and oxidation. The liver hepatocytes are the major site of metabolism for the majority of drugs (Caldwell *et al.* 1995). Drugs can be metabolised directly following absorption, being subject to first-pass metabolism. This describes the process in which a part of the drug is absorbed from the gastrointestinal tract but is then metabolised in the gut wall or the liver before reaching the blood circulation (Brenner & Stevens 2010).

Drug metabolism (biotransformation) mostly happens in two phases. Phase I metabolism serves to create or unmask a chemical group required for a phase II reaction, e.g. by oxidative reactions (Brenner & Stevens 2010). The most important group of enzymes for metabolism is the cytochrome P-450 family which is involved in oxidative metabolism of many compounds including most drugs (Glue & Banfield 1996; Furge & Guengerich 2006). Phase II metabolism involves conjugation with substances such as acetate or glucuronate, which renders most metabolites inactive and transforms them into a constitution which promotes elimination (Brenner & Stevens 2010). However, drug elimination or retention can also occur with the drug being unchanged by metabolism.

1.3.5 Excretion

Excretion deals with the removal of a drug from the organism. This can appear along different routes, the major ones being the kidneys and the liver (Caldwell *et al.* 1995). Other routes include pulmonary excretion as well as excretion via saliva, sweat and breast milk (Caldwell *et al.* 1995). For most drugs excretion takes place via the urine with renal excretion involving different steps: filtration, secretion, reabsorption and excretion (Brenner & Stevens 2010). In contrast, in the liver mostly active transport processes play a role in excreting larger, both polar and lipophilic compounds, facilitated e.g. by conjugated glucuronate (Brenner & Stevens 2010).

1.3.6 Calculation of pharmacokinetic parameters

In order to determine the parameters describing the pharmacokinetic profile of a drug, mathematical models are used to analyse the data. One category of mathematical modelling is compartmental pharmacokinetic analysis. Compartmental analysis is needed to simulate the passage of the drug through the body which is represented as a system of different compartments (Brenner & Stevens 2010). However, often non-compartmental analysis is performed to determine the pharmacokinetic properties. Pharmacokinetic parameters are here determined without the use of a specific compartmental model. This is based on the theory of statistical moments and parameters and is done under the assumption that the data follows linear pharmacokinetics, which is the case if the plasma concentration can be described by first order exponential equations and is proportional to the dose (Leucuta & Vlase 2006).

Parameters as the area under the concentration time curve (AUC) are used to calculate the amount of drug that was absorbed into the body. Regarding the drug's plasma concentration time curve, the peak plasma concentration (C_{max}) and the time to reach the maximum concentration (t_{max}) can be assessed (Jang *et al.* 2001). Furthermore, the plasma bioavailability (F) is calculated, it is defined as the fraction of the administered dose that reaches the systemic circulation (Brenner & Stevens 2010). It was defined that a drug has 100 % bioavailability upon intravenous administration; therefore the bioavailability of other administration routes is calculated relative to intravenous

administration. This is of importance for oral administration of drugs, since their bioavailability can be especially low, often due to pharmaceutical factors (e.g. tablet disintegration) as well as biological factors (e.g. presence of food and first-pass metabolism) (Brenner & Stevens 2010).

Furthermore, to gain more information about the distribution, e.g. the volume of distribution (V_d) is determined, which is defined as the volume of fluid wherein a drug would have to be dissolved to have the same concentration as it does in plasma (Brenner & Stevens 2010). Low V_d values similar to the plasma volume indicate a restricted distribution; high V_d volumes approaching the total body water indicate the drug reaching intracellular fluid (Brenner & Stevens 2010). To assess elimination, parameters such as the clearance (Cl) and terminal half-life ($t_{1/2}$) as well as the elimination rate constant (λ_z) are determined. The clearance is the volume of blood from which a drug is removed per unit time and the terminal half-life is the time necessary to reduce the plasma drug concentration by half and can be calculated from the elimination rate constant which describes the rate of terminal elimination (Brenner & Stevens 2010).

1.3.7 Plasma protein binding

Early assessment of drug availability is an important tool to predict *in vivo* efficacy of a drug candidate. However, the distribution of the drug can be limited by binding to plasma proteins which can result in a reduced free concentration available for therapeutic action (Tillement *et al.* 2006; Trainor 2007). Especially the free drug concentration at the therapeutic target is thought to determine the efficacy of a drug (Smith *et al.* 2010). For most organs the free drug concentration is identical to that in blood, because there is no barrier between the blood and the target organ. This is not true for the brain where the blood brain barrier restricts the access of many substances (Liu *et al.* 2014).

Additionally, plasma protein binding can also provide a reservoir to prolong the availability of the drug (Kratochwil *et al.* 2002). It is therefore important to monitor plasma protein binding in pharmacokinetic studies, especially in elderly patients where age as well as physiological and pathophysiological changes can lead to altered free drug concentrations (Grandison & Boudinot 2000).

The major drug-binding components in plasma are human serum albumin (HSA), α_1-acid glycoprotein (AGP), lipoproteins and erythrocytes, with the first two thought to be predominant (Bohnert & Gan 2013). HSA is the most abundant protein in human blood plasma (50 - 60 %, 66 kDa, 0.53 - 0.75 mM concentration) (Kratochwil *et al.* 2002). It is mainly responsible for binding of acidic drugs (Brenner & Stevens 2010; Liu *et al.* 2014). HSA has several hydrophobic binding sites and is therefore able to bind a wide diversity of ligands reversibly with high affinity (Kratochwil *et al.* 2002). AGP, sometimes also called orosomucoid, accounts for 1-3 % of total plasma protein (about

40 kDa, 12 - 31 µM in plasma) and is an acute-phase protein which is synthesised in the liver (Colombo *et al.* 2006; Trainor 2007). Therefore, its concentration fluctuates with a person's health as well as it depends on age, gender and other circumstances (Blain *et al.* 1985; Bohnert & Gan 2013). Basic and neutral (lipophilic) drugs mainly bind to AGP (Brenner & Stevens 2010; Liu *et al.* 2014).

However, it was shown that the available drugs indicated for the central nervous system exhibit no general preference for high or low HSA binding (Kratochwil *et al.* 2002). In contrast, newly approved drugs often show high plasma protein binding (Zhang *et al.* 2012a; Liu *et al.* 2014). Furthermore, it was also reported for frequently prescribed drugs with indication for the central nervous system that binding to brain tissue does not hamper a drug's efficacy (Maurer *et al.* 2005). Plasma protein binding has also been found to be stereoselective (Brocks 2006; Shen *et al.* 2013).

Plasma protein binding therefore is not a criterion that needs to be optimised in drug candidates, but nevertheless remains a parameter that should be investigated in the process of drug development (Liu *et al.* 2014).

2 Objective

Alzheimer's disease is the most common form of dementia. As the population ages, more people will develop Alzheimer's disease and suffering and costs increase. To date, only short symptomatic relief is possible, but no causative treatment is available. Therefore, research on novel potential therapeutics is very important. Pharmacokinetic studies are a means to gain important information on the behaviour of a drug in the body. This can help improving the therapeutic agent and it provides a tool for lead compound selection for further processing to preclinical research.

The aim of the presented study is the analysis of pharmacokinetic properties of the D-enantiomeric peptide D3 and its derivatives. Of special interest is the question whether and to what extent the peptides are taken up across the blood brain barrier. D3 and its derivatives were developed as potential therapeutic agent for treatment of Alzheimer's disease, therefore access to the brain is considered a requirement for therapeutic activity. Moreover, due to the patients' age and often compromised state of health, the possibility of oral administration or availability of another easy route of administration is of high importance.

To analyse the pharmacokinetic properties of the chosen D-peptides, they were radioactively labelled and administered to mice via different routes of administration. After different durations of time specific organs were harvested and the presence of radioactive peptide was analysed. Furthermore, binding to plasma proteins was analysed as this could prevent the peptides from reaching the brain. From this data, pharmacokinetic parameters were calculated and compared.

Ideally, the peptides should be able to access the brain in considerable amounts. Additionally, a relatively long half-live and a high bioavailability especially upon oral administration represent favourable results.

3 Manuscripts

3.1 Preclinical pharmacokinetic studies of the tritium labelled D-enantiomeric peptide D3 developed for the treatment of Alzheimer´s disease

Nan Jiang, Leonie H.E. Leithold, Julia Post, Tamar Ziehm, Jörg Mauler, Lothar Gremer, Markus Cremer, Elena Schartmann, N. Jon Shah, Janine Kutzsche, Karl-Josef Langen, Jörg Breitkreutz, Dieter Willbold, Antje Willuweit

Journal: PloS One, published

Impact Factor (2013): 3.534

Contributions: 20 %; Experimental design of plasma protein binding experiments, performance and data analysis; contribution to development of pharmacokinetic data analysis; manuscript writing

PLOS | ONE

RESEARCH ARTICLE

Preclinical Pharmacokinetic Studies of the Tritium Labelled D-Enantiomeric Peptide D3 Developed for the Treatment of Alzheimer´s Disease

Nan Jiang[1], Leonie H. E. Leithold[1], Julia Post[1], Tamar Ziehm[1], Jörg Mauler[2], Lothar Gremer[1], Markus Cremer[3], Elena Schartmann[1], N. Jon Shah[2], Janine Kutzsche[1], Karl-Josef Langen[2,4], Jörg Breitkreutz[5], Dieter Willbold[1,6]*, Antje Willuweit[2]*

1 Structural Biochemistry, Institute of Complex Systems (ICS-6), Forschungszentrum Jülich GmbH, Jülich, Germany, **2** Medical Imaging Physics, Institute of Neuroscience and Medicine (INM-4), Forschungszentrum Jülich GmbH, Jülich, Germany, **3** Structural and functional organisation of the brain, Institute of Neuroscience and Medicine (INM-1), Forschungszentrum Jülich GmbH, Jülich, Germany, **4** Department of Nuclear Medicine, Universitätsklinikum der RWTH Aachen, Aachen, Germany, **5** Institute of Pharmaceutics and Biopharmaceutics, Heinrich-Heine-Universität Düsseldorf, Düsseldorf, Germany, **6** Institut für Physikalische Biologie, Heinrich-Heine-Universität Düsseldorf, Düsseldorf, Germany

* D.Willbold@fz-juelich.de (DW); A.Willuweit@fz-juelich.de (AW)

OPEN ACCESS

Citation: Jiang N, Leithold LHE, Post J, Ziehm T, Mauler J, Gremer L, et al. (2015) Preclinical Pharmacokinetic Studies of the Tritium Labelled D-Enantiomeric Peptide D3 Developed for the Treatment of Alzheimer´s Disease. PLoS ONE 10(6): e0128553. doi:10.1371/journal.pone.0128553

Academic Editor: Riqiang Yan, Cleveland Clinic Foundation, UNITED STATES

Received: March 4, 2015

Accepted: April 28, 2015

Published: June 5, 2015

Data Availability Statement: All relevant data are within the paper and its Supporting Information files.

Funding: DW was supported by grants from the "Portfolio Technology and Medicine" and the Helmholtz-Validierungsfonds of the Impuls und Vernetzungs-Fonds der Helmholtzgemeinschaft; KJL and DW were supported by the "Portfolio Drug Design" of the Impuls und Vernetzungs-Fonds der Helmholtzgemeinschaft (http://www.helmholtz.de/ueber_uns/impuls_und_vernetzungsfonds; no grant numbers available). The funders had no role in study

Abstract

Targeting toxic amyloid beta (Aβ) oligomers is currently a very attractive drug development strategy for treatment of Alzheimer´s disease. Using mirror-image phage display against Aβ1-42, we have previously identified the fully D-enantiomeric peptide D3, which is able to eliminate Aβ oligomers and has proven therapeutic potential in transgenic Alzheimer´s disease animal models. However, there is little information on the pharmacokinetic behaviour of D-enantiomeric peptides in general. Therefore, we conducted experiments with the tritium labelled D-peptide D3 (^{3}H-D3) in mice with different administration routes to study its distribution in liver, kidney, brain, plasma and gastrointestinal tract, as well as its bioavailability by i.p. and p.o. administration. In addition, we investigated the metabolic stability in liver microsomes, mouse plasma, brain, liver and kidney homogenates, and estimated the plasma protein binding. Based on its high stability and long biological half-life, our pharmacokinetic results support the therapeutic potential of D-peptides in general, with D3 being a new promising drug candidate for Alzheimer´s disease treatment.

Introduction

After the initial description by Alois Alzheimer in 1906 [1], Alzheimer's disease (AD), a progressive neurodegenerative disorder, has become nowadays the most common form (60–80%) of dementia [2]. According to the World Alzheimer Report 2014, nearly 36 million people worldwide are suffering from AD or related dementia. Even after years of intensive

design, data collection and analysis, decision to publish, or preparation of the manuscript.

Competing Interests: The authors have declared that no competing interests exist.

investigation and research, it is still an incurable disease [3]. Current treatments are only supportive against some of its symptoms. Clinical duration of AD varies from one to 25 years, typically eight to ten years [4].

Amyloid beta (Aβ) is produced by sequential cleavage of a type I integral transmembrane protein, called amyloid precursor protein (APP) by β- and γ-secretases. Variable lengths of Aβ isomers differing at the C-terminus are produced due to imprecise cleavage by γ-secretase [5, 6]. The most abundant isomers are Aβ1–40 (approximately 80–90%) and Aβ1–42 (approximately 5–10%). Aβ1–42 is more hydrophobic and fibrillogenic, and therefore the main component of Aβ plaques in the brain of AD patients [7]. It also aggregates readily into oligomers, which are considered to be the most toxic form of Aβ [8–10].

In recent years, many substances have been developed targeting Aβ production and clearance [11], including peptide-based drugs [12, 13]. In spite of the many advantages of peptide drugs, for example high specificity and low toxicity, their short half-life time *in vivo* due to rapid degradation by proteases, and low bioavailability by oral administration, restrict their clinical usage. In comparison to naturally occurring L-form peptides, peptides derived from partial D-amino acid substitutions or D-enantiomeric peptides, which are composed entirely of D-amino acids, have advantages over L-enantiomers. Because of the stereoisomeric selectivity of proteolytic enzymes they are less prone to proteolysis, therefore longer half-lives and higher bioavailability after oral administration are to be expected [14–16]. Furthermore, they are less or even not immunogenic at all [13].

The fully D-enantiomeric peptide D3, which was identified by mirror-image phage display [17, 18] for binding to Aβ (1–42), has been shown to have interesting properties. D3 inhibits Aβ fibril formation and eliminates Aβ-oligomers *in vitro*. *Ex vivo*, D3 has been shown to specifically bind to amyloid plaques in transgenic mice [19]. *In vivo*, D3 was able to reduce plaque load and inflammation markers in the brains of treated transgenic mice, as well as improve their cognition even after oral administration [20–23]. Here we investigate the pharmacokinetic properties of D3 in mice.

We present the first comprehensive preclinical pharmacokinetic study of a peptide consisting solely of D-enantiomeric amino acid residues in general and in particular for such a D-peptide developed for the treatment of Alzheimer's disease.

Materials and Methods

Materials

^{3}H-D3 (rprtr-(4,5-^{3}H-Leu)-hthrnr) and its L-form enantiomer ^{3}H-(L)-D3 (RPRTR-(4,5-^{3}H-Leu)-HTHRNR) were purchased from Quotient Bioresearch (Radiochemicals) Ltd. (Cardiff, United Kingdom) with 10–100 Ci/mmol, 1 mCi/ml and purity >95%.

All chemicals were supplied by Fluka Chemie AG (Buchs, Switzerland), Merck (Darmstadt, Germany), AppliChem (Darmstadt, Germany) and VWR (Darmstadt, Germany) in research grade. Micro-osmotic pumps (model 1007D) were purchased from Alzet DURECT Corporation, (Cupertino, CA, USA).

Animals

Male C57Bl/6 mice (Charles River, Sulzfeld Germany) with an average age of 13 weeks and body weight of 28.5 g were used in this study. For micro-osmotic pump i.p. implantation experiment, 19 months old mice were used with average body weight of 34 g. The mice were hosted in the animal facility of the Forschungszentrum Juelich under standard housing conditions with free access to food and water for at least 2 weeks before experiment. All animal experiments were approved by the Animal Protection Committee of the local government

(LANUV (Landesamt für Natur, Umwelt und Verbraucherschutz), North-Rhine-Westphalia, Germany, AZ84-02.04.2011. A359 and AZ84-02.04.2011. A356) according to the Deutsche Tierschutzgesetz). All sections of this study adhere to the ARRIVE Guidelines for reporting animal research [24]. A completed ARRIVE guidelines checklist was included in Supporting Information (S1 File).

Pharmacokinetic studies

Mice were administered with 100 μl radioactive working solution consisting of 5 μCi ^{3}H-D3 in 5 μl with 95 μl buffer (0.1 M phosphate buffer, pH 8) as a single bolus dose either i.v. (tail vein), i.p. or p.o. (gavaging). In order to achieve the desired total D3 concentration, non-radioactive D3 was added to a concentration of 1 mg/ml (i.v.) or 3 mg/ml (i.p. and p.o.). Doses were selected from previous tolerability studies and were not causing any adverse effects. I.v. injections and i.p micro-osmotic pump implantations were performed under anaesthesia with ketamine/medetomidine per i.p. administration. Antisedan was administered s.c. to reverse the anaesthesia directly after the intervention, which took about 10 min. Sampling times were chosen depending on the route of administration (i.p.: 10, 20, 30, 60, 120, 240, 360, 1440 and 2880 min.; p.o.: 10, 20, 30, 60, 120, 240, 360, 1080, 1440, 2880 and 4320 min.; i.v.: 3, 5, 10, 15, 30, 60, 240, 1440 and 2880 min.; 3 animals per time point). For i.p. micro-osmotic pump implantation, delivery dose of pumps was set to 5 μCi ^{3}H-D3 plus 0.3 mg non-radioactive D3 per 24 hours per mouse. Sampling times were 2, 4 and 6 days after implantation (3 mice per time point).

Upon sampling time, blood was drawn per heart puncture under isoflurane anaesthesia and heparinized plasma was isolated. A small piece of liver (approx. 0.2 g), the left kidney and the right brain hemisphere were sampled. To study the gastrointestinal absorption and elimination by p.o. administration, mice were fasted 18 hours before the experiment and their complete gastrointestinal tracts were prepared. Small intestine was dissected into 4 equal parts and marked from oral to aboral as 1 to 4, respectively. Organ samples were weighted and homogenized in homogenizer tubes (Precellys Ceramic Kit 1.4 mm, Precellys 24, Bertin technologies SAS, Montigny le Bretonneux, France) with 500 μl PBS. 10 ml scintillation cocktail (Ultima Gold XR, PerkinElmer, Waltham, Massachusetts, USA) was added to 100 μl of each organ homogenate or plasma (diluted 1:1 with PBS) and mixed well. Disintegrations per unit time (dpm) were obtained in triplicates with a liquid scintillation counter (Packard Tri-Carb 2100TR Liquid Scintillation Analyser, PerkinElmer, Waltham, MA, USA). Blank values of each sample were obtained by omitting radioactive substance following the same protocol.

Radioactivity counted in each sample was adjusted (subtraction of the blank value) and was expressed as percentage injected dose per gram tissue or millilitre plasma (%ID/g or %ID/ml), or as milligram of total D3 per gram tissue or millilitre plasma (mg/g or mg/ml).

Pharmacokinetic analysis

Pharmacokinetic parameters were calculated with non-compartmental analysis using Phoenix WinNonlin, version 6.3 (Pharsight Corp., St. Louis, USA). Mean D3 concentrations per time point were used to calculate the PK parameters (model type: plasma (200–202); calculation method: linear trapezoidal linear interpolation; dose options: "IV Bolus" for i.v. or "Extravascular" for i.p. and p.o. administration). The same model setting was used to estimate pharmacokinetic parameters of brain. For i.v. administration, plasma concentration at time zero (C0) was back extrapolated with a log-linear regression of the first two observed plasma concentrations, while brain C0 was set to be zero. For the i.p. and p.o. administrations, all concentrations at time zero were set to be zero.

The last three to five observed mean plasma concentrations were used to estimate the first order rate constant in the terminal elimination phase (Lambda_z) based on the largest adjusted square of the correlation coefficient (R^2) of the log-linear regression lines. The area under the curve (AUC) from C0 extrapolated to infinity ($AUC_{C0\text{-}inf}$) was calculated as the sum of $AUC_{C0\text{-}last}$+(Clast/Lambda_z), calculated from the last determined concentration derived by Lambda_z, and $AUC_{C0\text{-}last}$ representing the AUC from time point zero to the last observed concentration (Clast). Parameters that do not require Lambda_z were calculated for brain data: time of maximal observed concentration (Tmax), maximal observed concentration (Cmax), maximal observed concentration normalized to dose (Cmax/D), $AUC_{C0\text{-}last}$ and mean residence time from the time of dosing to the last time point ($MRT_{C0\text{-}last}$). Additional parameters requiring estimated Lambda_z were calculated for plasma data: Lambda_z, terminal half-life (HL_Lambda_z), $AUC_{C0\text{-}inf}$, terminal volume of distribution (Vz), plasma clearance (Cl), $MRT_{C0\text{-}inf}$ and volume of distribution at steady state (Vss). Absolute bioavailability of i.p. and p.o. administration was calculated with $AUC_{C0\text{-}inf}$ by: F(bioavailability) = [AUC(non-iv)*Dose (iv)]/[AUC(iv)*Dose(non-iv)]*100.

To minimize the time dependence of brain-plasma ratio by bolus dosing, brain-plasma ratio was calculated from the areas under the brain and plasma concentration curves in the terminal elimination phase starting from 4 hours to infinity ($brain\_AUC_{4h\text{-}inf}$/$plasma\_AUC_{4h\text{-}inf}$).

Plasma protein binding

Plasma protein binding was estimated by incubation of D3 with varying concentrations of protein using TRANSIL^{XL} binding kits (Sovicell GmbH, Leipzig, Germany). K_D values were determined by titrating a constant drug concentration against different concentrations of human serum albumin (HSA) and α_1-acid glycoprotein (AGP). Experiments were performed as recommended for the kit. To obtain the desired D3 stock solution of 80 μM, non-radioactively labelled D3 was dissolved in PBS and 5% ^{3}H-labelled D3 solution was added for detection purposes. A final concentration of 5 μM D3 was applied in the assay. After incubation and centrifugation 15 μl supernatant were taken and scintillation cocktail was added. This was done in triplicate. Radioactivity was then quantified using liquid scintillation counting. After measuring the disintegrations per minute (dpm) of the supernatant containing the unbound peptide, the D3 fraction bound to the titrated protein was calculated and plotted against the protein concentrations. The curves were fitted to the Michaelis Menten ligand binding equation (SigmaPlot 11.0, Systat Software, Inc., San Jose, California, USA) to obtain the K_D. Mean and relative standard error (%) of multiple measurements are given (AGP n = 3, HSA n = 2).

For bioavailability determination, the unbound fraction of D3 (f_u) was calculated using the equation below:

$$f_u = 100 * \frac{\frac{C_{D3}-K_D-C_{physiol}}{2} + \sqrt{K_D * C_{D3} + \left(\frac{C_{D3}-K_D-C_{physiol}}{2}\right)^2}}{C_{D3}} \quad (1)$$

For very low D3 concentrations in blood (C_{D3}), Eq (1) can be simplified by Eq (2), where the unbound fraction of D3 can be calculated independently of the applied D3 concentration. Since this is true for our *in vivo* experiments we used Eq (2) for the total free fraction of D3, combining the binding of D3 to HSA and AGP. For calculation of the overall unbound fraction according to Eq (2), physiological concentrations ($C_{physiol}$) of 0.65 mM HSA and 0.02 mM

AGP were assumed.

$$f_{u,total} = 100 * \frac{1}{1 + \frac{C_{physiolHSA}}{K_D HSA} + \frac{C_{physiolAGP}}{K_D AGP}} \quad (2)$$

Calibration curves and internal standard

Calibration curves were prepared by adding a corresponding ^{3}H-D3 dilution series with certain dpm range to plasma or organ homogenates in comparison to those diluted in PBS. The dpm ranges of each ^{3}H-D3 dilution series were set to cover the measured dpm ranges of each sample (for plasma 400–40000; for brain 100–1200; for liver 3000–15000; for kidney 40000–400000). Plasma and organ homogenates obtained from C57Bl/6 mice were prepared following the same procedure as outlined above.

No differences were found comparing the calibration curves of ^{3}H-D3 in organ homogenates or plasma to those in PBS. The measured dpm values of the internal standard with ^{3}H-D3 in PBS matched closely the expected ones.

Thin layer chromatography

In order to study the proteolytic stability of peptides in biological extracts, tritium labelled peptides were incubated with liver microsomes (pooled from mouse (CD-1), Sigma-Aldrich), freshly prepared mouse plasma or extracts of brain, liver and kidney at 37°C for different time periods (from 0 min to 2 days). 1 μCi (approx. 0.08–0.8 μg) radioactive labelled peptide was mixed with 1 μl microsomes stock solution, plasma or organ extracts, respectively (in great excess to peptide). Mixtures containing tritium-labelled peptides were applied onto HPTLC Silica Gel 60 plates (OMNILAB, Essen, Germany) for thin layer chromatography (TLC) with a mobile solvent (2-Butanol/Pyridine/Ammonia(28%)/Water(39/34/10/26)). After development, a phosphor imaging plate for ^{3}H-autoradiography (FUJIFILM, Tokyo, Japan) was exposed to the TLC plates for 3 days. Images were acquired with a BAS reader and AIDA software (Raytest, Freiburg, Germany). Retardation factor (Rf) of each substance was defined as the ratio of the migration distance of the centre of a separated spot to the migration distance of the solvent front.

Results

Proteolytic stability of D3 in comparison to its L-enantiomer

Before meaningful pharmacokinetic studies could be performed with ^{3}H-D3, it was essential to show that the D-peptide is stable under near *in vivo* conditions. First, we compared the stability of ^{3}H-D3 with its exact enantiomer, ^{3}H-(L)-D3 in plasma (Fig 1). ^{3}H-(L)-D3 shows significant degradation already after 60 min incubation in plasma as concluded by the appearance of additional bands as compared to the mixture at 0 min on the TLC plate after detection by autoradiography. In contrast, ^{3}H-D3 did not show any degradation products even after 2 d incubation in the same plasma preparation.

More importantly, ^{3}H-D3, was neither degraded after 2 h incubation in liver microsomes nor after 2 days incubation in homogenates of kidney, brain and liver as shown by TLC and detection by autoradiography (Fig 2). Microsomes were checked for proteolytic activity using L-peptide substrates.

Due to high but unspecific affinity of D3 and (L)-D3 to the TLC plate support material (glass), artefacts were observed at the starting points of the TLC as well as light smears

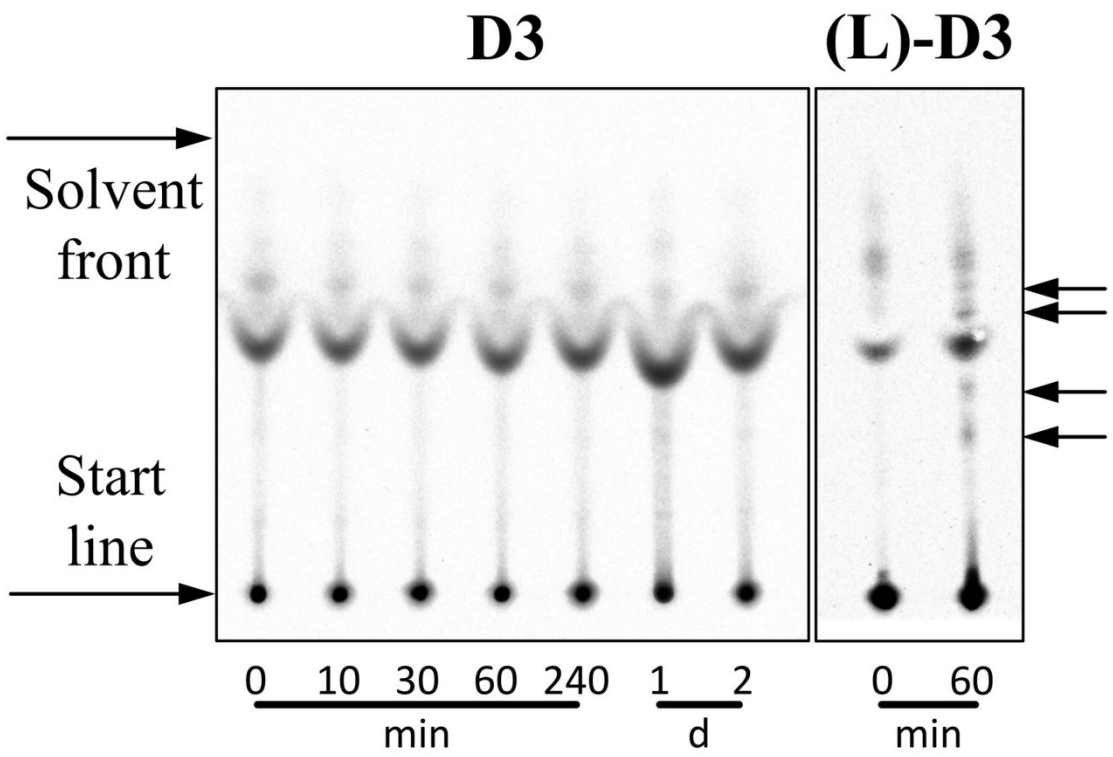

Fig 1. Autoradiogram demonstrating proteolytic stability of ^{3}H labelled peptides in plasma. ^{3}H-D3 was incubated with plasma for different times at 37°C and developed on TLC plates. For comparison, the exact enantiomer of D3, (L)-D3, was used in this stability assay. ^{3}H-(L)-D3 was incubated with plasma for 0 and 60 min at 37°C. Please note that free ^{3}H-(L)-D3 and free ^{3}H-D3 are perfect enantiomers to each other and because the TLC material is not chiral, both compounds show identical Rf values. Additional bands in the 0 min lanes of ^{3}H-(L)-D3 and ^{3}H-D3 that arise from binding and co-migration of ^{3}H-D3 and ^{3}H-(L)-D3 to plasma components do not necessarily have identical Rf values in the 0 min lanes of ^{3}H-(L)-D3 and ^{3}H-D3, because some of the plasma components are enantiomers themselves. Therefore, any effect of degradation will lead to extra additional bands as compared to the 0 min lane of the very same compound. Obvious proteolytic degradation can be observed for ^{3}H-(L)-D3 already after 60 min incubation with plasma leading to additionally appearing bands (black arrows) as compared to the 0 min lane ^{3}H-(L)-D3. Additionally appearing bands as compared to 0 min incubation are not observed for ^{3}H-D3 even after 2 days incubation.

doi:10.1371/journal.pone.0128553.g001

originating thereof. To prove that these compounds were not located in the layer of the TLC matrices, a control experiment was performed by placing a new TLC plate to a freshly developed plate to transfer only the ^{3}H-peptides within matrices, but not those on the glass surface support (Fig 3). Artefacts could thus be eliminated.

Pharmacokinetics

Time dependent distribution of D3 in organs and plasma after different administration routes was analysed using tritium labelled D3 (^{3}H-D3) as shown in Fig 4. The corresponding pharmacokinetic parameters calculated with non-compartmental analysis based on the absolute amount of administered D3 are shown in Tables 1 and 2.

After i.v. and i.p. administration, pharmacokinetic curves showed similar patterns with highest concentration of tritium per gram tissue found in kidney, followed by liver and plasma.

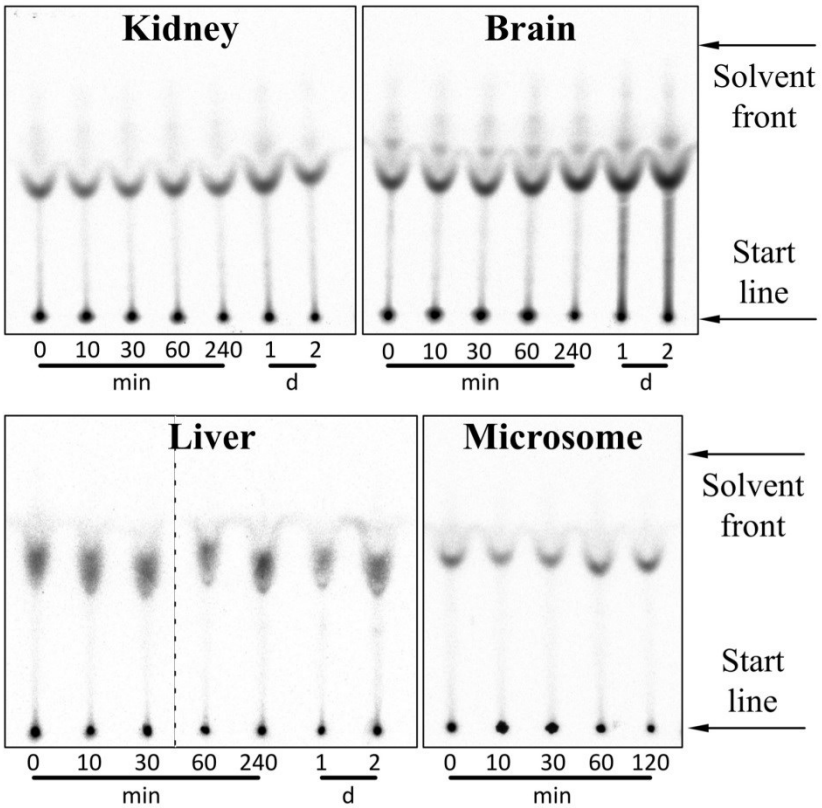

Fig 2. Autoradiogram demonstrating proteolytic stability of ^{3}H labelled peptides in liver microsomes and organ homogenates. ^{3}H-D3 was incubated with kidney, brain and liver homogenate for 0, 10, 30, 60, 240 min and 1, 2 days at 37°C and developed on TLC plates. For liver microsomes, the incubation time was 0, 10, 30, 60 and 120 min. Slight difference in Rf values of ^{3}H-D3 in liver homogenate might be due to incompletely homogenized liver tissues, which was not observed after incubation with liver microsomes. (Two autoradiograms of liver homogenate were presented in one image and separated through a dashed line.) No obvious proteolytic degradation of D3 can be observed in all the organ homogenates with up to two days' incubation.

doi:10.1371/journal.pone.0128553.g002

However, after oral administration ^{3}H-D3 concentrations measured in kidney and liver did not exceed concentrations in plasma (Fig 4). Plasma Cmax/D after i.v. administration reached 78 μg/ml/mg at Tmax 3 min (the first sampling time point), while after i.p. and p.o. administration plasma Cmax/D were 47 μg/ml/mg at 10 min and 1.5 μg/ml/mg at 240 min (Table 1). In brain, the Cmax/D and their corresponding Tmax values for i.v., i.p. and p.o. administration were 2.8, 2.2 and 1.3 μg/ml/mg at 3, 20 and 240 min, respectively (Table 2). However, after 4 hours concentrations in brain reached similar concentrations irrespectively of the administration route (Fig 4). Although plasma concentrations after p.o. administration appeared to be very low in comparison to i.v. and i.p. administration, comparable concentrations of ^{3}H-D3 were found in the brain resulting in high brain/plasma ratio after 4 h (Fig 5).

4 hours after a ^{3}H-D3 bolus dose, brain/plasma ratio of all administration routes reached a plateau between 0.7 and 1.0 (Fig 5). To minimize the time dependence of brain/plasma ratio, the absolute ratios were calculated from the area under the brain and plasma concentration

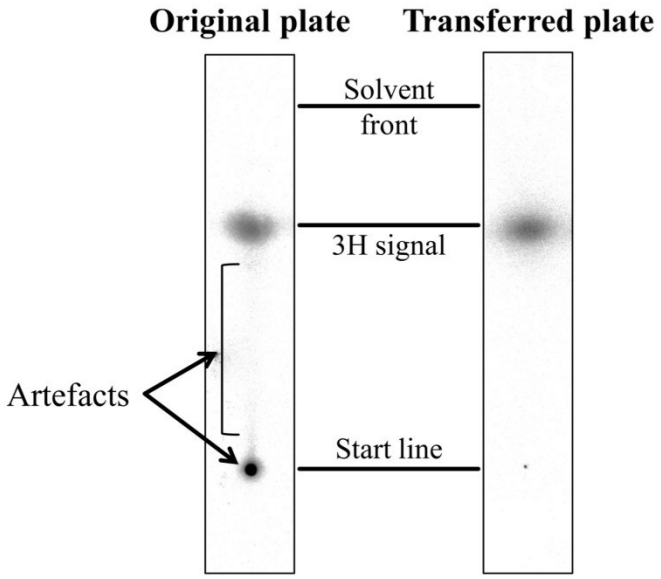

Fig 3. Plate-transfer of ^{3}H-D3 in TLC matrices. A control experiment was performed by placing a new TLC plate to a freshly developed plate to transfer only the ^{3}H-D3 within matrices. On the mirror image of the transferred plate, the ^{3}H signals at the start points as well as the smears were obviously reduced, while the intensity of separated ^{3}H-D3 did only change slightly. This result suggests that the observed artefacts arise from unspecific ^{3}H-D3 binding to the glass surface.

doi:10.1371/journal.pone.0128553.g003

curves from 4 hours to infinity (brain_$AUC_{4h\text{-}inf}$/plasma_$AUC_{4h\text{-}inf}$) with 1.07 for i.v., 0.69 for i.p., and 0.85 for p.o. administration.

After bolus administration, D3 showed relatively long elimination half-lives in plasma of 31.8 h, 41.2 h and 40.7 h after i.v., i.p. and p.o. administration, respectively. Plasma clearance was 0.12 ml/min after i.v. administration. Apparent volumes of distribution were different among i.v., i.p. and p.o. administration with 316, 444 and 684 ml, respectively (Table 1).

Absolute bioavailability was high with 92.2% after i.p. administration and 58.3% after p.o. administration (Table 1). When studying gastrointestinal distribution of D3 after p.o. administration (Fig 6), most of the radioactivity was found in the lower intestinal tract after 4 hours, which suggested that the majority of D3 did not enter the system circulation within 4 hours. Still, the AUC of D3 in brain after p.o. administration was comparable to those after i.p. and i. v. administration (Table 2).

We were also interested in answering the question, whether continuous dosing over several days using an i.p. implanted osmotic pump is showing specific effects in D3 distribution. We found linearly increasing D3 concentrations in plasma and all tested organs over 6 days (Fig 7). Although D3 highly accumulated in liver and kidney at day 6, the mice did not show any obvious signs of intoxication. The brain/plasma ratio increased with time from 0.53 at day 2 to 0.77 at day 6.

Plasma protein binding of D3

To estimate the free fraction of D3 in plasma *in vivo* ($f_{u,total}$), D3 was incubated with human serum albumin (HSA) and α_1-acid glycoprotein (AGP) in an *in vitro* assay (Fig 8). The plasma

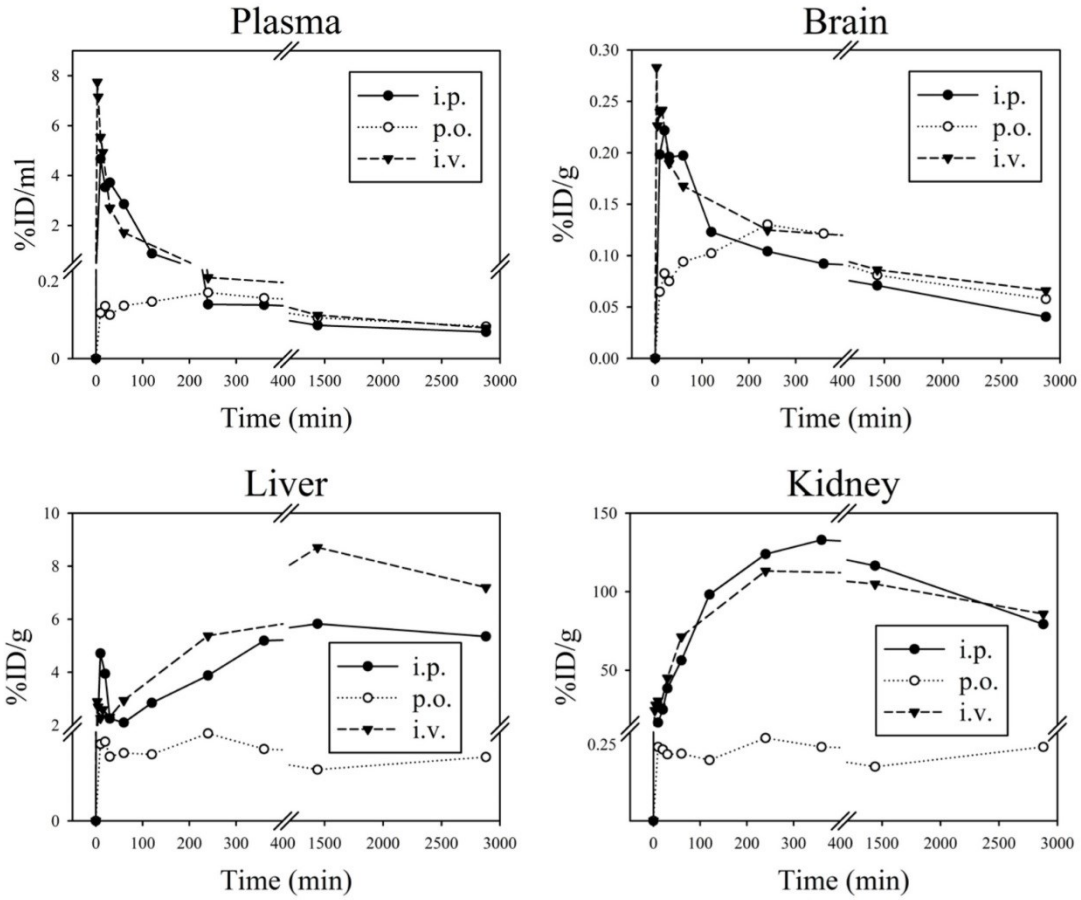

Fig 4. Mean pharmacokinetic profiles of ^{3}H-D3 in organs and plasma after i.p., p.o. and i.v. administration. ^{3}H-D3 (5 μCi) mixed with D3 in a total concentration of 3.5 mg/kg (i.v.) or 10.5 mg/kg (i.p. and p.o.) was applied per mouse. D3 concentrations are shown as percentage of injected dose per gram tissue or milliliter plasma (%ID/g or %ID/ml) dependent of time after administration. Mean values from 3 mice are shown.

doi:10.1371/journal.pone.0128553.g004

protein binding assay for AGP resulted in a K_D of 1.8 μM ± 7.9%. Assuming a D3 concentration in blood of 0.1 μM (C_{D3}, measured 4 h after i.p. injection) calculation of binding to AGP according to Eq (1) predicts a free fraction of 8.3%. For HSA, the K_D was above the detection limit of the kit (> 1.4 mM) indicating very low affinity of D3 to HSA. Nevertheless, calculation of the free fraction with an assumed K_D of 1.4 mM resulted in 68.3% free D3. Taken together, using Eq (2), the estimated free fraction of D3 in plasma was calculated to be approximately 8%.

Discussion

In the current study we have analysed the distribution of the D-enantiomeric peptide D3 after single intravenous, intraperitoneal and per oral administration, as well as continuous dosing

Table 1. Pharmacokinetic parameters for D3 from noncompartmental analysis of plasma.

Parameter	Units	i.v. (3.5 mg/kg)	i.p. (10.5 mg/kg)	p.o. (10.5 mg/kg)
Tmax	min	3	10	240
Cmax	µg/ml	7.75	14	0.45
Cmax/D	µg/ml/mg	77.5	46.7	1.48
$AUC_{C0\text{-}last}$	min*µg/ml	679	1763	1095
$MRT_{C0\text{-}last}$	min	547	527	1718
Lambda_z	1/min	0.00036	0.00028	0.00028
HL_Lambda_z	min	1907	2471	2439
$AUC_{C0\text{-}inf}$	min*µg/ml	869	2404	1521
$MRT_{C0\text{-}inf}$	min	1658	2104	3430
Vz	ml	317	445	684
Cl	ml/min	0.115	N.A.	N.A.
Vss	ml	190	N.A.	N.A.
Bioavailability	%	N.A.	92.2	58.3

N.A.: Parameters not applicable for this administration route. For abbreviations see methods section.

doi:10.1371/journal.pone.0128553.t001

via intraperitoneally implanted osmotic pumps. To the best of our knowledge, this is the first report of a comprehensive pharmacokinetic study of a peptide consisting solely of D-enantiomeric amino acid residues in rodents demonstrating excellent proteolytic stability, long plasma half-life and very high oral bioavailability.

D3 showed high proteolytic resistance exactly as it was shown *in vitro* previously with other all-D-peptides [14–16]. Thanks to this stability, metabolites can be neglected and the measured ^{3}H radioactivity represents the concentration of D3 after administration *in vivo*.

Estimated terminal plasma half-lives of D3 were between 32 and 41 h and were thus much higher than those reported for L-enantiomeric peptides which are typically only a few minutes [25]. Four hours after administration, irrespective of the administration routes, the temporal distribution of D3 in brain closely followed that in plasma resulting in brain/plasma ratios between 0.7 and 1.0 (Fig 5). While substances with a brain/plasma ratio larger than 0.3 are considered to have sufficient access to the central nervous system [26], our results suggest that D3 efficiently overcomes the blood-brain barrier.

Interestingly, by p.o. administration of D3, in spite of only a small rate of D3 being absorbed via the enteric tract, the bioavailability was 58.3% (Table 1), which is relatively high in comparison to that of L-peptide drugs, which were described to be less than 1% without delivery enhancement [27–30]. This finding can be explained by slow oral absorption of D3 and particularly long terminal half-life in plasma resulting in high AUC-values after p.o.

Table 2. Pharmacokinetic parameters for D3 from noncompartmental analysis of brain.

Parameter	Units	i.v. (3.5 mg/kg)	i.p. (10.5 mg/kg)	p.o. (10.5 mg/kg)
Tmax	min	3	20	240
Cmax	µg/g	0.283	0.665	0.390
Cmax/D	µg/g/mg	2.83	2.22	1.30
$AUC_{C0\text{-}last}$	min*µg/g	275	643	935
$MRT_{C0\text{-}last}$	min	1173	1108	1693

For abbreviations see methods section.

doi:10.1371/journal.pone.0128553.t002

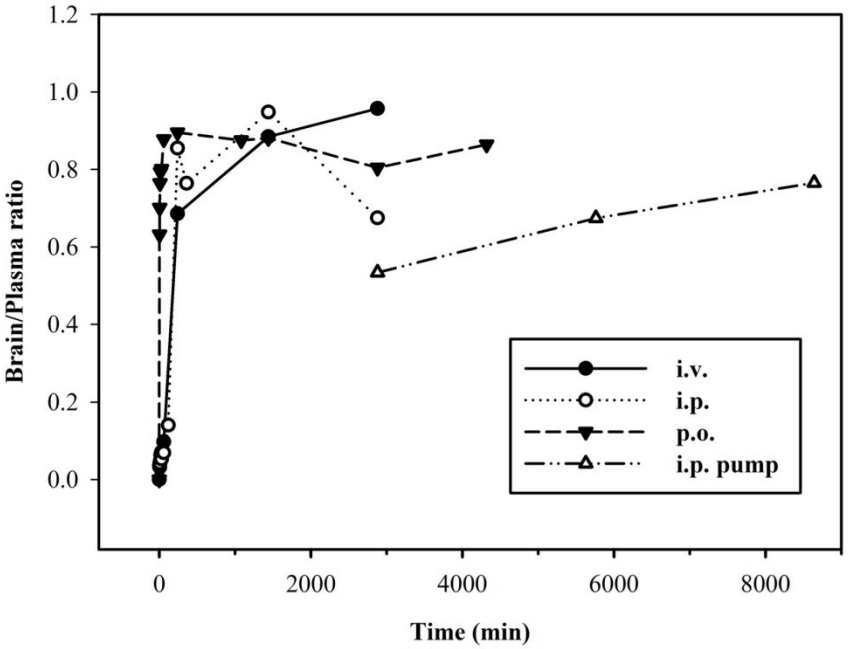

Fig 5. Temporal distribution of brain/plasma ratio of ^{3}H-D3 after different administration routes. Following bolus dose administration, low brain/plasma ratios were found at the starting time points. After 4 hours, the ratios reached relative high values and varied between 0.7–1.0. Upon i.p. pump implantation the ratio increased constantly with time.

doi:10.1371/journal.pone.0128553.g005

administration (Table 1). Low concentrations of D3 as found in kidney and liver after p.o. administration are desirable because this lowers the risk of possible intoxication of important organs. With absorption enhancers and a more suitable formulation of D3, even higher oral bioavailabilities seem to be feasible. Due to the observed high stability of D3 against proteolysis under biological conditions and its hydrophilic properties, elimination via biliary excretion (without re-absorption) and renal clearance in unchanged form could be expected.

Estimated volumes of distribution were 11.1 (i.v.), 15.6 (i.p.) and 24.0 l/kg (p.o.), respectively considering the body weight of the mice (28.5 g in average). The total body water in C57Bl/6 mice is approximately 0.6 l/kg [31], suggesting a distribution of D3 beyond the body fluid and some uptake in peripheral tissues.

Plasma volume of distribution at steady state was also high with 191 ml and 6.69 l/kg considering the body weight of the mice and the fraction of unbound D3 in plasma was predicted to be around 8%. High volume of distribution promotes low plasma clearance, which in our study was approximately between 0.12–0.19 ml/min observed in all routes of administration.

In summary, the current study demonstrates high proteolytic stability for the D-enantiomeric peptide D3. Furthermore, D3 enters the brain very efficiently and shows high oral bioavailability. The terminal half-life in mice after p.o. administration was approximately 41 hours with a brain/plasma ratio between 0.7 and 1.0, and a bioavailability of about 60%.

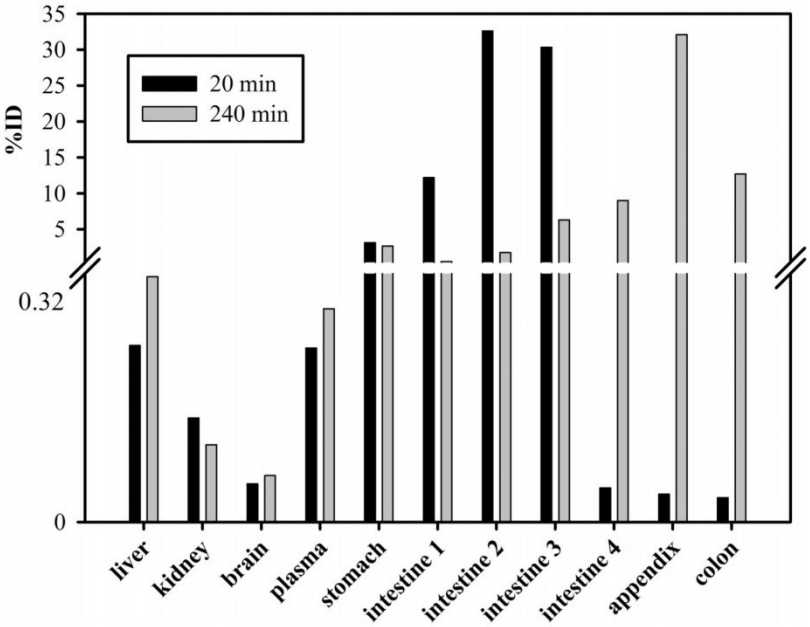

Fig 6. Distribution of ^{3}H-D3 after p.o. administration in organs and plasma. 20 min after gavaging of 100 µl, 5 µCi ^{3}H-D3 with a total D3 concentration of 10.5 mg/kg, most of the radioactivity was located in the middle of small intestine (intestine 2 and 3); 4 hours later, it spread to the lower intestinal tract. Of note is the high concentration of D3 observed in the appendix. At this time point, D3 could already be detected in feces. In comparison to the gastrointestinal tract, the amount of D3 in other organs or plasma after p.o. administration was very low.

doi:10.1371/journal.pone.0128553.g006

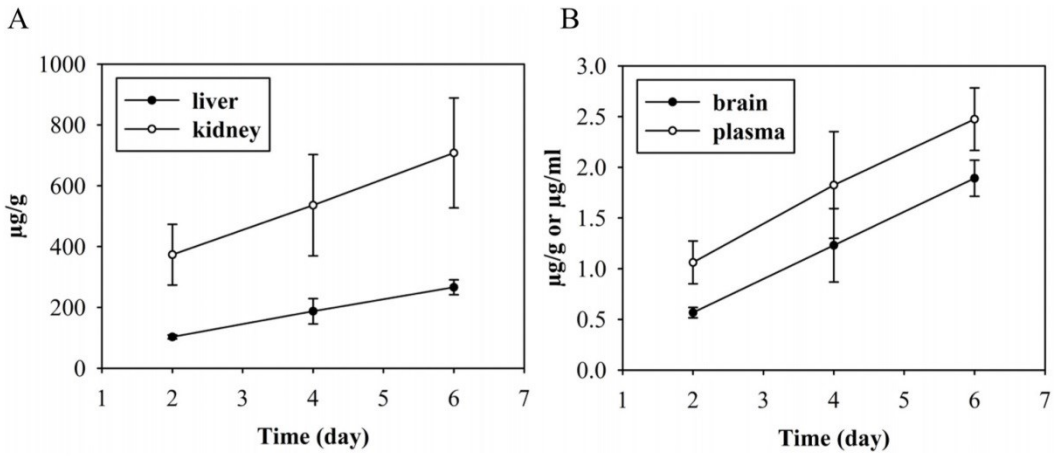

Fig 7. Concentration of ^{3}H-D3 in kidney, liver, brain and plasma administered via i.p. implanted osmotic pump. Alzet mini pumps with a delivery rate of 0.3 mg D3 (plus 5 µCi ^{3}H-D3) per 24 hours were implanted i.p. and organs were sampled after 2 to 6 days. Similar to bolus i.p. administration, more ^{3}H-D3 was found in kidney than in liver (A), whereas D3 concentrations in plasma and brain were considerably lower (B). The concentration of D3 was increasing linearly over time suggesting that the saturation concentration in the respective organs and plasma was not reached by 6 days of continuous dosing.

doi:10.1371/journal.pone.0128553.g007

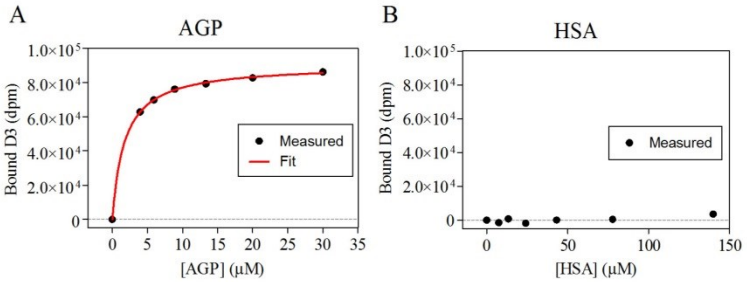

Fig 8. The bound D3 (in dpm) over the protein concentration as determined using the TRANSIL^{XL} kits. Each sample contained 5 μM D3 added to varying concentrations of AGP or HSA. (A) AGP fitted to the Michaelis Menten equation (red). (B) The binding of D3 to HSA was below the detection limit of the kit (K_D > 1.4 mM).

doi:10.1371/journal.pone.0128553.g008

In our previous studies, D3 already proved to be therapeutically active in reversing cognitive deficits and amyloid plaque load *in vivo*. Given its high oral bioavailability, suitably formulated D3 with multiple dosing might be a promising drug candidate against Alzheimer's disease.

Supporting Information

S1 File. ARRIVE Checklist. Completed "The ARRIVE Guidelines Checklist" for reporting animal data in this manuscript.
(DOCX)

Acknowledgments

We thank Michael Schöneck, Nicole Niemietz and Daniela Schumacher for excellent technical assistance and Dr. Dagmar Jürgens for discussions on the data analysis.

Author Contributions

Conceived and designed the experiments: NJ LL JB LG MC NJS JK KJL DW AW. Performed the experiments: NJ LL JP ES. Analyzed the data: NJ LL JP TZ JM DW AW. Wrote the paper: NJ LL NJS JB DW AW.

References

1. Berchtold NC, Cotman CW. Evolution in the conceptualization of dementia and Alzheimer's disease: Greco-Roman period to the 1960s. Neurobiology of aging. 1998; 19(3):173–89. Epub 1998/07/14. PMID: 9661992.
2. Fletcher LC, Burke KE, Caine PL, Rinne NL, Braniff CA, Davis HR, et al. Diagnosing Alzheimer's disease: are we any nearer to useful biomarker-based, non-invasive tests? GMS health technology assessment. 2013; 9:Doc01. Epub 2013/06/12. doi: 10.3205/hta000107 PMID: 23755087; PubMed Central PMCID: PMC3677379.
3. Nygaard HB. Current and emerging therapies for Alzheimer's disease. Clinical therapeutics. 2013; 35 (10):1480–9. Epub 2013/10/22. doi: 10.1016/j.clinthera.2013.09.009 PMID: 24139420.
4. TD B. Alzheimer Disease Overview. 1993. In: GeneReviews(R) [Internet]. University of Washington, Seattle.
5. Mikulca JA, Nguyen V, Gajdosik DA, Teklu SG, Giunta EA, Lessa EA, et al. Potential novel targets for Alzheimer pharmacotherapy: II. Update on secretase inhibitors and related approaches. Journal of clinical pharmacy and therapeutics. 2014; 39(1):25–37. Epub 2013/12/10. doi: 10.1111/jcpt.12112 PMID: 24313554.

6. Stockley JH, O'Neill C. Understanding BACE1: essential protease for amyloid-beta production in Alzheimer's disease. Cellular and molecular life sciences: CMLS. 2008; 65(20):3265–89. Epub 2008/08/13. doi: 10.1007/s00018-008-8271-3 PMID: 18695942.
7. Selkoe DJ. Alzheimer's disease: genes, proteins, and therapy. Physiological reviews. 2001; 81(2):741–66. Epub 2001/03/29. PMID: 11274343.
8. Bitan G, Kirkitadze MD, Lomakin A, Vollers SS, Benedek GB, Teplow DB. Amyloid beta-protein (Abeta) assembly: Abeta 40 and Abeta 42 oligomerize through distinct pathways. Proceedings of the National Academy of Sciences of the United States of America. 2003; 100(1):330–5. Epub 2002/12/31. doi: 10.1073/pnas.222681699 PMID: 12506200; PubMed Central PMCID: PMC140968.
9. Kayed R, Lasagna-Reeves CA. Molecular mechanisms of amyloid oligomers toxicity. Journal of Alzheimer's disease: JAD. 2013; 33 Suppl 1:S67–78. Epub 2012/04/26. doi: 10.3233/JAD-2012-129001 PMID: 22531422.
10. Tamaoka A. [The pathophysiology of Alzheimer's disease with special reference to "amyloid cascade hypothesis"]. Rinsho byori The Japanese journal of clinical pathology. 2013; 61(11):1060–9. Epub 2014/01/24. PMID: 24450113.
11. Schenk D, Basi GS, Pangalos MN. Treatment strategies targeting amyloid beta-protein. Cold Spring Harbor perspectives in medicine. 2012; 2(9):a006387. Epub 2012/09/07. doi: 10.1101/cshperspect.a006387 PMID: 22951439; PubMed Central PMCID: PMC3426815.
12. Citron M. Alzheimer's disease: strategies for disease modification. Nature reviews Drug discovery. 2010; 9(5):387–98. doi: 10.1038/nrd2896 PMID: 20431570
13. Sun N, Funke SA, Willbold D. A Survey of Peptides with Effective Therapeutic Potential in Alzheimer's Disease Rodent Models or in Human Clinical Studies. Mini-Rev Med Chem. 2012; 12(5):388–98. PMID: ISI:000303103600005.
14. Liu M, Li C, Pazgier M, Mao Y, Lv Y, Gu B, et al. D-peptide inhibitors of the p53-MDM2 interaction for targeted molecular therapy of malignant neoplasms. Proceedings of the National Academy of Sciences of the United States of America. 2010; 107(32):14321–6. Epub 2010/07/28. doi: 10.1073/pnas.1008930107 PMID: 20660730; PubMed Central PMCID: PMC2922601.
15. Zawadzke LE, Berg JM. A Racemic Protein. Journal of the American Chemical Society. 1992; 114 (10):4002–3. doi: 10.1021/Ja00036a073 PMID: ISI:A1992HT80100073.
16. Milton RCD, Milton SCF, Kent SBH. Total Chemical Synthesis of a D-Enzyme—the Enantiomers of Hiv-1 Protease Show Demonstration of Reciprocal Chiral Substrate-Specificity. Science. 1992; 256 (5062):1445–8. doi: 10.1126/science.1604320 PMID: ISI:A1992HX33700036.
17. Wiesehan K, Willbold D. Mirror-image phage display: aiming at the mirror. Chembiochem: a European journal of chemical biology. 2003; 4(9):811–5. Epub 2003/09/10. doi: 10.1002/cbic.200300570 PMID: 12964153.
18. Schumacher TN, Mayr LM, Minor DL Jr., Milhollen MA, Burgess MW, Kim PS. Identification of D-peptide ligands through mirror-image phage display. Science. 1996; 271(5257):1854–7. PMID: 8596952
19. van Groen T, Kadish I, Wiesehan K, Funke SA, Willbold D. In vitro and in vivo staining characteristics of small, fluorescent, Abeta42-binding D-enantiomeric peptides in transgenic AD mouse models. ChemMedChem. 2009; 4(2):276–82. Epub 2008/12/17. doi: 10.1002/cmdc.200800289 PMID: 19072935.
20. van Groen T, Kadish I, Funke SA, Bartnik D, Willbold D. Treatment with D3 removes amyloid deposits, reduces inflammation, and improves cognition in aged AbetaPP/PS1 double transgenic mice. J Alzheimers Dis. 2013; 34(3):609–20. Epub 2012/12/29. doi: 10.3233/JAD-121792 PMID: 23271316.
21. van Groen T, Kadish I, Funke A, Bartnik D, Willbold D. Treatment with Abeta42 binding D-amino acid peptides reduce amyloid deposition and inflammation in APP/PS1 double transgenic mice. Advances in protein chemistry and structural biology. 2012; 88:133–52. Epub 2012/07/21. doi: 10.1016/B978-0-12-398314-5.00005-2 PMID: 22814708.
22. Aileen Funke S, van Groen T, Kadish I, Bartnik D, Nagel-Steger L, Brener O, et al. Oral treatment with the d-enantiomeric peptide D3 improves the pathology and behavior of Alzheimer's Disease transgenic mice. ACS chemical neuroscience. 2010; 1(9):639–48. Epub 2010/09/15. doi: 10.1021/cn100057j PMID: 22778851; PubMed Central PMCID: PMC3368690.
23. van Groen T, Wiesehan K, Funke SA, Kadish I, Nagel-Steger L, Willbold D. Reduction of Alzheimer's disease amyloid plaque load in transgenic mice by D3, A D-enantiomeric peptide identified by mirror image phage display. ChemMedChem. 2008; 3(12):1848–52. Epub 2008/11/19. doi: 10.1002/cmdc.200800273 PMID: 19016284.
24. Kilkenny C, Browne WJ, Cuthill IC, Emerson M, Altman DG. Improving Bioscience Research Reporting: The ARRIVE Guidelines for Reporting Animal Research. Plos Biol. 2010; 8(6). ARTN e1000412 doi: 10.1371/journal.pbio.1000412 PMID: ISI:000279355600022.

25. Pollaro L, Heinis C. Strategies to prolong the plasma residence time of peptide drugs. MedChemComm. 2010; 1(5):319–24. doi: 10.1039/c0md00111b

26. Reichel A. The role of blood-brain barrier studies in the pharmaceutical industry. Current drug metabolism. 2006; 7(2):183–203. Epub 2006/02/14. PMID: 16472107.

27. Wong TW. Design of oral insulin delivery systems. Journal of drug targeting. 2010; 18(2):79–92. Epub 2009/12/09. doi: 10.3109/10611860903302815 PMID: 19968567.

28. Takagi H, Hiroi T, Hirose S, Yang L, Takaiwa F. Rice seed ER-derived protein body as an efficient delivery vehicle for oral tolerogenic peptides. Peptides. 2010; 31(8):1421–5. Epub 2010/05/12. doi: 10.1016/j.peptides.2010.04.032 PMID: 20457197.

29. Mason JM. Design and development of peptides and peptide mimetics as antagonists for therapeutic intervention. Future medicinal chemistry. 2010; 2(12):1813–22. Epub 2011/03/25. doi: 10.4155/fmc.10.259 PMID: 21428804.

30. Lalatsa A, Garrett NL, Ferrarelli T, Moger J, Schatzlein AG, Uchegbu IF. Delivery of Peptides to the Blood and Brain after Oral Uptake of Quaternary Ammonium Palmitoyl Glycol Chitosan Nanoparticles. Molecular pharmaceutics. 2012; 9(6):1764–74. doi: 10.1021/Mp300068j PMID: ISI:000304728700022.

31. Chapman ME, Hu L, Plato CF, Kohan DE. Bioimpedance spectroscopy for the estimation of body fluid volumes in mice. American journal of physiology Renal physiology. 2010; 299(1):F280–3. Epub 2010/05/14. doi: 10.1152/ajprenal.00113.2010 PMID: 20462974; PubMed Central PMCID: PMC2904176.

3.2 Pharmacokinetic properties of a novel D-peptide developed to be therapeutically active against toxic β-amyloid oligomers

Leonie H.E. Leithold, Nan Jiang, Julia Post, Tamar Ziehm, Elena Schartmann, Janine Kutzsche, N. Jon Shah, Jörg Breitkreutz, Karl-Josef Langen, Antje Willuweit, Dieter Willbold

Journal: Pharmaceutical Research, published online first

Impact Factor (2013): 3.952

Contributions: 60 %; Experimental design of plasma protein binding experiments, performance and data analysis; pharmacokinetic experiments and analysis; manuscript writing

Pharm Res
DOI 10.1007/s11095-015-1791-2

RESEARCH PAPER

Pharmacokinetic Properties of a Novel D-Peptide Developed to be Therapeutically Active Against Toxic β-Amyloid Oligomers

Leonie H. E. Leithold[1] • Nan Jiang[1] • Julia Post[1] • Tamar Ziehm[1] • Elena Schartmann[1] • Janine Kutzsche[1] • N. Jon Shah[2] • Jörg Breitkreutz[3] • Karl-Josef Langen[2,4] • Antje Willuweit[2] • Dieter Willbold[1,5]

Received: 29 April 2015 / Accepted: 8 September 2015

ABSTRACT

Purpose It has been shown that amyloid β (Aβ) oligomers play an important role in the pathology of Alzheimer's disease (AD). D3, a peptide consisting solely of D-enantiomeric amino acid residues, was developed to specifically eliminate Aβ oligomers and is therapeutically active in transgenic AD mice. D-peptides have several advantages over L-peptides, but little is known about their pharmacokinetic potential *in vivo*. Here, we analysed the pharmacokinetic properties of RD2, a rationally designed and potent D3 derivative.

Methods The pharmacokinetic analysis was performed using ^{3}H-RD2 after administration via several routes in mice. The time dependent amount of radiolabelled RD2 was measured in plasma and several organ homogenates by liquid scintillation counting. Furthermore, binding to plasma proteins was estimated.

Results RD2 penetrates into the brain, where it is thought to implement its therapeutic function. All administration routes result in a maximal brain concentration per dose (C_{max}/D) of 0.06 (µg/g)/(mg/kg) with brain/plasma ratios ranging between 0.7 and 1.0. RD2 shows a small elimination constant and a long terminal half-life in plasma of more than 2 days. It also exhibits high bioavailability after i.p., s.c. or p.o. administration.

Conclusions These excellent pharmacokinetic properties confirm that RD2 is a very promising drug candidate for AD.

KEY WORDS Alzheimer's disease · D-enantiomer · peptide · pharmacokinetics · preclinical

ABBREVIATIONS

%ID	Relative injected dose
AD	Alzheimer's disease
AGP	α_1-acid glycoprotein
AUC	Area under the concentration-time curve
AUMC	Area under the moment curve
Aβ	Amyloid β
C	Concentration
Cl	Clearance
D	Dose
dpm	Disintegrations per minute
F	Bioavailability
f_u	Unbound fraction
HSA	Human serum albumin
i.p.	Intraperitoneal
i.v.	Intravenous
inf	Infinity
MAT	Mean absorption time
MRT	Mean residence time
n.i.v.	Non-intravenous
p.o.	*per os*, oral delivery
r^2	Correlation coefficient
s.c.	Subcutaneous
$t_{1/2}$	Terminal half-life
TLC	Thin layer chromatography

✉ Antje Willuweit
a.willuweit@fz-juelich.de

✉ Dieter Willbold
d.willbold@fz-juelich.de

[1] Institute of Complex Systems, Structural Biochemistry (ICS-6), Forschungszentrum Jülich GmbH, 52425 Jülich, Germany

[2] Institute of Neuroscience and Medicine, Medical Imaging Physics (INM-4), Forschungszentrum Jülich GmbH, 52425 Jülich, Germany

[3] Institute of Pharmaceutics and Biopharmaceutics, Heinrich-Heine-Universität Düsseldorf, Düsseldorf, Germany

[4] Clinic for Nuclear Medicine, RWTH Aachen University, Aachen, Germany

[5] Institut für Physikalische Biologie, Heinrich-Heine-Universität Düsseldorf, Düsseldorf, Germany

Published online: 17 September 2015

V_{ss} Distribution volume in steady state
V_z Terminal distribution volume
λ_z Terminal elimination rate constant

INTRODUCTION

Alzheimer's disease (AD) is a progressive neurodegenerative disorder and the most common form of dementia. It currently affects about 24 million people worldwide, but to date, no curative treatment exists (1,2).

The pathology of Alzheimer's disease is mainly characterised by extracellular amyloid plaques and intracellular neurofibrillary tangles. Research suggests that amyloid β (Aβ) aggregation plays a major role in the development of AD (3,4), while Aβ oligomers are thought to be the most toxic species (5–7). Therefore, various strategies to develop AD therapeutics address Aβ, trying to reduce its formation, inhibit aggregation to fibrils or enhance its clearance (3,8). Several studies on potential therapeutics considered peptides, e.g. designed to prevent β-sheet conformation (3,9). However, peptide drugs show several disadvantages since they can be immunogenic, instable due to degradation by proteases and often show rapid clearance (10). Additionally, they generally have a very low oral bioavailability and short *in vivo* half-lives (11).

D-peptides, which are entirely composed of D-amino acids, are more protease resistant than L- peptides, due to the stereoisomeric selectivity of most proteolytic enzymes (12,13). As a result, system elimination is slower and they remain stable in the body for longer periods of time than L-peptides, thereby providing more time to be therapeutically active *in vivo* (14,15). This was for instance shown for all D-enantiomeric peptides in rat plasma and Rhesus monkey cerebrospinal fluid (16,17). In addition it has been shown that they are not immunogenic or at least significantly less than L-peptides (15).

Previously, a D-peptide, called D3, has been identified by mirror image phage display for binding to Aβ (18,19). It has been shown that it is able to improve both pathology and cognition of AD transgenic mice e.g. after 4 weeks of i.p. treatment or after 8 weeks of oral delivery (20–24).

RD2 is a derivative of D3 consisting of a rationally repositioned sequence, resulting in improved binding to Aβ oligomers (25) which are currently widely believed to be the most toxic Aβ species (26,27).

Here, we determined and compared the pharmacokinetic properties of RD2 in mice after intraperitoneal, subcutaneous, oral and intravenous delivery. This is the first systematic preclinical pharmacokinetic study of a D-enantiomeric peptide to such an extent.

METHODS

Peptides

RD2 (H-ptlhthnrrrrr-NH_2, all amino acid residues are D-enantiomers, 1.6 kDa) was purchased from Cambridge Peptides Ltd. (Birmingham, United Kingdom). The Lewis structure of RD2 can be found in Fig. 1.

Radioactively labelled peptides were purchased from Quotient Bioresearch (Radiochemicals) Ltd. (Cardiff, United Kingdom) containing 1 mCi/ml and were supplied as solution in water:ethanol (1:1). RD2 (H-pt-[4,5-^{3}H-D-Leu]-hthnrrrrr-NH_2) was supplied with > 95% purity, containing 124 Ci/mmol. Radioactively labelled L-peptide (H-RPRTR-[4,5-^{3}H-Leu]-HTHRNR-NH_2), 103 Ci/mmol was used as control for stability assessment.

Animals

C57BL/6 mice (Charles River Laboratories, Sulzfeld, Germany) were housed in groups of up to four mice in standard mouse individually ventilated cages with standard chip aspen bedding, a nestlet was provided as cage enrichment. Water as well as food were available *ad libitum*. Housing rooms were maintained on a 12/12 h light–dark cycle (7 a.m. – 7 p.m.), with a temperature of 22°C and approx. 54% humidity. All animal experiments were carried out in conformance with the German Protection of Animals Act (TierSchG §§ 7–9) and with permit of an Animal Protection Committee (AZ84-02.04.2011.A356).

Proteolytic Stability

To assess the stability of RD2 in different organs, thin layer chromatography (TLC) was applied using the ^{3}H-radioactively labelled RD2. As positive control an L-peptide was included. Blood and organs were sampled from C57BL/6 mice (25 g body weight). The animal was anaesthetised with isoflurane (Actavis Deutschland GmbH & Co. KG, Langenfeld, Germany) and blood was taken by cardiac puncture with a heparin containing needle before the mouse was sacrificed by cervical dislocation. Blood was spun down at 4°C and 1200 g for 15 min and plasma was taken. A small piece of liver (approx. 0.2 g), the left kidney and the right brain hemisphere were taken. All organ weights were measured and homogenised with 500 µl PBS per 0.2 g organ weight. Afterwards, organ homogenates were centrifuged at 4°C and 1200 g for 10 to 15 min and supernatant was taken off. 5 µl radioactively labelled peptide (5 µCi) were then added to 1 µl mouse plasma or organ homogenate supernatant. After different incubation times the reaction was stopped by adding 4 µl mobile solvent (2-butanol/pyridine/ammonia (28%)/water, 39/34/10/26 ml respectively) to each sample which was

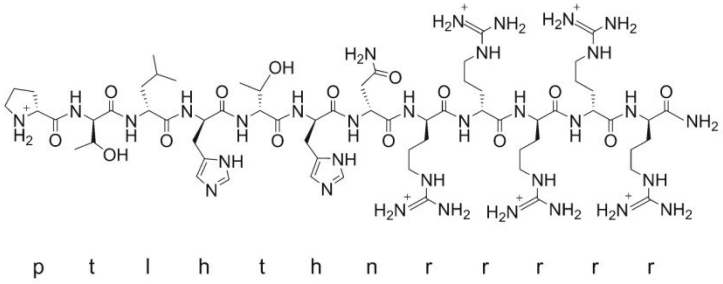

Fig. 1 Lewis structure and single letter amino acid code of the D-enantiomeric peptide RD2 (1.6 kDa).

then stored at - 20°C until further use. Samples were then dotted on the TLC membrane (HPTLC Silica 60 gel plates, Merck, Darmstadt, Germany) and placed into the solvent. Upon drying, start- and endpoint were marked with spots of ^{3}H-labelled peptide. For ^{3}H detection plates were then placed on phosphor imaging plates (Fujifilm, Tokyo, Japan) for 3 days and afterwards detected using a BAS reader with AIDA software (Raytest GmbH, Freiburg, Germany).

Pharmacokinetic Studies

Pharmacokinetic properties of ^{3}H-radioactively labelled RD2 in male C57BL/6 mice were studied using different administration routes. The applied amount contained 10 mg/kg for subcutaneous (s.c.) and intraperitoneal (i.p.) injection as well as oral gavage (p.o.) and 3.3 mg/kg for intravenous (i.v.) injection.

To achieve sufficiently high total concentrations of RD2, a combination of ^{3}H-labelled "hot" RD2 and non-radioactive "cold" RD2 was used, as detailed below. The working solution was prepared in phosphate buffer (0.1 M, pH 8.0). To achieve the appropriate dose each mouse received ^{3}H-labelled RD2 together with non-radioactive "cold" RD2, resulting in a total dose of 10 mg/kg (i.p., p.o., s.c.) or 3.3 mg/kg (i.v.) RD2 per mouse. I.v. injection was given into the tail vain under anaesthesia. Animals were sacrificed after different incubation times as detailed in Table I, for each time point three mice were used. Just before sampling time, the animal was anaesthetised with isoflurane and blood was taken by cardiac puncture with a heparin containing needle before the mouse was sacrificed by cervical dislocation. Blood was spun down at 4°C and 1200 g for 15 min and plasma was taken. A small piece of liver, the left kidney and the right brain hemisphere were taken at all time points. Additionally, at the late time points of 7 and 28 days, the spleen and the inguinal lymph nodes were harvested (spleen all administration routes, lymph nodes i.p. and i.v. only). 24 h after i.v. and i.p. administration urine and faeces were taken freshly (urine $n=2$ (i.p.) $n=4$ (i.v.), faeces $n=5$). All weights were measured and organs were homogenised with 500 µl PBS. After mixing with 10 ml scintillation cocktail (Ultima Gold XR, PerkinElmer, Waltham, MA, USA) ^{3}H-radioactivity was then measured in triplicate with a liquid scintillation analyser beta radiation counter (PerkinElmer, Waltham, MA, USA) in form of disintegrations per minute (dpm). The same procedure was performed on three animals without RD2 application, thereby creating blank reference values for each organ that were subtracted from all dpm values.

From the activity of the working solution subtracted with blank values and the organ weight the relative injected dose (%ID/g or %ID/ml) and total amount of RD2 (mg/g or mg/ml) per gram organ or millilitre plasma were calculated. All calculations of pharmacokinetic parameters were based on the total RD2 concentration. For calculation of pharmacokinetic parameters of the brain the radioactivity resulting from residual blood was subtracted assuming a plasma fraction of 1.5% in brain. The relative injected dose was only used for presentation purposes of the time dependent distribution in organs and plasma and displayed as mean and standard error of the mean where numbers are given.

Calculation of Pharmacokinetic Parameters

A non-compartmental analysis of pharmacokinetic parameters was performed. The area under the curve (AUC) as well as the area under the moment curve (AUMC) for the total RD2 concentrations was calculated (SigmaPlot 11.0, Systat Software, Inc., San José, CA, USA). The mean residence time (MRT) was calculated according to MRT = AUMC/AUC. The RD2 concentration at time zero was assumed to be zero for all applications except for plasma after i.v. delivery where it was back extrapolated from the first two observed concentrations in the semi-logarithmic time-concentration plot (SigmaPlot). The terminal elimination rate constant (λ_z) was obtained by logarithmic extrapolation based on the last observed concentrations starting from 2 days post administration (the correlation coefficient (r^2) was between 0.92 and 1.0 for all extrapolations). Parameters containing the suffix "0–28" were calculated from the measured data points while "0-inf" denotes values reaching into infinity being calculated based on λ_z. The AUC and AUMC reaching into infinity were

Table I Pharmacokinetic Experiments were Performed According to this Scheme

Administration method	Time points	RD2 dose
i.v.	3 min, 5 min, 10 min, 15 min, 30 min, 1 h, 4 h, 1 d, 2 d, 7 d, 28 d	3.3 mg/kg
i.p.	10 min, 20 min, 30 min, 1 h, 2 h, 4 h, 6 h, 1 d, 2 d, 7 d, 28 d	10 mg/kg
s.c.	10 min, 20 min, 30 min, 1 h, 2 h, 4 h, 6 h, 1 d, 2 d, 7 d, 28 d	10 mg/kg
p.o.	30 min, 1 h, 2 h, 4 h, 6 h, 8 h, 18 h, 1 d, 2 d, 3 d, 7 d, 28 d	10 mg/kg

Assessed durations post administration and concentrations of RD2 per route of administration are given. For each time point three mice were used

calculated by $AUC_{0-inf}=AUC_{0-28}+C_{28}/\lambda_z$ and $AUMC_{0-inf}=AUMC_{0-28}+(C_{28}*t_{28})/\lambda_z+C_{28}/\lambda_z^2$. The bioavailability (F) was calculated on the basis of the respective AUC according to $F=100*(D_{i.v.}*AUC_{n.i.v.})/(D_{n.i.v.}*AUC_{i.v.})$ with n.i.v. denoting the respective extravascular administration route. Parameters describing the terminal elimination phase were calculated based on λ_z: the terminal half-life ($t_{1/2}=\ln 2/\lambda_z$) and clearance ($Cl_{i.v.}=\lambda_z*V_z$), the terminal distribution volume ($V_z=D/(\lambda_z*AUC_{inf})$ (for n.i.v. Cl and V_z were calculated including the bioavailability: $Cl_{n.i.v.}=\lambda_z*V_z/F$ and $V_z=(D*F)/(\lambda_z*AUC_{inf})$) was calculated as well as the distribution volume in steady state ($V_{ss}=(D*AUMC)/AUC^2$).

The overall brain/plasma ratio was determined using the respective AUC_{0-28} whereas the brain/plasma ratio over time was calculated from the individual values of each time point, both with subtracted radioactivity from residual blood, assuming a plasma fraction of 1.5% in brain (28).

Plasma Protein Binding

Plasma protein binding was estimated by incubation of RD2 with varying concentrations of protein using TRANSIL^{XL} binding kits (Sovicell GmbH, Leipzig, Germany). K_D values were determined by titrating a constant drug concentration against different concentrations of human serum albumin (HSA) and α_1-acid glycoprotein (AGP). Experiments were performed as recommended for the kit. To obtain the desired RD2 stock solution of 80 µM, non-radioactively RD2 was dissolved in PBS and 5% ^{3}H-labelled RD2 solution was added for detection purposes. A final concentration of 5 µM RD2 was applied in the assay. After incubation and centrifugation 15 µl supernatant were taken and scintillation cocktail was added for detection using liquid scintillation counting. This was done in triplicate. After measuring the disintegrations per minute (dpm) of the supernatant containing the unbound RD2, the fraction bound to the titrated protein was calculated and plotted against the protein concentrations. The curves were fitted to the Michaelis Menten ligand binding equation (SigmaPlot) to obtain a K_D. Mean and relative standard error (%) of multiple measurements are given where applicable (AGP $n=2$).

For determination of the unbound fraction of RD2 (f_u) Eq. (1) was used:

$$f_u = 100*\frac{\frac{C_{RD2}-K_D-C_{physiol}}{2}+\sqrt{K_D*C_{RD2}+\left(\frac{C_{RD2}-K_D-C_{physiol}}{2}\right)^2}}{C_{RD2}} \quad (1)$$

For very low RD2 concentrations in blood (C_{RD2}), Eq. (1) can be simplified by Eq. (2), where the unbound fraction of RD2 can be calculated independently of the applied RD2 concentration. Since this is true for our *in vivo* experiments we used Eq. (2) for the total free fraction of RD2, combining the binding of RD2 to HSA and AGP. For calculation of the unbound fraction according to Eq. (2), physiological concentrations ($C_{physiol}$) of 0.65 mM HSA and 0.02 mM AGP were assumed.

$$f_{u,total} = 100*\frac{1}{1+\frac{C_{physiol,HSA}}{K_{D,HSA}}+\frac{C_{physiol,AGP}}{K_{D,AGP}}} \quad (2)$$

RESULTS

Proteolytic Stability of RD2

To confirm stability of ^{3}H-labelled RD2 in mouse plasma, thin layer chromatography (TLC) was performed after incubation of ^{3}H-RD2 with plasma for up to 1 day and detected via autoradiography. This experiment was essential to consider potential metabolites in later pharmacokinetic analyses. TLC results showed that RD2 remained stable in mouse plasma (Fig. 2) for at least 24 h while a comparable L-peptide was proteolytically degraded within 2 h as is deduced from the appearance of additional bands at that time (marked by arrows) in comparison to those present at 0 h. Similarly, the pattern of RD2 after incubation with organ homogenates did not change over time, indicating that no proteolytic degradation took place (Fig. 2). Of note, the peptides bind to different components of the plasma and organ samples resulting in different patterns and intensities for each peptide.

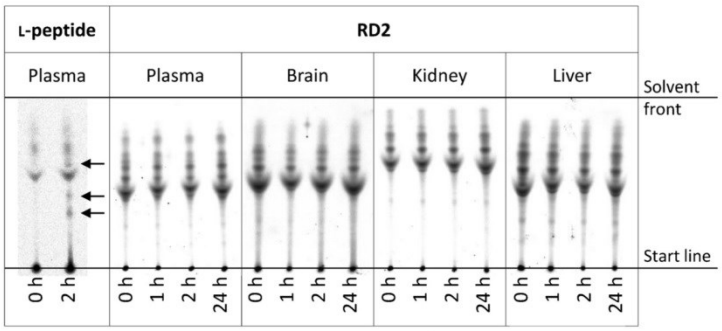

Fig. 2 Autoradiography of thin layer chromatogram demonstrating proteolytic stability of ^{3}H-labelled RD2 in mouse plasma, brain, kidney and liver. ^{3}H-RD2 was incubated at 37°C with mouse plasma for different durations and developed on TLC plates. For comparison, a very similar L-peptide was also incubated with mouse plasma. Multiple bands in the 0 h lanes arise from binding and co-migration of the ^{3}H-peptides with plasma and tissue components. Therefore, any effect of degradation will lead to extra additional bands as compared to the 0 h lane of the very same compound. Obvious proteolytic degradation can be observed for the ^{3}H-L-peptide already after 2 h of incubation with plasma leading to additionally appearing bands (*black arrows*) as compared to the 0 h lane. Additionally appearing bands as compared to 0 h incubation are not observed for ^{3}H-RD2 even after 24 h of incubation in plasma and tissue homogenates.

However, since the overall composition did not change with time, it can be concluded that RD2 was not subject to proteolytic degradation. The L-peptide showed appearance of additional bands after 2 h incubation, while the pattern of RD2 remained unchanged. Therefore, metabolites were considered negligible and the measured radioactivity was used to back calculate the total RD2 concentration.

Pharmacokinetic Properties

Pharmacokinetic analyses were performed using ^{3}H-labelled RD2 after i.v., i.p., s.c. or oral administration in mice. Graphs showing the relative injected dose per organ weight over time of the different administration routes can be found in Fig. 3.

Significant amounts of ^{3}H-RD2 were found in the analysed organs after i.v., i.p. or s.c. injection with highest concentrations present in kidney, followed by liver and plasma (Fig. 3). Oral administration resulted in very low ^{3}H-RD2 levels in liver, kidney and plasma. Interestingly, in brain ^{3}H-RD2 was found in amounts similar to the other administration routes. Exposure to all analysed organs was quite stable for a couple of days and declined gradually until 28 days after injection where it was still detectable in very low amounts.

Additionally, ^{3}H-RD2 amounts in urine and faeces were evaluated 24 h post i.p. and i.v. injection, showing only low doses in faeces (0.28±0.05 (i.p.) and 0.35±0.02%ID/g (i.v.), n=5). The amount of ^{3}H-RD2 in urine was higher, following i.p. administration it reached 2.3±0.09%ID/ml and 4.3±0.07%ID/ml upon i.v. administration (i.p. n=2; i.v. n=4). Furthermore, at 7 and 28 days post injection the presence of ^{3}H-RD2 in spleen and lymph nodes was determined, showing only low concentrations at 7 days (0.4 – 0.6±0.11%ID/g) decreasing with time (0.01 – 0.2±0.02%ID/g, except spleen i.v. 0.6 ±0.02%ID/g). Remarkably, upon oral application nearly no ^{3}H-RD2 was found in the spleen at 7 days post injection (0.04±0.004%ID/g).

Plasma Pharmacokinetic Parameters

A summary of all pharmacokinetic parameters in mouse plasma can be found in Table II, parameters were determined based on the back-calculated total RD2 concentration from measured radioactivity.

In contrast to the other administration routes, i.v. injection was performed with 3.3 mg/kg body weight. Results show low rate of terminal plasma clearance with Cl/F=1.68 ml/(kg*min) and a relatively long terminal half-life ($t_{1/2}$) of 59 h. Since the extrapolated part of the area under the curve (AUC) is small (≤1%) the AUC_{0-28} and $AUC_{0\text{-}inf}$ are very similar with $AUC_{0\text{-}inf}$=1.97 mg/ml*min.

Upon extravascular administration, absorption happened rapidly, as t_{max} was between 0.5 and 1 h, with oral administration showing the slowest absorption. The maximal observed concentration relative to the dose (C_{max}/D) was highest for i.v. administration (3.04 (µg/ml)/(mg/kg)), lower after i.p. and s.c. injection (0.79 and 0.98 (µg/ml)/(mg/kg)) and lowest following oral administration (0.09 (µg/ml)/(mg/kg)). The drug exposure in plasma, calculated as $AUC_{0\text{-}inf}$, showed the highest values after s.c. injection (5.42 mg/ml*min) and similar values upon i.p. and p.o. administration (4.57 and 4.54 mg/ml*min). The mean residence time (MRT), however, appeared to be comparable between all administration routes. The terminal half-life was about 60 h and independent of the administration route. The bioavailability (F) was similar for i.p. and p.o. administration (approx. 76%) and even higher upon s.c. injection (91%).

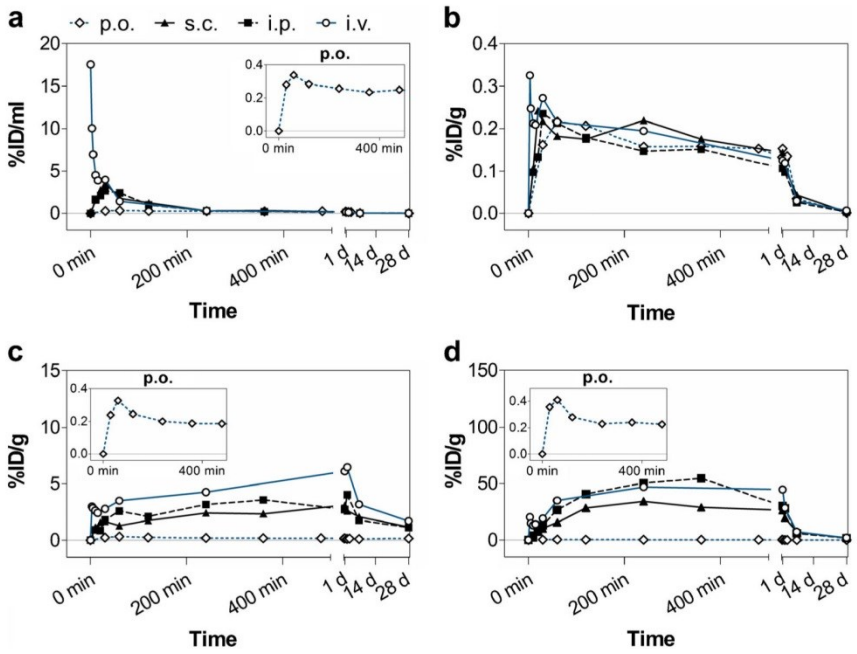

Fig. 3 Time dependent distribution of ^{3}H-RD2 in mouse organs and plasma after different administration routes. ^{3}H-RD2 was administered together with non-radioactive RD2 via different routes at 10 mg/kg or 3.3 mg/kg (i.v.). The concentration of ^{3}H-RD2 as expressed in relative injected dose per gram organ (%ID/g) or millilitre plasma (%ID/ml) is shown for plasma (**a**), brain (**b**), liver (**c**) and kidney (**d**) over time after different administration routes (p.o. *dashed line*, *open square*; s.c. *triangle*; i.p. *dashed line*, *closed square*; i.v. *open circle*). Graphs show the mean of three mice per time point.

Pharmacokinetic Parameters of RD2 in the Brain

Table III shows a summary of parameters calculated for the brain as this is expected to be the therapeutically relevant organ. The present study was performed in healthy C57BL/6 mice. The resulting pharmacokinetic parameters may be different in transgenic AD mouse models. Measured ^{3}H-RD2 radioactivity was used to extrapolate the total RD2 concentration in brain.

Brain/plasma ratios increased over time for i.v., i.p. and s.c. injection (Fig. 4), whereas for oral administration it remained relatively stable, all delivery routes almost reaching

Table II Determined Pharmacokinetic Parameters in Mouse Plasma for Different Administration Routes, based on Measured ^{3}H-RD2

Parameter	Units	i.v.	i.p.	s.c.	p.o.
Dose (D)	mg/kg	3.3	10	10	10
t_{max}	min	3	30	30	60
C_{max}/D	(μg/ml)/(mg/kg)	3.04	0.79	0.98	0.09
AUC_{0-28}	mg/ml*min	1.95	4.54	5.39	4.51
$AUMC_{0-28}$	min^2*mg/ml	9908	22,154	26,169	23,355
MRT_{0-28}	h	84.8	81.4	80.9	86.3
λ_z	min^{-1}	0.00020	0.00019	0.00019	0.00020
$t_{1/2}$	h	59	62	60	58
$AUC_{0\text{-}inf}$	mg/ml*min	1.97	4.57	5.42	4.54
$AUMC_{0\text{-}inf}$	min^2*mg/ml	10,794	23,676	27,514	24,748
$MRT_{0\text{-}inf}$	h	91.4	86.4	84.6	90.8
V_z	l/kg	8.57	8.95	8.77	8.46
Cl/F	ml/(min*kg)	1.68	2.19	1.84	2.20
V_{ss}	l/kg	9.20			
F_{AUC-28}	%		76.9	91.4	76.5
% AUC extrapolated	%	1.0	0.7	0.5	0.7

For comparison of absolute values, note that i.v. was administered at lower dose than extravascular administration. Clear fields are not applicable for this respective administration route. For abbreviations please refer to the abbreviation and methods sections

Table III Calculated Pharmacokinetic Parameters in Mouse Brains for Different Administration Routes, based on Measured ^{3}H-RD2

Parameter	Units	i.v.	i.p.	s.c.	p.o.
Dose (D)	mg/kg	3.3	10.0	10.0	10.0
t_{max}	min	3	30	20	60
C_{max}/D	(μg/g)/(mg/kg)	0.06	0.06	0.06	0.06
AUC_{0-28}	mg/g*min	1.48	3.37	4.51	4.49
$AUMC_{0-28}$	min^2*mg/g	11,408	22,656	31,419	27,039
MRT_{0-28}	h	128.4	111.9	116.1	100.3
λ_z	min^{-1}	0.00019	0.00019	0.00012	0.00016
$t_{1/2}$	h	60	61	94	73
F_{AUC-28}	%		75.2	100.6	100.1
Brain/plasma ratio AUC_{0-28}		0.8	0.7	0.8	1.0

Clear fields are not applicable for this respective administration route. For abbreviations please refer to the abbreviation and methods sections

1 at 2 days post administration. Overall, a good penetration of the brain was reached with AUC-based brain/plasma ratios reaching 0.8 (i.v. and s.c.) and even 1.0 (p.o.). Interestingly, C_{max}/D in brain was similar for all administration routes (0.06 (μg/ml)/(mg/kg)). The AUC_{0-28} was high for s.c. and p.o. administration (4.5 mg/g*min) but lower following i.p. injection (3.4 mg/g*min). After i.v. injection the AUC_{0-28} was found to be 1.5 mg/g*min but was performed using a lower dose of RD2. The terminal half-life of ^{3}H-RD2 in brain was very comparable to that in plasma, i.e. 61 h (i.v. and i.p.), 73 h (p.o.) and 94 h (s.c.). The bioavailability in the brain was calculated to be 75% for i.p. injection and 100% for s.c. and oral administration.

Plasma Protein Binding

For estimation of the *in vivo* free fraction of RD2 in blood ($f_{u,total}$), an *in vitro* assay was used, incubating RD2 with human serum albumin (HSA) and α_1-acid glycoprotein (AGP) (Fig. 5). For AGP this assay resulted in a K_D of 2.77 μM ± 9.97% (r^2 = 99.4%). The fraction unbound to AGP (f_u) was estimated using Eq. (1) under assumption of a RD2 blood concentration of 0.23 μM (C_{RD2}, measured 4 h after p.o. administration). This predicts a free fraction of 12.3%. For HSA, the K_D was above the detection limit of the kit (≥1.4 mM) indicating a very low affinity for HSA and leaving AGP as the main binding partner. Nevertheless, calculation of the RD2 fraction unbound to HSA with an assumed K_D of 1.4 mM results in 68.3% free RD2. Taken together, using Eq. (2), the estimated free fraction of RD2 in plasma was calculated to be approximately 11.5%.

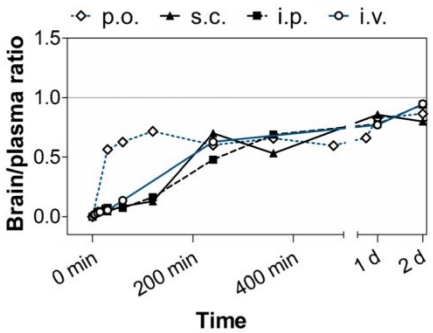

Fig. 4 Time dependent development of the brain/plasma ratio for different administration routes, corrected for residual blood in the brain.

DISCUSSION

In the present study we have analysed the pharmacokinetic properties of the D-peptide RD2, an improved derivative of D3, which has previously been shown to be therapeutically active *in vivo* (20,22).

It has previously been shown *in vivo* for rat plasma and rhesus monkey CSF that D-peptides are proteolytically more stable than their L-forms (16,17). Here, we also demonstrated that RD2 remains intact in mouse plasma and organ homogenates for at least 24 h. Thus, we considered metabolites negligible and used the measured ^{3}H-radioactivity to calculate the RD2 concentrations *in vivo*. Nevertheless, it needs to be clearly stated that all obtained pharmacokinetic values are based on the assumption that the measured radioactivity represents the non-metabolised RD2. Although we have shown that RD2 is stable for at least 24 h in plasma and tissue homogenates, we cannot exclude for later time points partial conversion of RD2 into metabolites that may or may not have reduced therapeutic activities. However, because we did not see any RD2 metabolism at 24 h, there was no reason to expect significant metabolism at 48 h or even 7 days. Furthermore, incubation in organ homogenates or plasma beyond 24 h appeared not to be meaningful because after longer incubation times enzymes

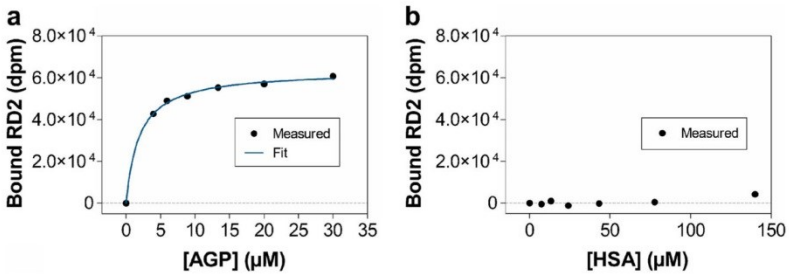

Fig. 5 Plasma protein binding of RD2. Bound ^{3}H-RD2 (in dpm) dependent on AGP (**a**) and HSA (**b**) concentration (*dots*). For binding of RD2 to AGP the fit according to the Michaelis Menten binding equation (*line*) is shown, indicating an almost perfect fit ($r^2 = 99.4\%$, **a**). Binding of RD2 to HSA was below the detection limit of the applied kit ($K_D \geq 1.4$ mM).

in those biological samples will have digested themselves leading to artefacts.

In the present study non-compartmental analysis was performed because a simplistic analysis of the data at hand is possible without making assumptions regarding the number of compartments as is necessary for other analyses such as compartmental or physiologically based models. We quantified RD2 in plasma and brain by measuring the radioactivity and assumed based on the 24 h stability data in plasma and organ homogenates that the measured radioactivity parallels RD2 concentration. Any minor metabolite would influence a more complex model, e.g. a minimal physiologically based model, to produce inaccurate data. However, non-compartmental analysis assumes linear kinetics and may therefore not be the optimal model for pharmacokinetic analysis of RD2. This may result in over- or under-estimation of certain values. Nevertheless, non-compartmental analysis is often used to give an indication of the pharmacokinetic properties of a candidate. Therefore, the more simple non-compartmental analysis was used to avoid additional over-interpretation of our data towards the pharmacokinetic properties of RD2.

Summarised, the pharmacokinetic results yielded a low terminal plasma clearance (Cl/F = 1.68 ml/(min*kg)) of RD2 resulting in long terminal half-lives of about 60 h upon all assessed administration routes. Since L-peptides are typically cleared from the blood relatively fast after administration, often within minutes, this long half-life represents a major advantage of RD2 since it provides more time to reach the target tissue and to be therapeutically active (10,29). The plasma bioavailability was exceptionally high following extravascular administration, with 77% upon intraperitoneal and oral administration and 91% after subcutaneous injection. In comparison to other peptide drugs especially the bioavailability upon oral application is very high (11,30).

It is noteworthy that irrespective of the administration route similar concentrations of RD2 reached the brain where it is thought to be therapeutically active. Irrespective of the administration route an overall brain/plasma ratio of 1 was reached. This indicates sufficient transport of RD2 into the target organ.

RD2 levels found in urine at 24 h post injection agree with the relatively high values obtained at the 24 h time point in the kidney. In general, values are higher upon i.v. injection than those obtained following i.p. administration. Hence, even 1 day after dosing the kidney still seems to be a major excretion route, illustrated also by the high RD2 concentrations observed in the kidney for at least 2 days. Additionally, excretion of RD2 also appears to take place via faeces although rather low doses of RD2 are measured at 24 h post i.v. or i.p. administration, indicating that this excretion pathway is not the dominating one for these administration routes. Furthermore, measurements of RD2 in spleen and inguinal lymph nodes indicate that after 28 days post administration only very low amounts of RD2 remain in the lymphatic system.

Prediction of plasma protein binding based on binding to HSA and AGP suggested a plasma free fraction of about 12%, which is also a very favourable property of RD2 as potential AD drug candidate. It has been reported that only the minority of the examined drugs developed for the central nervous system exhibit free plasma fractions above 10% (31).

Here, we compare RD2 distribution after different administration routes as well as the predicted plasma protein binding. In this pharmacokinetic study we were able to demonstrate high stability, long plasma half-life of several days and favourable oral and subcutaneous bioavailability of this all D-enantiomeric peptide in mice.

CONCLUSION

Taken together, the current study demonstrates favourable pharmacokinetic properties of the D-enantiomeric peptide RD2. Based on the long terminal half-life, high oral bioavailability and drug exposure to the brain it can be concluded, that D-peptides in general may be very well suited as drug candidates. Particularly, providing therapeutic efficiency

in vivo, RD2 may be a very promising candidate for the treatment of Alzheimer's disease.

ACKNOWLEDGMENTS AND DISCLOSURES

We thank Daniela Schumacher, Elias Bissong and Nicole Niemietz for the excellent technical assistance. Additionally, we thank Jörg Mauler for helping with the data analysis. D.W. was supported by grants from the "Portfolio Technology and Medicine" and the Helmholtz-Validierungsfonds of the Impuls und Vernetzungs-Fonds der Helmholtzgemeinschaft; K.J.L. and D.W. were supported by the "Portfolio Drug Research" of the Impuls und Vernetzungs-Fonds der Helmholtzgemeinschaft. The authors declare that they have no conflict of interest.

REFERENCES

1. Reitz C, Mayeux R. Alzheimer disease: epidemiology, diagnostic criteria, risk factors and biomarkers. Biochem Pharmacol. 2014;88(4):640–51.
2. Alzheimer's Association. 2014 Alzheimer's disease facts and figures. Alzheimers Dement. 2014;10(2):e47–92.
3. Soto C. Plaque busters: strategies to inhibit amyloid formation in Alzheimer's disease. Mol Med Today. 1999;5(8):343–50.
4. Hardy JA, Higgins GA. Alzheimer's disease: the amyloid cascade hypothesis. Science. 1992;256(5054):184–5.
5. Benilova I, Karran E, De Strooper B. The toxic a beta oligomer and Alzheimer's disease: an emperor in need of clothes. Nat Neurosci. 2012;15(3):349–57.
6. DaRocha-Souto B, Scotton TC, Coma M, Serrano-Pozo A, Hashimoto T, Serenó L, *et al.* Brain oligomeric beta-amyloid but not total amyloid plaque burden correlates with neuronal loss and astrocyte inflammatory response in amyloid precursor protein/tau transgenic mice. J Neuropathol Exp Neurol. 2011;70(5):360–76.
7. Decker H, Lo KY, Unger SM, Ferreira ST, Silverman MA. Amyloid-beta peptide oligomers disrupt axonal transport through an NMDA receptor-dependent mechanism that is mediated by glycogen synthase kinase 3 beta in primary cultured hippocampal neurons. J Neurosci. 2010;30(27):9166–71.
8. Hardy J, Selkoe DJ. The amyloid hypothesis of Alzheimer's disease: progress and problems on the road to therapeutics. Science. 2002;297(5580):353–6.
9. Sun N, Funke SA, Willbold D. A survey of peptides with effective therapeutic potential in Alzheimer's disease rodent models or in human clinical studies. Mini Rev Med Chem. 2012;12(5):388–98.
10. Sato AK, Viswanathan M, Kent RB, Wood CR. Therapeutic peptides: technological advances driving peptides into development. Curr Opin Biotechnol. 2006;17(6):638–42.
11. Pauletti GM, Gangwar S, Siahaan TJ, Aubé J, Borchardt RT. Improvement of oral peptide bioavailability: peptidomimetics and prodrug strategies. Adv Drug Deliv Rev. 1997;27(2–3):235–56.
12. van Regenmortel MHV, Muller S. D-peptides as immunogens and diagnostic reagents. Curr Opin Biotechnol. 1998;9(4):377–82.
13. Soto C, Kindy MS, Baumann M, Frangione B. Inhibition of Alzheimer's amyloidosis by peptides that prevent beta-sheet conformation. Biochem Biophys Res Commun. 1996;226(3):672–80.
14. Sela M, Zisman E. Different roles of D-amino acids in immune phenomena. FASEB J. 1997;11(6):449–56.
15. Dintzis HM, Symer DE, Dintzis RZ, Zawadzke LE, Berg JM. A comparison of the immunogenicity of a pair of enantiomeric proteins. Proteins Struct Funct Genet. 1993;16(3):306–8.
16. Findeis MA, Musso GM, Arico-Muendel CC, Benjamin HW, Hundal AM, Lee JJ, *et al.* Modified-peptide inhibitors of amyloid beta-peptide polymerization. Biochemistry. 1999;38(21):6791–800.
17. Poduslo JF, Curran GL, Kumar A, Frangione B, Soto C. beta-sheet breaker peptide inhibitor of Alzheimer's amyloidogenesis with increased blood–brain barrier permeability and resistance to proteolytic degradation in plasma. J Neurobiol. 1999;39(3):371–82.
18. Schumacher TNM, Mayr LM, Minor DL, Milhollen MA, Burgess MW, Kim PS. Identification of D-peptide ligands through mirror-image phage display. Science. 1996;271(5257):1854–7.
19. Wiesehan K, Willbold D. Mirror-image phage display: aiming at the mirror. Chembiochem. 2003;4(9):811–5.
20. Funke SA, van Groen T, Kadish I, Bartnik D, Nagel-Steger L, Brener O, *et al.* Oral treatment with the D-enantiomeric peptide D3 improves the pathology and behavior of Alzheimer's disease transgenic mice. ACS Chem Neurosci. 2010;1(9):639–48.
21. van Groen T, Kadish I, Funke A, Bartnik D, Willbold D. Treatment with a beta 42 binding D-amino acid peptides reduce amyloid deposition and inflammation in APP/PS1 double transgenic mice. Adv Protein Chem Struct Biol. 2012;88:133–52.
22. van Groen T, Wiesehan K, Funke SA, Kadish I, Nagel-Steger L, Willbold D. Reduction of Alzheimer's disease amyloid plaque load in transgenic mice by D3, a D-enantiomeric peptide identified by mirror image phage display. ChemMedChem. 2008;3(12):1848–52.
23. van Groen T, Kadish I, Wiesehan K, Funke SA, Willbold D. In vitro and in vivo staining characteristics of small, fluorescent, Aβ42-binding D-enantiomeric peptides in transgenic AD mouse models. ChemMedChem. 2009;4(2):276–82.
24. van Groen T, Kadish I, Funke SA, Bartnik D, Willbold D. Treatment with D3 removes amyloid deposits, reduces inflammation, and improves cognition in aged AbetaPP/PS1 double transgenic mice. J Alzheimers Dis. 2013;34(3):609–20.
25. Olubiyi OO, Frenzel D, Bartnik D, Glück JM, Brener O, Nagel-Steger L, *et al.* Amyloid aggregation inhibitory mechanism of arginine-rich D-peptides. Curr Med Chem. 2014;21(12):1448–57.
26. Larson ME, Lesne SE. Soluble Abeta oligomer production and toxicity. J Neurochem. 2012;120 Suppl 1:125–39.
27. Ferreira ST, Klein WL. The Abeta oligomer hypothesis for synapse failure and memory loss in Alzheimer's disease. Neurobiol Learn Mem. 2011;96(4):529–43.
28. Brown RP, Delp MD, Lindstedt SL, Rhomberg LR, Beliles RP. Physiological parameter values for physiologically based pharmacokinetic models. Toxicol Ind Health. 1997;13(4):407–84.
29. Pollaro L, Heinis C. Strategies to prolong the plasma residence time of peptide drugs. Med Chem Commun. 2010;1(5):319–24.
30. Renukuntla J, Vadlapudi AD, Patel A, Boddu SH, Mitra AK. Approaches for enhancing oral bioavailability of peptides and proteins. Int J Pharm. 2013;447(1–2):75–93.
31. Kratochwil NA, Huber W, Muller F, Kansy M, Gerber PR. Predicting plasma protein binding of drugs: a new approach. Biochem Pharmacol. 2002;64(9):1355–74.

3.3 Pharmacokinetic properties of tandem D-peptides designed for treatment of Alzheimer's disease

Leonie H.E. Leithold, Nan Jiang, Julia Post, Nicole Niemietz, Elena Schartmann, Tamar Ziehm, Janine Kutzsche, N. Jon Shah, Jörg Breitkreutz, Karl-Josef Langen, Antje Willuweit, Dieter Willbold

Journal: European Journal of Pharmaceutical Sciences, submitted

Impact Factor (2013): 3.005

Contributions: 45 %; Experimental design of plasma protein binding experiments, performance and data analysis; pharmacokinetic experiments and analysis; manuscript writing

Pharmacokinetic properties of tandem D-peptides designed for treatment of Alzheimer's disease

Leonie H.E. Leithold[a*] and Nan Jiang[a*], Julia Post[a], Nicole Niemietz[b], Elena Schartmann[a], Tamar Ziehm[a], Janine Kutzsche[a], N. Jon Shah[b,c], Jörg Breitkreutz[d], Karl-Josef Langen[b,e], Antje Willuweit[b], Dieter Willbold[a,f]

Affiliations:

[a]Institute of Complex Systems, Structural Biochemistry, Forschungszentrum Jülich GmbH, 52425 Jülich, Germany, e-mail addresses: l.hofmann@fz-juelich.de, n.jiang@fz-juelich.de, j.post@fz-juelich.de, e.schartmann@fz-juelich.de, t.ziehm@fz-juelich.de, j.kutzsche@fz-juelich.de, d.willbold@fz-juelich.de

[c]Department of Neurology, Universitätsklinikum der RWTH Aachen, 52074 Aachen, Germany

[d]Institute of Pharmaceutics and Biopharmaceutics, Heinrich-Heine-Universität Düsseldorf, 40225 Düsseldorf, Germany, joerg.breitkreutz@uni-duesseldorf.de

[e]Department of Nuclear Medicine, Universitätsklinikum der RWTH Aachen, 52074 Aachen, Germany

[f]Institut für Physikalische Biologie, Heinrich-Heine-Universität Düsseldorf, 40225 Düsseldorf, Germany

*authors contributed equally

Corresponding authors:

Dieter Willbold

Institute of Complex Systems

Structural Biochemistry (ICS-6)

Forschungszentrum Jülich GmbH

52425 Jülich

Germany

Phone: +49 2461 61 2100

Fax: +49 2461 61 2023

d.willbold@fz-juelich.de

Antje Willuweit

Institute of Neuroscience and Medicine

Medical Imaging Physics (INM-4)

Forschungszentrum Jülich GmbH

52425 Jülich

Germany

Phone: +49 2461 61 96358

Fax: +49 2461 61 2302

a.willuweit@fz-juelich.de

Abstract

Peptides are considered as promising substances for development of drug candidates. However, they frequently exhibit severe disadvantages such as instability and unfavourable pharmacokinetic properties. Many peptides are rapidly cleared from the organism and oral bioavailabilities as well as *in vivo* half-lives often remain low. Peptides consisting solely of d-enantiomeric amino acid residues combine promising therapeutic properties with high proteolytic stability and enhanced pharmacokinetic parameters. Recently, we have shown that D3 and RD2 have highly advantageous pharmacokinetic properties. Especially D3 has already proven promising properties suitable for treatment of Alzheimer's disease. Here, we analyse the pharmacokinetic profiles of D3D3 and RD2D3, which are head-to-tail tandem D-peptides built of D3 and its derivative RD2. Both D3D3 and RD2D3 show proteolytic stability in mouse plasma and organ homogenates for at least 24 h and liver microsomes for 4 h. Notwithstanding their high affinity to plasma proteins, both peptides are taken up into the brain following i.v. as well as i.p. administration. Although both peptides contain identical d-amino acid residues, they are arranged in a different sequence order and the peptides show differences in pharmacokinetic properties. After i.p. administration RD2D3 exhibits lower plasma clearance and higher bioavailability than D3D3. We therefore concluded that the amino acid sequence of RD2 leads to more favourable pharmacokinetic properties within the tandem peptide, which underlines the importance of particular sequence motifs, even in short peptides, for the design of further therapeutic D-peptides.

Graphical Abstract

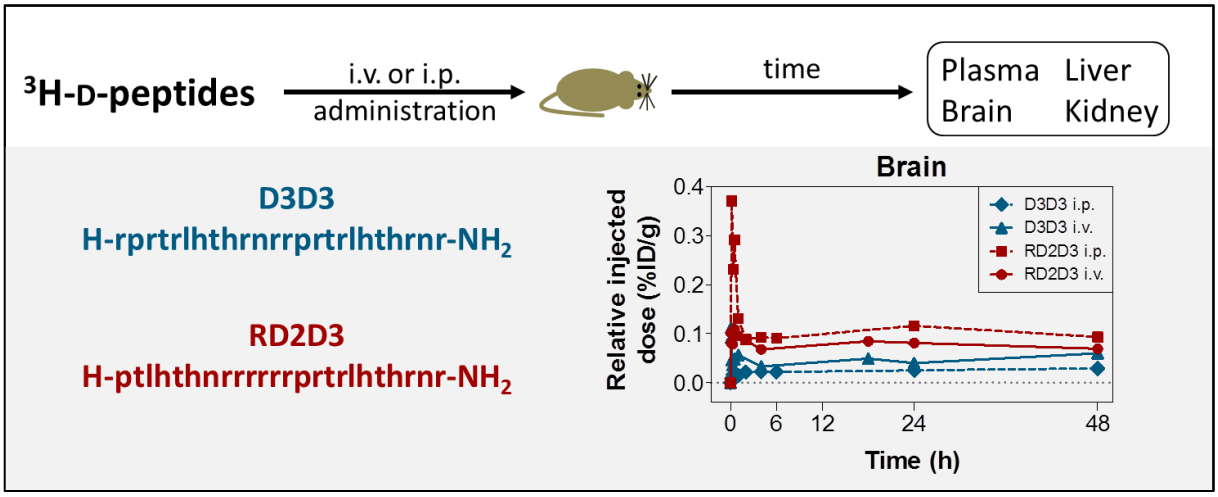

Keywords

Pharmacokinetics; Alzheimer's disease; D-enantiomeric peptide; beta amyloid ligand; therapy

Abbreviations

%ID, relative injected dose; AD, Alzheimer's disease; AGP, α_1-acid glycoprotein; AUC, area under the concentration-time curve; AUMC, area under the moment curve; Aβ, β-amyloid; C, concentration; Cl, clearance; D, dose; dpm, disintegrations per minute; F, bioavailability; f_u, unbound fraction; HSA, human serum albumin; i.p., intraperitoneal; i.v., intravenous; inf, infinity; K_D, dissociation constant; MRT, mean residence time; p.o., *per os*, oral delivery; s.c., subcutaneous; r^2, correlation coefficient; $t_{1/2}$, terminal half-life; TLC, thin layer chromatography; V_{ss}, distribution volume in steady state; V_z, terminal distribution volume; λ_z, terminal elimination rate constant

Introduction

Despite remarkable efforts to develop curative and disease modifying treatments against Alzheimer's disease (AD), thus far only symptomatic treatment is available (Nygaard 2013). Amongst other substance classes, peptides are being investigated as promising drug candidates (Sun *et al.* 2012). Currently, however, most peptides have shown severe disadvantages due to their immunogenicity and instability as well as unfavourable pharmacokinetic properties such as rapid clearance, low oral bioavailability and short *in vivo* half-lives (Pauletti *et al.* 1997; Sato *et al.* 2006).

To overcome those disadvantages, D-enantiomeric peptides are being developed. They combine high protease resistance due to stereoisomeric selectivity of mammalian proteolytic enzymes with low, if any, immunogenicity, leading to slower system elimination and thereby providing more time for therapeutic activity (Dintzis *et al.* 1993; van Regenmortel & Muller 1998).

Using mirror image phage display against β-amyloid (Aβ) monomers as target (Schumacher *et al.* 1996; Wiesehan & Willbold 2003), we have previously identified the D-peptide D3 which has been shown to improve pathology and cognition in transgenic AD mice (van Groen *et al.* 2008; Funke *et al.* 2010; van Groen *et al.* 2012; van Groen *et al.* 2013). Additionally, a number of derivatives have also been designed. Among those, RD2 has shown enhanced properties *in vitro* and *in silico*, while containing the same D-amino acid residues in a rationally reordered sequence (Olubiyi *et al.* 2014). Studies assessing pharmacokinetic properties of both D3 (Jiang *et al.* 2015) and RD2 (Leithold *et al.* 2015) have demonstrated auspicious characteristics such as long half-lives and high oral bioavailability.

Here, we determined the pharmacokinetic properties of D3D3 and RD2D3, which can be thought of as head-to-tail tandem homo- and heteropeptides made of D3 and RD2. The rationale behind the design of the tandem peptides is that multivalent D-peptides can be expected to target their multivalent target molecules, here Aβ oligomers, with increased efficiency. Recently, this was shown to be true for D3D3 *in vitro* and *in vivo* (Brener *et al.* 2015).

Methods

Peptides

D3D3 (H-rprtrlhthrnrrprtrlhthrnr-NH_2, 3.2 kDa) and RD2D3 (H-ptlhthnrrrrrrprtrlhthrnr-NH_2, 3.2 kDa) were purchased from peptides&elephants GmbH (Potsdam, Germany). All peptides consist solely of D-enantiomeric amino acids. The Lewis structures of both peptides can be found in fig. 1.

The tritium-labelled peptides ^{3}H-D3D3 (H-rprtrlhthrnrrprtrlhthrnr-NH_2, 110 Ci/mmol) and ^{3}H-RD2D3 (H-ptlhthnrrrrrrprtrlhthrnr-NH_2, 73 Ci/mmol) were purchased from Quotient Bioresearch (Radiochemicals) Ltd. (Cardiff, United Kingdom) to contain 1 mCi/ml respectively 37 MBq/ml and were supplied as solution in water and ethanol (1:1). The radioactively labelled L-enantiomer of D3 (H-RPRTRLHTHRNR-NH_2, 103 Ci/mmol, Quotient Bioresearch), was used as control peptide for stability assessment.

Proteolytic stability

Proteolytic stability of ^{3}H-D3D3 and ^{3}H-RD2D3 in mouse organ homogenates was assessed as described previously (Leithold *et al.* 2015). Additionally, 2 µl of a ^{3}H-L-peptide were incubated with 1 µl mouse plasma as control.

Furthermore, proteolytic stability of all peptides against degradation by microsomes was analysed using liver microsomes (pooled from CD-1 mice, 10 mg/ml, Sigma-Aldrich). 6 µl ^{3}H-peptide were added to 4 µl pre-warmed microsome solution and incubated at 37°C. After different incubation times the reaction was stopped by addition of 6 µl mobile solvent (2-butanol/pyridine/ammonia (28 %)/water, 39/34/10/26 ml respectively) and samples were stored at -20°C until further use. For detection, thin layer chromatography and autoradiography were performed as described before (Leithold *et al.* 2015).

Pharmacokinetic studies

Pharmacokinetic analysis of the 3H-peptides was assessed as previously described, with the exceptions explained below (Leithold *et al.* 2015). For pharmacokinetic analysis different doses and time points of organ harvesting were chosen per route of administration: i.v. injection 3.3 mg/kg, 3 min, 5 min, 10 min, 15 min, 30 min, 1 h, 4 h, 18 h, 1 d, 2 d; i.p. administration 10 mg/kg, 10 min, 20 min, 30 min, 1 h, 2 h, 4 h, 6 h, 1 d, 2 d. For each time point three mice were administered with the respective dose. The terminal elimination rate constant (λz) was obtained by logarithmic extrapolation of the last five to six observed concentrations based on the highest correlation coefficient obtained (r2 = 0.99 for all calculations).

Plasma protein binding

The plasma protein binding assay was performed twice per peptide as described previously (Leithold *et al.* 2015).

Animals

C57BL/6 mice were used for plasma extraction and pharmacokinetic studies. All animal experiments were carried out in conformance with the German Protection of Animals Act (TierSchG §§ 7-9) and with permit from an Animal Protection Committee (AZ84-02.04.2011.A356).

Results

Proteolytic stability

It was shown previously that both D3 and RD2 are proteolytically stable in organ homogenates and plasma (Jiang *et al.* 2015; Leithold *et al.* 2015). To confirm the proteolytic stability for both tandem peptides, ^{3}H-D3D3 and ^{3}H-RD2D3 were incubated with mouse plasma (fig. 2) and organ homogenates (fig. 3) for up to 24 h and analysed by thin layer chromatography (TLC). It is noteworthy that under TLC conditions the peptides bound differently to plasma and organ constituents, thereby exhibiting different patterns and intensities on the TLC plate as detected by autoradiography. Results show that overall composition of both D3D3 and RD2D3 did not change over time, but remained stable for at least 24 h. In contrast, the L-peptide used for control was proteolytically degraded within 2 h as visible by the time dependent appearance of additional bands (fig. 2).

Moreover, neither D-peptide was degraded after 4 h incubation with liver microsomes, in contrast to the L-peptide (fig. 2). Confirmation of proteolytic stability of D3D3 and RD2D3 was important to ensure that measured radioactivity in the pharmacokinetic studies correlated with ^{3}H-D3D3 and ^{3}H-RD2D3 total concentrations.

Pharmacokinetic properties

To assess pharmacokinetic parameters ^{3}H-labelled D3D3 and RD2D3 were used for i.p. and i.v. administration in mice. Following the radioactive label, both peptides were successfully quantitated in all analysed organs and upon all administration routes. Fig. 4 shows the relative injected dose per millilitre plasma or gram brain, liver and kidney over the time course of two days as well as the brain/plasma ratio.

Remarkably, for RD2D3 intraperitoneal rather than intravenous administration resulted in higher values in all organs, whereas this was the opposite for D3D3 where i.v. resulted in higher amounts present in all assessed organs. Higher concentration of D3D3 and RD2D3 in the liver as compared to the kidney suggests the liver as the major pathway for excretion for both peptides. It is noteworthy that after 2 days post administration both peptides were still present in all organs and especially high in liver and kidney. RD2D3 reached higher levels than D3D3 in the brain as well as in liver and kidney (fig. 4), which is most prominent following i.p. administration.

Plasma pharmacokinetic parameters

Plasma pharmacokinetic parameters were calculated based on back calculated peptide concentrations from measured radioactivity in plasma and are summarised in table 1. The maximally observed concentration relative to the Dose (C_{max}/D) was similar for i.v. injection (D3D3 0.54 and RD2D3 0.58 (µg/ml)/(mg/kg)) but differed upon i.p.

administration between 0.16 (µg/ml)/(mg/kg) for D3D3 and 0.47 (µg/ml)/(mg/kg) for RD2D3. For both D-peptides the areas under the curve $AUC_{0\text{-last}}$ and $AUC_{0\text{-inf}}$ do not differ much, which is due to the very low extrapolated part of the $AUC_{0\text{-inf}}$ (< 3 %). RD2D3 showed higher plasma $AUC_{0\text{-inf}}$ for both administration routes (i.v. 0.32 mg/ml*min and i.p. 1.87 mg/ml*min) as compared to D3D3 (i.v. 0.18 mg/ml*min and i.p. 0.62 mg/ml*min). The mean retention time ($MRT_{0\text{-inf}}$) was around 11 and 12 h and similar for all administration routes and both peptides. The rate of i.v. terminal plasma clearance was higher for D3D3 with Cl/F = 17.9 ml/(min*kg) than for RD2D3 with Cl/F = 10.2 ml/(min*kg). Additionally, upon i.p. administration the clearance was found to be lower than after i.v. administration for both peptides. This results in longer half-lives ($t_{1/2}$) for RD2D3 (i.v. 0.8 h and i.p. 2.3 h) compared to D3D3 (i.v. 0.7 h and i.p. 1.5 h). Furthermore, the bioavailability (F) upon i.p. administration of RD2D3 was very high with about 190 %, while D3D3 reached 110 %.

Brain pharmacokinetic parameters

Since the brain is thought to be the therapeutically relevant target organ, pharmacokinetic parameters were also calculated for the brain (table 2). Both peptides showed an increasing brain/plasma ratio over time, reaching 1 after about 6 to 12 hours (fig. 5), which resulted in an overall brain/plasma ratio based on the $AUC_{0\text{-last}}$ of 0.6 (i.v.) and 0.3 (i.p.) for D3D3 and 0.6 (i.v.) and 0.5 (i.p.) for RD2D3. The time-dependent The brain exposure ($AUC_{0\text{-last}}$) was higher for RD2D3 than for D3D3, especially upon i.p. administration (RD2D3 i.v. 0.19 and i.p. 0.88 mg/g*min and D3D3 i.v. 0.12 and i.p. 0.20 mg/g*min). The C_{max}/D was 0.02 (µg/g)/(mg/kg) for i.v. administration. I.p. injection lead to a C_{max}/D of 0.01 for D3D3 and was higher for RD2D3 with 0.11 (µg/g)/(mg/kg). The MRT was calculated to be about one day for both

peptides and administration routes. Furthermore, the bioavailability of the i.p. administration was low for D3D3 with 55 % and very high for RD2D3 with 157 %.

Table 1: Pharmacokinetic parameters determined from mouse plasma for i.v. and i.p. administration. Clear fields are not applicable for the respective administration route. For abbreviations please refer to the abbreviations section.

Parameter	**Units**	**D3D3**		**RD2D3**	
		i.v.	**i.p.**	**i.v.**	**i.p.**
Dose (D)	mg/kg	3.3	10	3.3	10
t_{max}	min	3	60	3	60
C_{max}/D	(µg/ml)/(mg/kg)	0.54	0.16	0.58	0.47
$AUC_{0\text{-}last}$	mg/ml*min	0.18	0.61	0.32	1.82
$AUMC_{0\text{-}last}$	min^2*mg/ml	131	424	229	1091
$MRT_{0\text{-}last}$	h	11.9	11.6	11.9	10.0
λ_z	min^{-1}	0.0155	0.0075	0.0137	0.0050
$t_{1/2}$	h	0.7	1.5	0.8	2.3
$AUC_{0\text{-}inf}$	mg/ml*min	0.18	0.62	0.32	1.87
$AUMC_{0\text{-}inf}$	min^2*mg/ml	137	461	240	1225
$MRT_{0\text{-}inf}$	h	12.3	12.3	12.3	10.9
V_z	l/kg	1.15	2.37	0.74	1.99
Cl/F	ml/(min*kg)	17.9	16.1	10.2	5.4
V_{ss}	l/kg	13.2		7.5	
$F_{AUC\text{-}last}$	%		110		187
% AUC extrapolated	%	1.1	1.9	1.2	2.3

Table 2: Brain pharmacokinetic parameters determined for i.v. and i.p. administration. Clear fields are not applicable for the respective administration route. For abbreviations please refer to the abbreviations section.

Parameter	Units	D3D3		RD2D3	
		i.v.	i.p.	i.v.	i.p.
Dose (D)	mg/kg	3.3	10	3.3	10
t_{max}	min	3	2880	30	10
C_{max}/D	(µg/g)/(mg/kg)	0.02	0.01	0.02	0.11
$AUC_{0\text{-last}}$	mg/g*min	0.12	0.20	0.19	0.88
$AUMC_{0\text{-last}}$	min^2*mg/g	189	315	269	1264
$MRT_{0\text{-last}}$	h	26.8	26.5	24.2	23.8
$F_{AUC\text{-last}}$	%		55		157
Brain/plasma ratio $AUC_{0\text{-last}}$		0.6	0.3	0.6	0.5

Plasma protein binding

In vivo plasma protein binding was estimated by *in vitro* incubation of ^{3}H-labelled D3D3 and RD2D3 with human serum albumin (HSA) and α_1-acid glycoprotein (AGP) (fig. 6). For AGP the binding curves of both peptides reached saturation even at the lowest AGP concentration. This indicates strong binding affinities to AGP. Results yielded for RD2D3 a K_D of 0.04 µM ± 18 % and for D3D3 a K_D of 0.03 µM ± 18 %. Binding to HSA did not reach saturation and could therefore not be determined reliably, with K_D values being in the hundreds micromolar range. It could be deduced that both peptides showed much higher affinity to AGP than to HSA and plasma protein binding therefore is mainly determined by AGP binding. The expected free fraction in plasma was calculated disregarding HSA binding and under the assumption of peptide

concentrations in plasma of C_{RD2D3} = 0.027 µM and C_{D3D3} = 0.013 µM (concentrations 24 h after administration). Results showed a fraction unbound (f_u) for RD2D3 of 0.20 % and for D3D3 of 0.16 %.

Discussion

Here, we have assessed the pharmacokinetic properties of two D-peptides which are head-to-tail tandem derivatives of the previously described peptides D3 and its derivative RD2. D3 has been selected by mirror image phage display for binding against Aβ(1-42) and both D3 and RD2 have demonstrated therapeutic potential *in vitro* and *in vivo* (van Groen *et al.* 2008; Bartnik *et al.* 2010; Funke *et al.* 2010; Olubiyi *et al.* 2014). Furthermore, D3 and RD2 exhibited excellent pharmacokinetic properties as has been shown previously (Jiang *et al.* 2015; Leithold *et al.* 2015). In a next step, tandem peptides were created in order to enhance the affinity to Aβ (Brener *et al.* 2015). Thereafter, pharmacokinetic assessment was performed to determine their ability to reach the target organ brain.

For both D3 and RD2 it could previously be shown that they remain stable in mouse organ homogenates and plasma (Jiang *et al.* 2015; Leithold *et al.* 2015). Here, we demonstrated that the homo- and heteropeptides D3D3 and RD2D3 are likewise proteolytically stable for at least 24 h in mouse plasma, organ homogenates and liver microsomes. We used the measured ^{3}H-radioactivity of the administered peptides in the pharmacokinetic study to calculate the peptide concentrations. This assumes that the non-metabolised peptides are represented by the measured radioactivity which is then used to obtain the pharmacokinetic parameters. Although we have shown that the peptides are stable in mouse plasma for 24 h we cannot exclude partial

metabolism at later time points which might or might not influence their therapeutic effectivity. Incubation in plasma and organ homogenates beyond 24 h and microsomes beyond 4 h appeared not to be meaningful since enzyme activities in biological samples cannot be expected to last for long incubation times at 37 °C. Furthermore, due to the complete lack of metabolism of RD2D3 and D3D3 after 24 h incubation with organ homogenates as well as after incubation with microsomes there was no reason to expect significant metabolism at 48 h. Nevertheless, for pharmacokinetic assessment we performed a non-compartmental analysis since this is a simplistic analysis without the need for assumptions regarding the number of compartments. Any minor metabolite would influence more complex pharmacokinetic models and would lead to inaccurate data. The authors are aware that non-compartmental analysis may not be the optimal model for the pharmacokinetic analysis. It assumes linear kinetics and may therefore result in over- or under-estimation of certain parameters. However, it is often used as an initial indication of the pharmacokinetic properties of a substance and avoids additional over-interpretation of the data at hand.

To summarise, the pharmacokinetic analysis showed that RD2D3 has a lower clearance than D3D3, resulting in higher drug exposure in plasma and brain as well as a high bioavailability after i.p. administration. Both peptides have higher AUC values upon i.p. administration compared to i.v. administration. However, both D3D3 and RD2D3 have relatively high elimination rate constants and therefore short half-lives of only few hours that are in the same range as other peptides assessed as potential drugs (Pollaro & Heinis 2010). Furthermore, D3D3 and RD2D3 have a low predicted free fraction in plasma and may therefore only be available for therapeutic action in the target organ

in small amounts. However, it was shown that high plasma protein binding does not necessarily impede drug efficacy (Smith *et al.* 2010; Liu *et al.* 2014).

The i.p. plasma drug exposure especially of RD2D3 is considerably higher than upon i.v. administration. This could possibly be explained by the higher rate of clearance observed for i.v. administration. Entero-hepatic recirculation or renal reabsorption can lead to a prolonged presence of the peptide in the organism (Bendayan 1996; Roberts *et al.* 2002). This is underlined by the results showing no apparent decrease of the peptide concentration in liver and kidney after 2 days (fig. 4). For RD2D3 the concentration in both organs is higher than for D3D3, indicating that this effect is more pronounced for RD2D3, explaining the much higher bioavailability of RD2D3 than D3D3.

It was shown that D3 itself has a half-life in plasma of 32 h for i.v. and more than 40 h upon i.p. or oral administration (Jiang *et al.* 2015). Remarkably, RD2 showed a plasma half-life of about 60 h for all assessed administration routes (Leithold *et al.* 2015). In contrast, both tandem peptides have remarkably short half-lives of only few hours. This is also reflected in the clearance, with D3D3 exhibiting the highest rate, followed by RD2D3, D3 and RD2 having the slowest clearance. Interestingly, the MRT in both plasma and brain was higher for the tandem peptides than for D3 for both i.p. and i.v. administration, while RD2 had much higher MRT values for all administration routes. RD2 also showed the highest brain/plasma ratio when calculated using the $AUC_{0\text{-last}}$ of all peptides. Since also the drug exposure in plasma, as calculated by plasma $AUC_{0\text{-inf}}$, is highest in RD2 and D3, it is concluded that the larger size of the tandem peptides results in less favourable pharmacokinetic parameters. Furthermore, resorption from

the peritoneum into the blood seems to be least effective for the tandem peptides. Plasma levels of D3D3 are very low, higher for RD2D3 followed by D3, while RD2 is resorbed very efficiently. Similarly, peptide levels in the brain are highest for RD2, followed by D3 and the tandem peptides with RD2D3 exhibiting higher levels than D3D3. Considering the brain/plasma ratios which do not differ much, the low brain levels of the tandem peptides may result primarily from their insufficient resorption rather than from an inferior ability to enter the brain.

Conclusions

Taken together, the tandem peptides exhibit less favourable pharmacokinetic properties than the single peptides. Resorption of D3D3 and RD2D3 is less effective, resulting in lower brain concentrations as compared to the single peptides D3 and RD2. This disadvantage of the tandem peptides could possibly be outweighed by higher efficiency of the tandem compounds as was indicated by recent data for D3D3 (Brener *et al.* 2015). Furthermore, it is concluded that the sequence order of the D-enantiomeric amino acid residues has a considerable impact on pharmacokinetic properties of the peptide. Peptides harbouring the amino acid residue sequence of RD2 were found to exhibit enhanced pharmacokinetic properties than those harbouring the D3 sequence. This can be seen both in RD2 alone when compared to D3 and similarly within RD2D3 in comparison to D3D3.

Acknowledgements

We thank Jörg Mauler for helping with the data analysis. D.W. and N.J.S. were supported by grants from the “Portfolio Technology and Medicine” of the Impuls und Vernetzungs-Fonds der Helmholtzgemeinschaft. D.W. was supported by the Helmholtz-Validierungsfonds of the Impuls und Vernetzungs-Fonds der Helmholtzgemeinschaft; K.J.L. and D.W. were supported by the “Portfolio Drug Research” of the Impuls und Vernetzungs-Fonds der Helmholtzgemeinschaft.

Conflict of interest

The authors declare that they have no conflict of interest.

References

Bartnik, D., Funke, S.A., Andrei-Selmer, L.C., Bacher, M., Dodel, R., Willbold, D., 2010. Differently Selected D-Enantiomeric Peptides Act on Different Abeta Species. Rejuvenation research 13, 202-205.

Dintzis, H.M., Symer, D.E., Dintzis, R.Z., Zawadzke, L.E., Berg, J.M., 1993. A Comparison of the Immunogenicity of a Pair of Enantiomeric Proteins. Proteins-Structure Function and Genetics 16, 306-308.

Funke, S.A., van Groen, T., Kadish, I., Bartnik, D., Nagel-Steger, L., Brener, O., Sehl, T., Batra-Safferling, R., Moriscot, C., Schoehn, G., Horn, A.H.C., Mueller-Schiffmann, A., Korth, C., Sticht, H., Willbold, D., 2010. Oral Treatment with the D-Enantiomeric Peptide D3 Improves the Pathology and Behavior of Alzheimer's Disease Transgenic Mice. ACS Chem. Neurosci. 1, 639-648.

Liu, X., Wright, M., Hop, C.E.C.A., 2014. Rational Use of Plasma Protein and Tissue Binding Data in Drug Design. J. Med. Chem. 57, 8238-8248.

Nygaard, H.B., 2013. Current and emerging therapies for Alzheimer's disease. Clin. Ther. 35, 1480-1489.

Olubiyi, O.O., Frenzel, D., Bartnik, D., Glück, J.M., Brener, O., Nagel-Steger, L., Funke, S.A., Willbold, D., Strodel, B., 2014. Amyloid aggregation inhibitory mechanism of arginine-rich D-peptides. Curr. Med. Chem. 21, 1448-1457.

Pauletti, G.M., Gangwar, S., Siahaan, T.J., Aubé, J., Borchardt, R.T., 1997. Improvement of oral peptide bioavailability: Peptidomimetics and prodrug strategies. Adv Drug Deliv Rev 27, 235-256.

Pollaro, L., Heinis, C., 2010. Strategies to prolong the plasma residence time of peptide drugs. Medchemcomm 1, 319-324.

Sato, A.K., Viswanathan, M., Kent, R.B., Wood, C.R., 2006. Therapeutic peptides: technological advances driving peptides into development. Curr. Opin. Biotechnol. 17, 638-642.

Smith, D.A., Di, L., Kerns, E.H., 2010. The effect of plasma protein binding on in vivo efficacy: misconceptions in drug discovery. Nat Rev Drug Discov 9, 929-939.

Sun, N., Funke, S.A., Willbold, D., 2012. A survey of peptides with effective therapeutic potential in Alzheimer's disease rodent models or in human clinical studies. Mini Rev. Med. Chem. 12, 388-398.

van Groen, T., Kadish, I., Funke, A., Bartnik, D., Willbold, D., 2012. Treatment with A beta 42 Binding D-Amino Acid Peptides Reduce Amyloid Deposition and Inflammation in APP/PS1 Double Transgenic Mice. Adv. Protein Chem. Struct. Biol. 88, 133-152.

van Groen, T., Kadish, I., Funke, S.A., Bartnik, D., Willbold, D., 2013. Treatment with D3 removes amyloid deposits, reduces inflammation, and improves cognition in aged AbetaPP/PS1 double transgenic mice. J. Alzheimers Dis. 34, 609-620.

van Groen, T., Wiesehan, K., Funke, S.A., Kadish, I., Nagel-Steger, L., Willbold, D., 2008. Reduction of Alzheimer's Disease Amyloid Plaque Load in Transgenic Mice by D3, a D-Enantiomeric Peptide Identified by Mirror Image Phage Display. ChemMedChem 3, 1848-1852.

van Regenmortel, M.H.V., Muller, S., 1998. D-peptides as immunogens and diagnostic reagents. Curr. Opin. Biotechnol. 9, 377-382.

Legend to figures

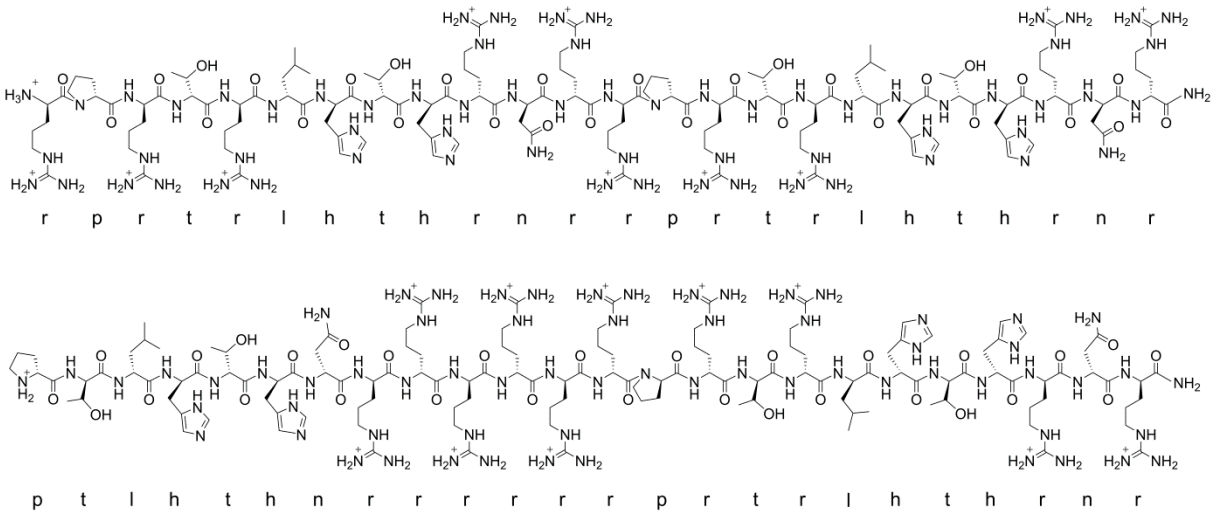

Fig. 1. Lewis structure and single letter amino acid code of D3D3 (top) and RD2D3 (bottom). Both peptides are D-enantiomeric peptides (3.2 kDa).

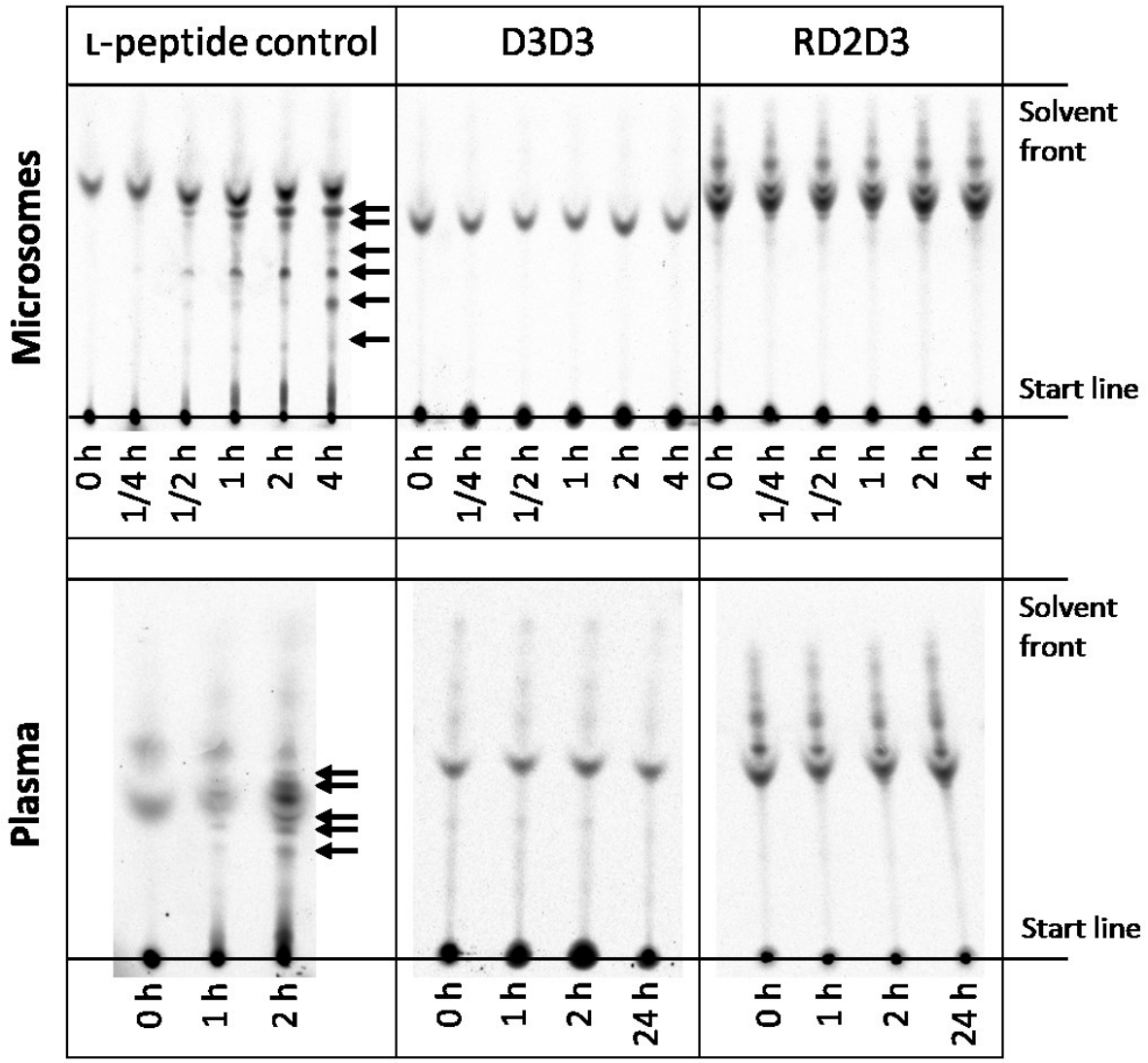

Fig. 2. Autoradiography of thin layer chromatogram, showing proteolytic stability of ^{3}H-D3D3 and ^{3}H-RD2D3 in mouse plasma and liver microsomes in comparison to an L-peptide control. The peptides were incubated with plasma or microsomes at 37 °C for the given amount of time and applied to thin layer chromatography plates. Proteolytic degradation is apparent from time dependent appearance of additional bands, as was obvious for the L-peptide control (arrows). In contrast, D3D3 and RD2D3 remained stable for 4 h in liver microsomes and plasma for up to 24 h of incubation.

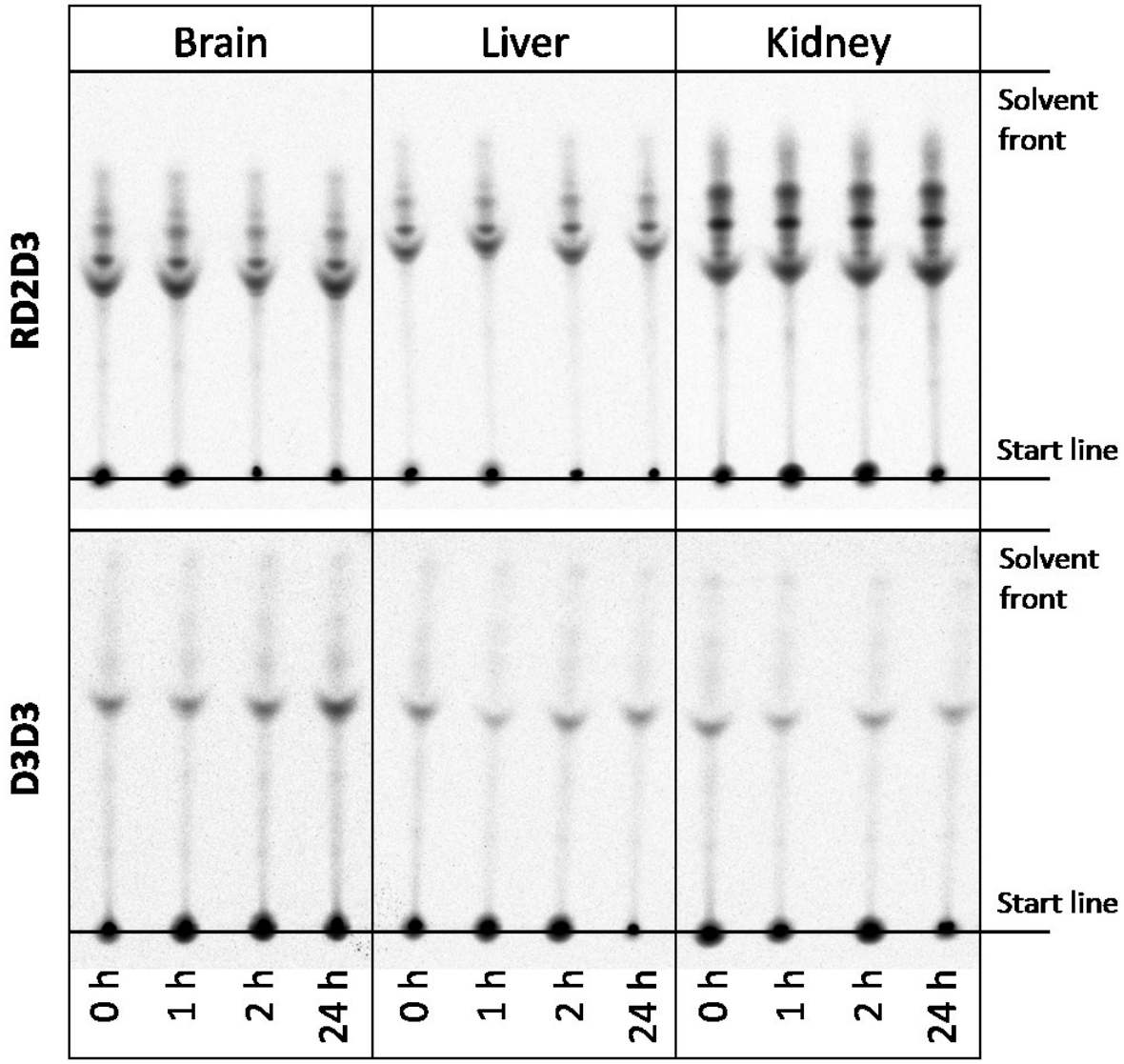

Fig. 3. Autoradiography of thin layer chromatogram, showing proteolytic stability of ^{3}H-D3D3 and ^{3}H-RD2D3 in mouse organ homogenates. The peptides were incubated with brain, liver and kidney homogenates at 37 °C for the given amount of time and applied to thin layer chromatography plates. No proteolytic degradation is apparent for both peptides for up to 24 h of incubation.

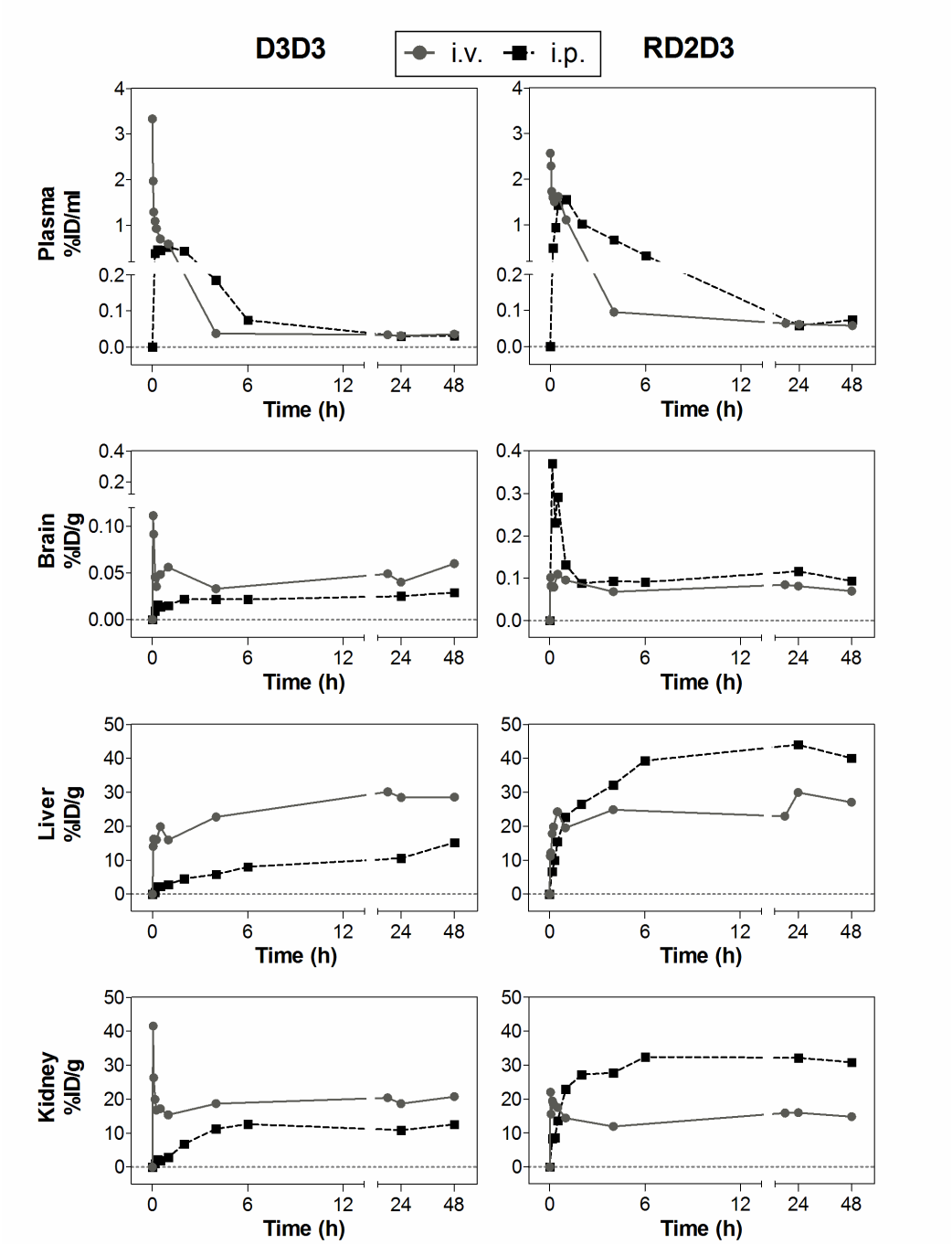

Fig. 4. Time-dependent distribution of ^{3}H-D3D3 and ^{3}H-RD2D3 in mouse plasma, brain, liver and kidney after i.v. and i.p. administration. Radioactively labelled D3D3 or RD2D3 was administered together with non-labelled peptide at total concentrations of 10 mg/kg (i.p.) or 3.3 mg/kg (i.v.). The concentration of D3D3 and RD2D3 is shown as percent of the injected dose per millilitre plasma (%ID/ml) or gram organ (%ID/g). Graphs show the means of three mice per time point.

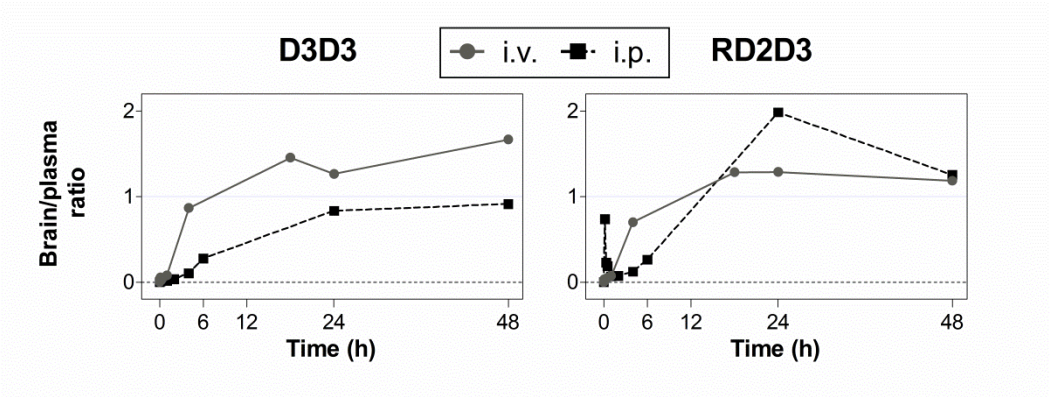

Fig. 5. Time-dependent development of ^{3}H-D3D3 and ^{3}H-RD2D3 brain/plasma ratio after i.v. and i.p. administration. Graphs show the means of three mice per time point, corrected for residual blood in the brain.

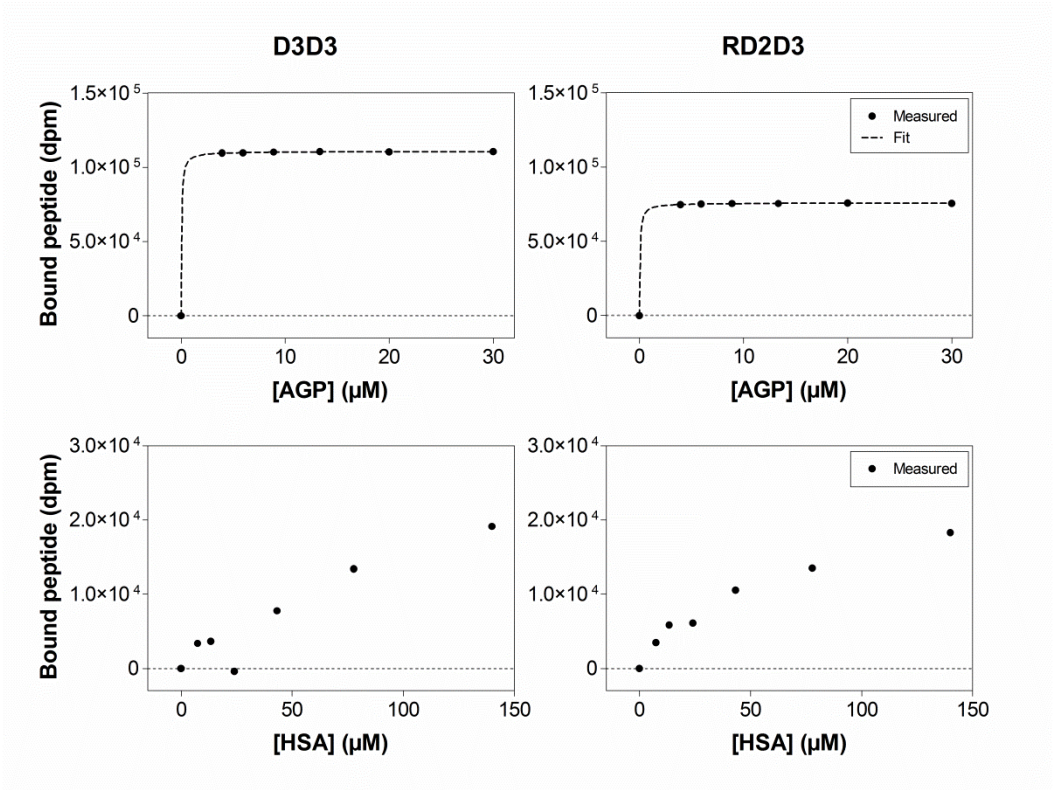

Fig. 6. Plasma protein binding of ^{3}H-D3D3 and ^{3}H-RD2D3. Graphs display the determined amount of D-peptide bound (in dpm) to α_1-acid glycoprotein (AGP) or human serum albumin (HSA) at different concentrations. Binding affinity to AGP was roughly estimated based on the Michaelis Menten binding equation (dotted lines). Dissociation constants for binding to HSA could be estimated to be in the hundreds µM range as the saturation was not reached even above 100 µM.

4 Summary and conclusion

Alzheimer's disease is predicted to affect an increasing number of people and thereby causes suffering of patients and their families as well as a considerable financial burden for societies (Alzheimer's Disease International 2010). However, causal treatment has yet to be developed and to date therapeutic intervention remains symptomatic (Alzheimer's Association 2014). Current research investigates various substances among different categories for potential therapeutic effect, amongst them the promising category of peptide drugs (Funke & Willbold 2012).

To improve their proteolytic stability and thereby the half-life, peptides can be built from D-enantiomeric amino acids. This modification lends them positive properties such as higher proteolytic stability resulting in longer half-lives and in some cases D-peptides showed lower immunogenicity (Dintzis *et al.* 1993; van Regenmortel & Muller 1998). Examples for D-peptides created as therapeutic intervention for Alzheimer's disease are D3, its derivative RD2 and their head-to-tail tandem forms D3D3 and RD2D3.

In the presented study pharmacokinetic properties of these four peptides were analysed and compared. Pharmacokinetics provide a tool for lead compound prioritisation for further progress to (pre-)clinical studies and can give insight into issues that may arise. Possible problems can arise during all steps of the ADME process and can include poor resorption, extensive metabolism or protein binding as well as insufficient penetration of the target tissue (Jang *et al.* 2001). Desirable are properties such as a relatively long half-live, in order to ensure sufficient time for therapeutic activity to take place. This, however, is often a problem for peptides, which are rapidly cleared from the organism (Pollaro & Heinis 2010). Furthermore, the drug should be available for therapeutic activity at sufficient concentrations, as represented by a high bioavailability (Feucht & Patel 2011). In case of drugs indicated for the central nervous system, brain penetration is thought to be of importance, too, but remains a delicate measurement as it does not necessarily have an impact on therapeutic activity (Reichel 2009). Especially oral administration is of interest for further therapeutic development.

4.1 Stability and plasma protein binding

Results showed that all D-peptides remained stable in mouse plasma and organ homogenates for at least 24 hours, while the control L-peptide was proteolytically degraded after short incubation times. For D3 and the tandem peptides, stability could also be shown in a preparation of microsomes from mouse liver. Interestingly, all peptides exhibited different thin layer chromatography patterns after incubation, showing binding of different plasma constituents.

Comparison of the predicted plasma protein binding of all four peptides showed that they all preferably bound to AGP than HSA, while exhibiting different affinities. The tandem peptides both showed high affinity binding to AGP, resulting in free fractions of peptide that are below 0.2 % which is considered very low (Liu *et al.* 2014). In contrast, the single peptides bound less strongly to AGP, resulting in approximately 8 % D3 and 11.5 % RD2 remaining unbound in plasma. It was shown that plasma protein binding does not necessarily have an influence on drug efficacy (Smith *et al.* 2010; Liu *et al.* 2014). However, higher amounts of free peptide could positively influence the uptake of peptide into the brain through the blood brain barrier, especially if the peptides are taken up by passive diffusion. The exact mechanism of uptake of the D-peptides into the brain remains to be clarified, but *in vitro* experiments indicated transcytosis as possible mechanism (Liu *et al.* 2010).

4.2 Intravenous and intraperitoneal administration – D3, RD2, D3D3 and RD2D3

Pharmacokinetic parameters of all four peptides were analysed after intraperitoneal and intravenous administration. It was observed, that in general i.p. injection lead to longer half-lives in plasma than i.v. administration. RD2 showed the by far longest half-life with over 60 hours. Furthermore, the clearance rate of RD2 was less than half of that of D3, while the tandem peptides exhibited high clearance rates. Consequently, the plasma $AUC_{0\text{-}inf}$, representing the exposure to the peptide, was much higher for RD2 than D3, followed by RD2D3 and even lower for D3D3.

Upon both routes of administration, all four peptides were shown to enter the brain (figure 6). D3D3 achieved the lowest brain exposure ($AUC_{0\text{-}last}$) and, remarkably, RD2D3 and D3 did not differ by much. The exposure of RD2D3 was a bit lower than D3 for i.v. administration but clearly higher after i.p. administration. Since RD2 was assessed for up to 28 days, the total exposure was not directly comparable to the other peptides and with about five times more much higher. However, the RD2 level reached in the brain was also about twice as high as for D3. Remarkably, the retention of D3 in the brain was the lowest of all peptides, whereas that of RD2 was considerably high.

Comparison of the brain/plasma ratio of all peptides (calculation from the $AUC_{0\text{-}last}$ as done for the other peptides showed that D3 had a ratio of 0.4 after both i.v. and i.p. administration) as an indicator for brain penetration, showed interestingly that after i.v. administration the brain/plasma ratio was lowest for D3, while after i.p. injection D3D3 showed the lowest ratio followed by D3. For both administration routes, RD2 had the highest brain/plasma ratio. In contrast, when regarding the time-dependent presentation of the brain/plasma ratio, all peptides reached quite similar values after 48 hours (figure 6).

Taken together, this indicated that the resorption of the tandem peptides was generally lower than that of the single peptides. Furthermore, uptake of D3 and D3D3 into the brain appeared to be lower, although they reached comparable levels after 24 hours. Therefore, it can be concluded that the amino acid sequence of RD2 seemed to hold advantages over D3, which also manifested in improved properties of the tandem peptide RD2D3 over D3D3.

The single peptides were primarily found in the kidney rather than the liver and it was shown that levels decreased within a reasonable amount of time. This suggests that the kidney formed the main excretion route for the single peptides. Interestingly, the tandem peptides showed high levels in the liver that remain high even 48 hours after administration. This might be due to their strong binding to the plasma proteins which might prevent excretion by renal filtration and together with their larger size might lead to excretion via the liver (Caldwell *et al.* 1995).

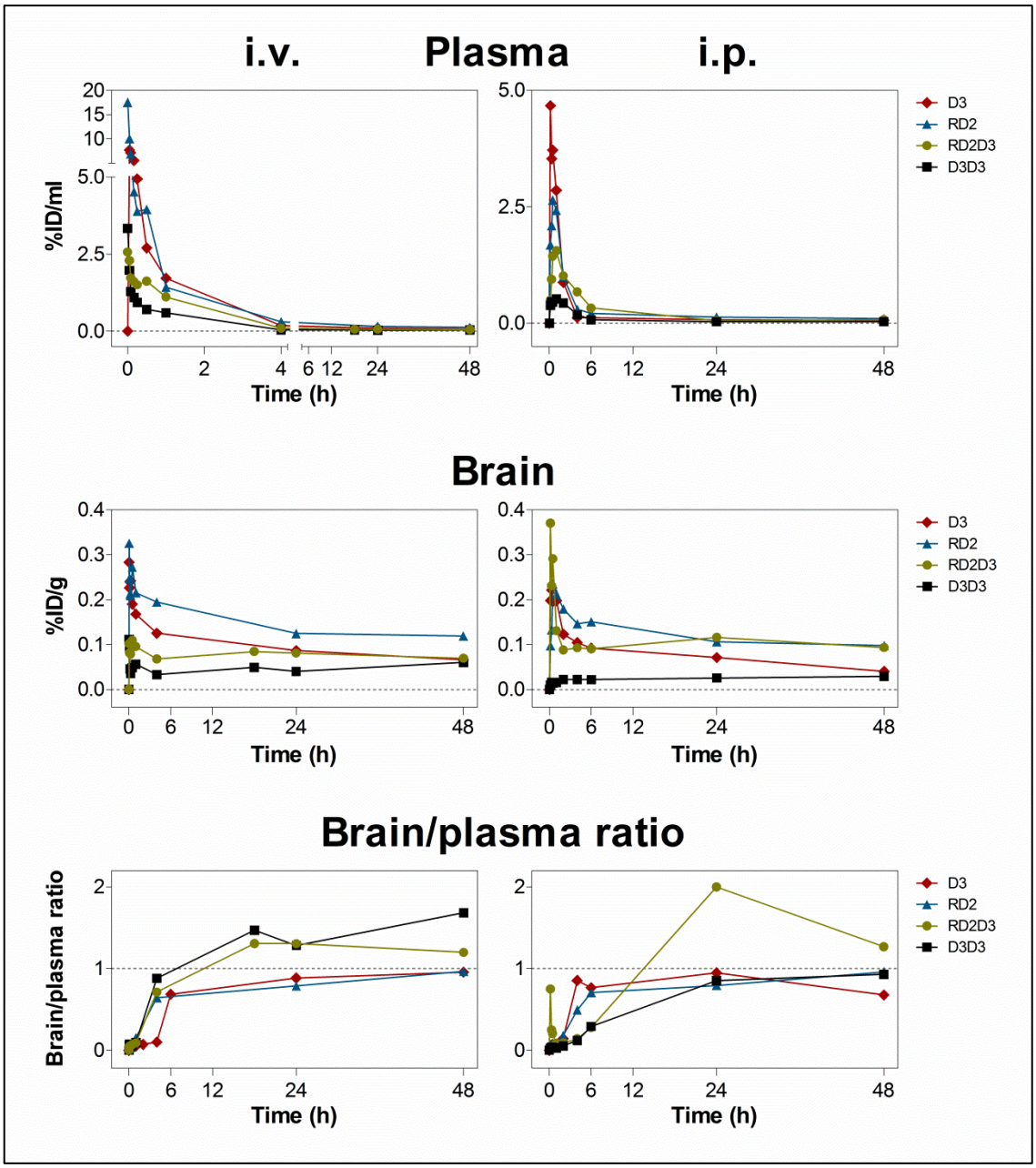

Figure 6: Comparison of all four peptides after i.v. and i.p. administration. Radioactively labelled peptide was administered to mice and organs were harvested at different time points afterwards. Time dependent peptide concentrations in plasma and brain are shown as well as the brain/plasma ratio. Concentrations are expressed as relative injected dose per gram organ (%ID/g) or millilitre plasma (%ID/ml) and presented as mean of three mice per time point.

4.3 Oral and subcutaneous administration – D3 and RD2

For both RD2 and D3 pharmacokinetic properties were also determined for oral administration, additionally, RD2 was also assessed upon subcutaneous administration. Results for oral administration showed that D3 had a half-life which was more than 7 hours longer than that of RD2. However, the exposure in the plasma ($AUC_{0\text{-}inf}$) was three times higher for RD2 than for D3. Similarly, the exposure of RD2 ($AUC_{0\text{-}last}$) in the brain was more than 4 times higher than that of D3.

Both peptides entered the brain sufficiently after oral administration as shown by the high brain/plasma ratios of 0.85 for D3 and 1.0 for RD2 which suggest efficient penetration of the brain (Reichel 2006). It is noteworthy that upon oral administration both peptides reached levels in the brain (figure 7) which were as high as (%ID/g) or even higher ($AUC_{0\text{-}last}$) than upon i.v. and i.p. administration, despite lacking the initial concentration peak observed in the other administration routes. This indicated the presence of an efficient transport mechanism into the brain, which was underlined by the much more rapid increase of the brain/plasma ratio seen after oral administration (figure 7). Furthermore, RD2 showed a much higher oral availability as could be seen in the higher bioavailability as well as plasma and brain levels. This advantage is of special interest as low oral bioavailability often is a problem of peptide drugs (Renukuntla *et al.* 2013).

Interestingly, RD2 also showed very promising results upon subcutaneous administration (figure 7). The plasma half-life was comparable to that determined after i.v. and i.p. administration and the exposure ($AUC_{0\text{-}inf}$) was the highest observed. Similarly, the bioavailability was higher than that of RD2 administered intraperitoneally or orally. The exposure in the brain ($AUC_{0\text{-}last}$) was comparable to that of oral administration, while the half-life of RD2 in the brain was another 30 hours longer than for i.v. or i.p. administration.

These results showed that oral and subcutaneous administration of both D-peptides were very promising approaches for their development as therapeutics. Oral administration is the most convenient and thus most commonly used administration route, but alternatives that provide easy administration and prolonged treatment are being assessed for practicality (Di Stefano *et al.* 2011). Since adjustment of formulation often is needed to optimise the chosen administration route, it is very beneficial that both D-peptides already showed promising properties without any special formulation applied.

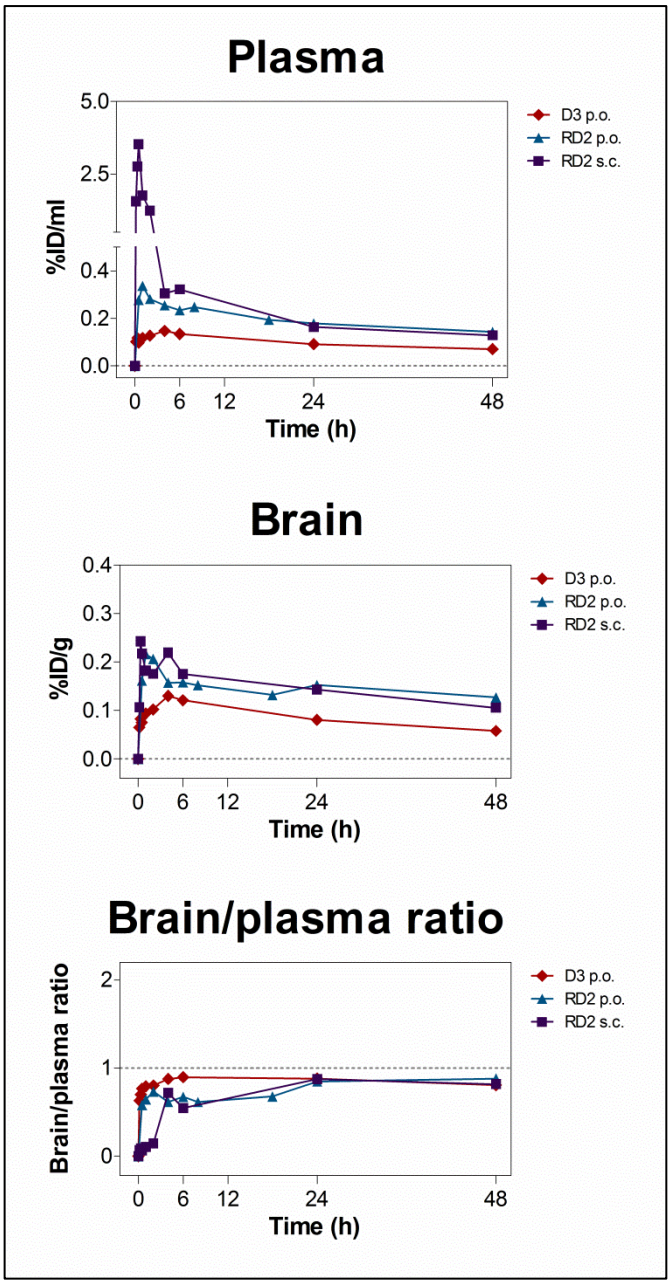

Figure 7: Comparison of D3 and RD2 following oral administration as well as RD2 after subcutaneous administration. Radioactively labelled peptide was administered to mice and organs were harvested at different time points afterwards. Time dependent peptide concentrations in plasma and brain are shown as well as the brain/plasma ratio. Concentrations are expressed as relative injected dose per gram organ (%ID/g) or millilitre plasma (%ID/ml) and presented as mean of three mice per time point.

4.4 General conclusion

In comparison with other therapeutically active peptides and drugs indicated for AD, the presented D-peptides showed suitable pharmacokinetic parameters. Particularly the half-life of the single peptides was high - without having undergone formulation or conjugation processes. It was much higher than that observed for other peptide drugs (Pollaro & Heinis 2010) and comparable to that of memantine or donepezil, two approved dementia therapeutics (Blennow *et al.* 2006; Noetzli & Eap 2013). Furthermore, especially RD2 provided high oral bioavailability, similar to that seen in most anti-dementia drugs (Noetzli & Eap 2013).

The tandem peptides exhibited pharmacokinetic properties which were less favourable than that of both single peptides. Since they are conjugates of D3 and/or RD2, they consist of identical amino acids. Therefore, the larger size and possibly a different structure of the tandem peptides seemed to influence the pharmacokinetic properties, giving them characteristics which are possibly disadvantageous for their intended use as AD therapeutics.

However, the crucial evaluation parameter remains the *in vivo* efficacy of the peptides. If a tandem peptide was shown to have a considerably higher therapeutic activity this could possibly counterbalance the disadvantageous pharmacokinetic properties as was indicated recently for D3D3 (Brener *et al.* 2015).

In vivo efficacy of D3 was already shown in transgenic AD mice, it was able to enhance cognition and reduce both plaque load and plaque-related inflammation in a number of studies (see 1.2.1). Preliminary research with RD2 shows that it is also therapeutically active, but profound studies examining its *in vivo* efficacy have not been published so far.

In contrast to D3, RD2 exhibited promising improvements in a number of pharmacokinetic parameters. Furthermore, it was shown to have higher affinity to Aβ oligomers (Olubiyi *et al.* 2014), which are currently thought to be the most toxic Aβ species. Taken together, provided that RD2 shows similar or enhanced therapeutic efficacy *in vivo*, RD2 is a very promising drug candidate for clinical research into its suitability as AD therapeutic.

IX References

Alzheimer's Association (2011). 2011 Alzheimer's disease facts and figures. *Alzheimer's & Dementia, 7*(2), 208-244.

Alzheimer's Association (2014). 2014 Alzheimer's disease facts and figures. *Alzheimer's & Dementia, 10*(2), e47-92.

Alzheimer's Disease International (2010). World Alzheimer Report 2010 - The Global Economic Impact of Dementia.

Alzheimer's disease International (2013a). The Global Impact of Dementia 2013-2050.

Alzheimer's Disease International (2013b). World Alzheimer Report 2013 - Journey of Caring: An analysis of long-term care for dementia.

Alzheimer's Disease International (2014). World Alzheimer Report 2014 - Dementia and Risk Reduction: an analysis of protective and modifiable factors.

Ballard C, Gauthier S, Corbett A, Brayne C, Aarsland D, & Jones E (2011). Alzheimer's disease. *Lancet, 377*(9770), 1019-1031.

Ballatore C, Lee VMY, & Trojanowski JQ (2007). Tau-mediated neurodegeneration in Alzheimer's disease and related disorders. *Nature Reviews Neuroscience, 8*(9), 663-672.

Bartnik D, Funke SA, Andrei-Selmer LC, Bacher M, Dodel R, & Willbold D (2010). Differently Selected D-Enantiomeric Peptides Act on Different Abeta Species. *Rejuvenation Res, 13*(2-3), 202-205.

Bendayan R (1996). Renal drug transport: a review. *Pharmacotherapy, 16*(6), 971-985.

Benilova I, Karran E, & De Strooper B (2012). The toxic A beta oligomer and Alzheimer's disease: an emperor in need of clothes. *Nature Neuroscience, 15*(3), 349-357.

Bertram L, Lill CM, & Tanzi RE (2010). The genetics of Alzheimer disease: back to the future. *Neuron, 68*(2), 270-281.

Bird TD (2008). Genetic aspects of Alzheimer disease. *Genetics in Medicine, 10*(4), 231-239.

Birks J (2006). Cholinesterase inhibitors for Alzheimer's disease. *Cochrane Database of Systematic Reviews*(1).

Blain PG, Mucklow JC, Rawlins MD, Roberts DF, Routledge PA, & Shand DG (1985). Determinants of plasma alpha 1-acid glycoprotein (AAG) concentrations in health. *British Journal of Clinical Pharmacology, 20*(5), 500-502.

Blanchard BJ, Konopka G, Russell M, & Ingram VM (1997). Mechanism and prevention of neurotoxicity caused by beta-amyloid peptides: relation to Alzheimer's disease. *Brain Research, 776*(1-2), 40-50.

Blennow K, de Leon MJ, & Zetterberg H (2006). Alzheimer's disease. *Lancet, 368*(9533), 387-403.

Blennow K, Hampel H, Weiner M, & Zetterberg H (2010). Cerebrospinal fluid and plasma biomarkers in Alzheimer disease. *Nature Reviews Neurology, 6*(3), 131-144.

Bloudek LM, Spackman DE, Blankenburg M, & Sullivan SD (2011). Review and meta-analysis of biomarkers and diagnostic imaging in Alzheimer's disease. *Journal of Alzheimer's Disease, 26*(4), 627-645.

Bohnert T, & Gan LS (2013). Plasma protein binding: from discovery to development. *Journal of Pharmaceutical Sciences, 102*(9), 2953-2994.

Brener O, Dunkelmann T, Gremer L, van Groen T, Mirecka EA, Kadish I, Willuweit A, Kutzsche J, Jurgens D, Rudolph S, Tusche M, Bongen P, Pietruszka J, Oesterhelt F, Langen KJ, Demuth HU, Janssen A, Hoyer W, Funke SA, Nagel-Steger L, & Willbold D (2015). QIAD assay for quantitating a compound's efficacy in elimination of toxic Abeta oligomers. *Scientific Reports, 5*, 13222.

Brenner GM, & Stevens CW. (2010). *Pharmacology* (3rd ed.): Saunders/Elsevier.

Brocks DR (2006). Drug disposition in three dimensions: An update on stereoselectivity in pharmacokinetics. *Biopharmaceutics and Drug Disposition, 27*(8), 387-406.

Caldwell J, Gardner I, & Swales N (1995). An introduction to drug disposition: the basic principles of absorption, distribution, metabolism, and excretion. *Toxicologic Pathology, 23*(2), 102-114.

Campo VL, Bernardes LSC, & Carvalho I (2009). Stereoselectivity in Drug Metabolism: Molecular Mechanisms and Analytical Methods. *Current Drug Metabolism, 10*(2), 188-205.

Chalifour RJ, McLaughlin RW, Lavoie L, Morissette C, Tremblay N, Boule M, Sarazin P, Stea D, Lacombe D, Tremblay P, & Gervais F (2003). Stereoselective interactions of peptide inhibitors with the beta-amyloid peptide. *Journal of Biological Chemistry, 278*(37), 34874-34881.

Chang JW, Siedlak S, Moreira P, Nunomura A, Castellani RJ, Smith MA, Zhu XW, Perry G, & Casadesus G (2011). Oxidative Stress in Alzheimer's Disease: A Critical Appraisal of the Causes and the Consequences. *Studies on Experimental Models*, 211-220.

Chaudhary K, Haddadin S, Nistala R, & Papageorgio C (2010). Intraperitoneal drug therapy: an advantage. *Current Clinical Pharmacology, 5*(2), 82-88.

Citron M, Oltersdorf T, Haass C, McConlogue L, Hung AY, Seubert P, Vigo-Pelfrey C, Lieberburg I, & Selkoe DJ (1992). Mutation of the beta-amyloid precursor protein in familial Alzheimer's disease increases beta-protein production. *Nature, 360*(6405), 672-674.

Colombo S, Buclin T, Decosterd LA, Telenti A, Furrer H, Lee BL, Biollaz J, Eap CB, & Swiss HIVCS (2006). Orosomucoid (alpha1-acid glycoprotein) plasma concentration and genetic variants: effects on human immunodeficiency virus protease inhibitor clearance and cellular accumulation. *Clinical Pharmacology and Therapeutics, 80*(4), 307-318.

Corder EH, Saunders AM, Strittmatter WJ, Schmechel DE, Gaskell PC, Small GW, Roses AD, Haines JL, & Pericak-Vance MA (1993). Gene dose of apolipoprotein E type 4 allele and the risk of Alzheimer's disease in late onset families. *Science (New York, N Y), 261*(5123), 921-923.

DaRocha-Souto B, Scotton TC, Coma M, Serrano-Pozo A, Hashimoto T, Serenó L, Rodríguez M, Sánchez B, Hyman BT, & Gómez-Isla T (2011). Brain Oligomeric beta-Amyloid but Not Total Amyloid Plaque Burden Correlates With Neuronal Loss and Astrocyte Inflammatory Response in Amyloid Precursor Protein/Tau Transgenic Mice. *Journal of Neuropathology and Experimental Neurology, 70*(5), 360-376.

de Silva HAR, & Patel AJ (1997). Presenilins and early-onset familial Alzheimer's disease. *Neuroreport, 8*(8), R1-R12.

Deary IJ, Corley J, Gow AJ, Harris SE, Houlihan LM, Marioni RE, Penke L, Rafnsson SB, & Starr JM (2009). Age-associated cognitive decline. *British Medical Bulletin, 92*(1), 135-152.

Decker H, Lo KY, Unger SM, Ferreira ST, & Silverman MA (2010). Amyloid-beta Peptide Oligomers Disrupt Axonal Transport through an NMDA Receptor-Dependent Mechanism That Is Mediated by Glycogen Synthase Kinase 3 beta in Primary Cultured Hippocampal Neurons. *Journal of Neuroscience, 30*(27), 9166-9171.

Di Stefano A, Iannitelli A, Laserra S, & Sozio P (2011). Drug delivery strategies for Alzheimer's disease treatment. *Expert Opin Drug Deliv, 8*(5), 581-603.

Dintzis HM, Symer DE, Dintzis RZ, Zawadzke LE, & Berg JM (1993). A Comparison of the Immunogenicity of a Pair of Enantiomeric Proteins. *Proteins-Structure Function and Genetics, 16*(3), 306-308.

Esch FS, Keim PS, Beattie EC, Blacher RW, Culwell AR, Oltersdorf T, McClure D, & Ward PJ (1990). Cleavage of Amyloid Beta Peptide During Constitutive Processing of Its Precursor. *Science, 248*(4959), 1122-1124.

Ferreira ST, Vieira MNN, & De Felice FG (2007). Soluble protein oligomers as emerging toxins in alzheimer's and other amyloid diseases. *IUBMB Life, 59*(4-5), 332-345.

Ferri CP, Prince M, Brayne C, Brodaty H, Fratiglioni L, Ganguli M, Hall K, Hasegawa K, Hendrie H, Huang Y, Jorm A, Mathers C, Menezes PR, Rimmer E, & Scazufca M (2005). Global prevalence of dementia: a Delphi consensus study. *The Lancet, 366*(9503), 2112-2117.

Feucht C, & Patel DR (2011). Principles of Pharmacology. *Pediatric Clinics of North America, 58*(1), 11-19.

Findeis MA, Musso GM, Arico-Muendel CC, Benjamin HW, Hundal AM, Lee JJ, Chin J, Kelley M, Wakefield J, Hayward NJ, & Molineaux SM (1999). Modified-peptide inhibitors of amyloid beta-peptide polymerization. *Biochemistry, 38*(21), 6791-6800.

Frydman-Marom A, Rechter M, Shefler I, Bram Y, Shalev DE, & Gazit E (2009). Cognitive-Performance Recovery of Alzheimer's Disease Model Mice by Modulation of Early Soluble Amyloidal Assemblies. *Angewandte Chemie-International Edition, 48*(11), 1981-1986.

Funke SA, van Groen T, Kadish I, Bartnik D, Nagel-Steger L, Brener O, Sehl T, Batra-Safferling R, Moriscot C, Schoehn G, Horn AHC, Mueller-Schiffmann A, Korth C, Sticht H, & Willbold D (2010). Oral Treatment with the D-Enantiomeric Peptide D3 Improves the Pathology and Behavior of Alzheimer's Disease Transgenic Mice. *ACS Chemical Neuroscience, 1*(9), 639-648.

Funke SA, & Willbold D (2012). Peptides for therapy and diagnosis of Alzheimer's disease. *Current Pharmaceutical Design, 18*(6), 755-767.

Furge LL, & Guengerich FP (2006). Cytochrome P450 enzymes in drug metabolism and chemical toxicology: An introduction. *Biochemistry and Molecular Biology Education, 34*(2), 66-74.

Glue P, & Banfield C (1996). Psychiatry, psychopharmacology and P-450s. *Human Psychopharmacology-Clinical and Experimental, 11*(2), 97-114.

Grandison MK, & Boudinot FD (2000). Age-related changes in protein binding of drugs: implications for therapy. *Clinical Pharmacokinetics, 38*(3), 271-290.

Handattu SP, Garber DW, Monroe CE, van Groen T, Kadish I, Nayyar G, Cao DF, Palgunachari MN, Li L, & Anantharamaiah GM (2009). Oral apolipoprotein A-I mimetic peptide improves cognitive function and reduces amyloid burden in a mouse model of Alzheimer's disease. *Neurobiology of Disease, 34*(3), 525-534.

Hardy J, & Selkoe DJ (2002). The Amyloid Hypothesis of Alzheimer's Disease: Progress and Problems on the Road to Therapeutics. *Science, 297*(5580), 353-356.

Hardy JA, & Higgins GA (1992). Alzheimer's Disease: The Amyloid Cascade Hypothesis. *Science, 256*(5054), 184-185.

Holtzman DM, Morris JC, & Goate AM (2011). Alzheimer's Disease: The Challenge of the Second Century. *Science Translational Medicine, 3*(77), 77sr71.

Hutton M, & Hardy J (1997). The presenilins and Alzheimer's disease. *Human Molecular Genetics, 6*(10), 1639-1646.

Hutton M, Lendon CL, Rizzu P, Baker M, Froelich S, Houlden H, Pickering-Brown S, Chakraverty S, Isaacs A, Grover A, Hackett J, Adamson J, Lincoln S, Dickson D, Davies P, Petersen RC, Stevens M, de Graaff E, Wauters E, van Baren J, Hillebrand M, Joosse M, Kwon JM, Nowotny P, Che LK, Norton J, Morris JC, Reed LA, Trojanowski J, Basun H, Lannfelt L, Neystat M, Fahn S, Dark F, Tannenberg T, Dodd PR, Hayward N, Kwok JB, Schofield PR, Andreadis A, Snowden J, Craufurd D, Neary D, Owen F, Oostra BA, Hardy J, Goate A, van Swieten J, Mann D, Lynch T, & Heutink P (1998). Association of missense and 5'-splice-site mutations in tau with the inherited dementia FTDP-17. *Nature, 393*(6686), 702-705.

Hyman BT, Phelps CH, Beach TG, Bigio EH, Cairns NJ, Carrillo MC, Dickson DW, Duyckaerts C, Frosch MP, Masliah E, Mirra SS, Nelson PT, Schneider JA, Thal DR, Thies B, Trojanowski JQ, Vinters HV, & Montine TJ (2012). National Institute on Aging-Alzheimer's Association guidelines for the neuropathologic assessment of Alzheimer's disease. *Alzheimers & Dementia, 8*(1), 1-13.

Ikonomovic MD, Klunk WE, Abrahamson EE, Mathis CA, Price JC, Tsopelas ND, Lopresti BJ, Ziolko S, Bi WZ, Paljug WR, Debnath ML, Hope CE, Isanski BA, Hamilton RL, & DeKosky ST (2008). Post-mortem correlates of in vivo PiB-PET amyloid imaging in a typical case of Alzheimer's disease. *Brain, 131*, 1630-1645.

Jang GR, Harris RZ, & Lau DT (2001). Pharmacokinetics and its role in small molecule drug discovery research. *Medicinal Research Reviews, 21*(5), 382-396.

Jiang N, Leithold LHE, Post J, Ziehm T, Mauler J, Gremer L, Cremer M, Schartmann E, Shah NJ, Kutzsche J, Langen K-J, Breitkreutz J, Willbold D, & Willuweit A (2015). Preclinical Pharmacokinetic Studies of the Tritium Labelled D-Enantiomeric Peptide D3 Developed for the Treatment of Alzheimer's Disease. *PloS One, 10*(6), e0128553.

Kratochwil NA, Huber W, Muller F, Kansy M, & Gerber PR (2002). Predicting plasma protein binding of drugs: a new approach. *Biochemical Pharmacology, 64*(9), 1355-1374.

Kumar J, & Sim V (2014). D-amino acid-based peptide inhibitors as early or preventative therapy in Alzheimer disease. *Prion, 8*(1), 119-124.

Kummer MP, & Heneka MT (2014). Truncated and modified amyloid-beta species. *Alzheimer's Research & Therapy, 6*(3), 28.

Lanctot KL, Herrmann N, Yau KK, Khan LR, Liu BA, Loulou MM, & Einarson TR (2003). Efficacy and safety of cholinesterase inhibitors in Alzheimer's disease: a meta-analysis. *Canadian Medical Association Journal, 169*(6), 557-564.

Leithold LHE, Jiang N, Post J, Ziehm T, Schartmann E, Kutzsche J, Shah NJ, Breitkreutz J, Langen KJ, Willuweit A, & Willbold D (2015). Pharmacokinetic Properties of a Novel D-Peptide Developed to be Therapeutically Active Against Toxic β-Amyloid Oligomers. *Pharmaceutical Research*.

Leucuta SE, & Vlase L (2006). Pharmacokinetics and metabolic drug interactions. *Current Clinical Pharmacology, 1*(1), 5-20.

Liu C, Zhao M, Jiang L, Cheng PN, Park J, Sawaya MR, Pensalfini A, Gou D, Berk AJ, Glabe CG, Nowick J, & Eisenberg D (2012). Out-of-register beta-sheets suggest a pathway to toxic amyloid aggregates. *Proceedings of the National Academy of Sciences of the United States of America, 109*(51), 20913-20918.

Liu H, Funke SA, & Willbold D (2010). Transport of Alzheimer disease amyloid-beta-binding D-amino acid peptides across an in vitro blood-brain barrier model. *Rejuvenation Res, 13*(2-3), 210-213.

Liu X, Wright M, & Hop CECA (2014). Rational Use of Plasma Protein and Tissue Binding Data in Drug Design. *Journal of Medicinal Chemistry, 57*(20), 8238-8248.

Massoud F, & Léger GC (2011). Pharmacological treatment of Alzheimer disease. *Canadian Journal of Psychiatry. Revue Canadienne de Psychiatrie, 56*(10), 579-588.

Maurer TS, Debartolo DB, Tess DA, & Scott DO (2005). Relationship between exposure and nonspecific binding of thirty-three central nervous system drugs in mice. *Drug Metabolism and Disposition: The Biological Fate of Chemicals, 33*(1), 175-181.

McKhann GM, Knopman DS, Chertkow H, Hyman BT, Jack CR, Kawas CH, Klunk WE, Koroshetz WJ, Manly JJ, Mayeux R, Mohs RC, Morris JC, Rossor MN, Scheltens P, Carrillo MC, Thies B, Weintraub S, & Phelps CH (2011). The diagnosis of dementia due to Alzheimer's disease: Recommendations from the National Institute on Aging-Alzheimer's Association workgroups on diagnostic guidelines for Alzheimer's disease. *Alzheimers & Dementia, 7*(3), 263-269.

McNaull BBA, Todd S, McGuinness B, & Passmore AP (2010). Inflammation and Anti-Inflammatory Strategies for Alzheimer's Disease - A Mini-Review. *Gerontology, 56*(1), 3-14.

Meyer UA (2000). Pharmacogenetics and adverse drug reactions. *Lancet, 356*(9242), 1667-1671.

Mullan M, Crawford F, Axelman K, Houlden H, Lilius L, Winblad B, & Lannfelt L (1992). A pathogenic mutation for probable Alzheimer's disease in the APP gene at the N-terminus of beta-amyloid. *Nature Genetics, 1*(5), 345-347.

Niwa T, Murayama N, & Yamazaki H (2011). Stereoselectivity of Human Cytochrome P450 in Metabolic and Inhibitory Activities. *Current Drug Metabolism, 12*(6), 549-569.

Noetzli M, & Eap CB (2013). Pharmacodynamic, Pharmacokinetic and Pharmacogenetic Aspects of Drugs Used in the Treatment of Alzheimer's Disease. *Clinical Pharmacokinetics, 52*(4), 225-241.

Nygaard HB (2013). Current and emerging therapies for Alzheimer's disease. *Clinical Therapeutics, 35*(10), 1480-1489.

Olubiyi OO, Frenzel D, Bartnik D, Glück JM, Brener O, Nagel-Steger L, Funke SA, Willbold D, & Strodel B (2014). Amyloid aggregation inhibitory mechanism of arginine-rich D-peptides. *Current Medicinal Chemistry, 21*(12), 1448-1457.

Olubiyi OO, & Strodel B (2012). Structures of the Amyloid beta-Peptides A beta(1-40) and A beta(1-42) as Influenced by pH and a D-Peptide. *Journal of Physical Chemistry B, 116*(10), 3280-3291.

Pauletti GM, Gangwar S, Siahaan TJ, Aubé J, & Borchardt RT (1997). Improvement of oral peptide bioavailability: Peptidomimetics and prodrug strategies. *Adv Drug Deliv Rev, 27*(2-3), 235-256.

Pike CJ, Cummings BJ, & Cotman CW (1995). Early association of reactive astrocytes with senile plaques in Alzheimer's disease. *Experimental Neurology, 132*(2), 172-179.

Pimplikar SW (2009). Reassessing the amyloid cascade hypothesis of Alzheimer's disease. *The International Journal of Biochemistry & Cell Biology, 41*(6), 1261-1268.

Poduslo JF, Curran GL, Kumar A, Frangione B, & Soto C (1999). beta-sheet breaker peptide inhibitor of Alzheimer's amyloidogenesis with increased blood-brain barrier permeability and resistance to proteolytic degradation in plasma. *Journal of Neurobiology, 39*(3), 371-382.

Pollaro L, & Heinis C (2010). Strategies to prolong the plasma residence time of peptide drugs. *Medchemcomm, 1*(5), 319-324.

Reichel A (2006). The role of blood-brain barrier studies in the pharmaceutical industry. *Curr Drug Metab, 7*(2), 183-203.

Reichel A (2009). Addressing central nervous system (CNS) penetration in drug discovery: basics and implications of the evolving new concept. *Chemistry & Biodiversity, 6*(11), 2030-2049.

Reitz C, & Mayeux R (2014). Alzheimer disease: Epidemiology, diagnostic criteria, risk factors and biomarkers. *Biochemical Pharmacology, 88*(4), 640-651.

Renukuntla J, Vadlapudi AD, Patel A, Boddu SH, & Mitra AK (2013). Approaches for enhancing oral bioavailability of peptides and proteins. *International Journal of Pharmaceutics, 447*(1-2), 75-93.

Roberts MS, Magnusson BM, Burczynski FJ, & Weiss M (2002). Enterohepatic circulation: physiological, pharmacokinetic and clinical implications. *Clinical Pharmacokinetics, 41*(10), 751-790.

Rogers J, & Lue LF (2001). Microglial chemotaxis, activation, and phagocytosis of amyloid beta-peptide as linked phenomena in Alzheimer's disease. *Neurochemistry International, 39*(5-6), 333-340.

Rojo LE, Fernandez JA, Maccioni AA, Jimenez JM, & Maccioni RB (2008). Neuroinflammation: Implications for the pathogenesis and molecular diagnosis of Alzheimer's disease. *Archives of Medical Research, 39*(1), 1-16.

Roy S, Zhang B, Lee VMY, & Trojanowski JQ (2005). Axonal transport defects: a common theme in neurodegenerative diseases. *Acta Neuropathologica, 109*(1), 5-13.

Sato AK, Viswanathan M, Kent RB, & Wood CR (2006). Therapeutic peptides: technological advances driving peptides into development. *Current Opinion in Biotechnology, 17*(6), 638-642.

Schumacher TNM, Mayr LM, Minor DL, Milhollen MA, Burgess MW, & Kim PS (1996). Identification of D-peptide ligands through mirror-image phage display. *Science, 271*(5257), 1854-1857.

Sela M, & Zisman E (1997). Different roles of D-amino acids in immune phenomena. *FASEB Journal, 11*(6), 449-456.

Selkoe DJ (1991). The molecular pathology of Alzheimer's disease. *Neuron, 6*(4), 487-498.

Serrano-Pozo A, Frosch MP, Masliah E, & Hyman BT (2011). Neuropathological alterations in Alzheimer disease. *Cold Spring Harbor Perspectives in Medicine, 1*(1), a006189.

Shen Q, Wang L, Zhou H, Jiang HD, Yu LS, & Zeng S (2013). Stereoselective binding of chiral drugs to plasma proteins. *Acta Pharmacologica Sinica, 34*(8), 998-1006.

Smith DA, Di L, & Kerns EH (2010). The effect of plasma protein binding on in vivo efficacy: misconceptions in drug discovery. *Nat Rev Drug Discov, 9*(12), 929-939.

Soto C (1999). Plaque busters: strategies to inhibit amyloid formation in Alzheimer's disease. *Molecular Medicine Today, 5*(8), 343-350.

Soto C, Kindy MS, Baumann M, & Frangione B (1996). Inhibition of Alzheimer's amyloidosis by peptides that prevent beta-sheet conformation. *Biochemical and Biophysical Research Communications, 226*(3), 672-680.

Sun N, Funke SA, & Willbold D (2012). A survey of peptides with effective therapeutic potential in Alzheimer's disease rodent models or in human clinical studies. *Mini Reviews in Medicinal Chemistry, 12*(5), 388-398.

Terry AV, & Buccafusco JJ (2003). The cholinergic hypothesis of age and Alzheimer's disease-related cognitive deficits: Recent challenges and their implications for novel drug development. *Journal of Pharmacology and Experimental Therapeutics, 306*(3), 821-827.

Thies W, Bleiler L, & Alzheimer's Association (2013). 2013 Alzheimer's disease facts and figures. *Alzheimer's & Dementia, 9*(2), 208-245.

Tillement JP, Duche JC, & Barre J (2006). Drug binding to blood proteins : characteristics, roles and pathophysiological changes. *Bulletin De L Academie Nationale De Medecine, 190*(4-5), 935-946.

Tjernberg LO, Lilliehook C, Callaway DJ, Naslund J, Hahne S, Thyberg J, Terenius L, & Nordstedt C (1997). Controlling amyloid beta-peptide fibril formation with protease-stable ligands. *Journal of Biological Chemistry, 272*(19), 12601-12605.

Trainor GL (2007). The importance of plasma protein binding in drug discovery. *Expert Opin Drug Discov, 2*(1), 51-64.

Trojanowski JQ, Smith AB, Huryn D, & Lee VMY (2005). Microtubule-stabilising drugs for therapy of Alzheimer's disease and other neurodegenerative disorders with axonal transport impairments. *Expert Opinion on Pharmacotherapy, 6*(5), 683-686.

Tuppo EE, & Arias HR (2005). The role of inflammation in Alzheimer's disease. *International Journal of Biochemistry and Cell Biology, 37*(2), 289-305.

van Groen T, Kadish I, Funke A, Bartnik D, & Willbold D (2012). Treatment with A beta 42 Binding D-Amino Acid Peptides Reduce Amyloid Deposition and Inflammation in APP/PS1 Double Transgenic Mice. *Advances in Protein Chemistry and Structural Biology, 88*, 133-152.

van Groen T, Kadish I, Funke SA, Bartnik D, & Willbold D (2013). Treatment with D3 removes amyloid deposits, reduces inflammation, and improves cognition in aged AbetaPP/PS1 double transgenic mice. *Journal of Alzheimer's Disease, 34*(3), 609-620.

van Groen T, Kadish I, Wiesehan K, Funke SA, & Willbold D (2009). In vitro and in vivo Staining Characteristics of Small, Fluorescent, Aβ42-Binding D-Enantiomeric Peptides in Transgenic AD Mouse Models. *ChemMedChem, 4*(2), 276-282.

van Groen T, Wiesehan K, Funke SA, Kadish I, Nagel-Steger L, & Willbold D (2008). Reduction of Alzheimer's Disease Amyloid Plaque Load in Transgenic Mice by D3, a D-Enantiomeric Peptide Identified by Mirror Image Phage Display. *ChemMedChem, 3*(12), 1848-1852.

van Marum RJ (2009). Update on the use of memantine in Alzheimer's disease. *Neuropsychiatric Disease and Treatment, 5*, 237-247.

van Regenmortel MHV, & Muller S (1998). D-peptides as immunogens and diagnostic reagents. *Current Opinion in Biotechnology, 9*(4), 377-382.

Walsh DM, & Selkoe DJ (2007). A beta oligomers - a decade of discovery. *Journal of Neurochemistry, 101*(5), 1172-1184.

Wang QX, Qiu J, Wang P, Jia GF, Wang P, Li JL, & Zhou ZQ (2005). Stereoselective kinetic study of hexaconazole enantiomers in the rabbit. *Chirality, 17*(4), 186-192.

Wiesehan K, & Willbold D (2003). Mirror-image phage display: Aiming at the mirror. *Chembiochem: A European Journal of Chemical Biology, 4*(9), 811-815.

Wilcock D, & Griffin WST (2013). Down's syndrome, neuroinflammation, and Alzheimer neuropathogenesis. *Journal of Neuroinflammation, 10*(1), 84.

Williams KM (1990). Enantiomers in arthritic disorders. *Pharmacology and Therapeutics, 46*(2), 273-295.

Zhang F, Xue J, Shao J, & Jia L (2012a). Compilation of 222 drugs' plasma protein binding data and guidance for study designs. *Drug Discov Today, 17*(9-10), 475-485.

Zhang W, Arteaga J, Cashion DK, Chen G, Gangadharmath U, Gomez LF, Kasi D, Lam C, Liang QW, Liu CH, Mocharla VP, Mu FR, Sinha A, Szardenings AK, Wang E, Walsh JC, Xia CF, Yu C, Zhao TM, & Kolb HC (2012b). A Highly Selective and Specific PET Tracer for Imaging of Tau Pathologies. *Journal of Alzheimers Disease, 31*(3), 601-612.

Zhu X, Su B, Wang X, Smith MA, & Perry G (2007). Causes of oxidative stress in Alzheimer disease. *Cellular and Molecular Life Sciences, 64*(17), 2202-2210.